Universitat Autònoma de Barcelona

The Ppz protein phosphatase as a potential novel antifungal target

Chunyi Zhang

The Ppz protein phosphatase as a potential novel antifungal target

Doctoral thesis presented by

Chunyi Zhang

for the degree of PhD in Bioquímica, Biología Molecular y Biomedicina from the Universitat Autònoma de Barcelona.

Thesis performed at the Departament de Bioquímica i Biologia Molecular and the Institut de Biotecnologia i de Biomedicina (Universitat Autònoma de Barcelona).

Thesis supervised by Dr. Joaquín Ariño Carmona

Cerdanyola del Vallès, April 2019

A. fumigatus	***A****spergillus* ***fumigatus***
A. nidulans	***A****spergillus* ***nidulans***
A. thaliana	***A****rabidopsis* ***thaliana***
AICAR	5'-phosphoribosyl-5-***a***mino-4-***i***midazole ***car***boxamide
AIDS	***A***cquired ***I***mmune ***D***eficiency ***S***yndrome
AMP	***A***denosine ***m***ono***p***hosphate
ATP	***A***denosine ***t***ri***p***hosphate
BLAST	***B***asic ***L***ocal ***A***lignment ***S***earch ***T***ool
C. albicans	***C****andida* ***albicans***
C. neoformans	***C****ryptococcus* ***neoformans***
CDK	***C***yclin-***d***ependent ***k***inase
cDNA	***c***omplementary ***DNA***
CoA	***Co***enzyme ***A***
CTD	***C***arboxy-***t***erminal ***d***omain
C-terminal	***C***arboxyl ***terminal***
CWI	***C***ell ***W***all ***I***ntegrity
D. hansenii	***D****ebaryomyces* ***hansenii***
DNA	***D***eoxyribo***n***ucleic ***a***cid
DTT	***D****i****t***hio***th***reitol
E. coli	***E****scherichia* ***coli***
FACS	***F***luorescence-***a***ctivated ***c***ell ***s***orting
FAD	***F***lavin ***A***denine ***D***inucleotide
FCP	***T***FIIF-associating component of RNA polymerase II ***C***TD ***p***hosphatase
FMN	***F***lavin ***m***ono***n***ucleotide
GDP	***G***uanosine ***di******p***hosphate
GST	***G***lutathione ***S***-***t***ransferase
GTP	***G***uanosine ***t***ri***p***hosphate

h	***h***our
HA	***H***em***a***gglutinin
HIV	***H***uman ***I***mmunodeficiency ***V***irus ***I***nfection
IMP	***I***nosine ***m***ono***p***hosphate
IPTG	**I**so***p***ropyl-β-***t***hio***g***alactopyranoside
kbp	***k***ilo ***b***ase ***p***air
kDa	***k***ilo ***Da***ltons
LB	***L***ysogeny ***B***roth
M	***M***olar concentration
MAP	***M***itogen-***a***ctivated ***p***rotein
MAPK	***M***itogen-***a***ctivated ***p***rotein ***k***inase
Mbp	***M***ega ***b***ase ***p***airs
MEK	***M***APK***/E***RK ***K***inase
MEKK	***M***APK***/E***RK ***K***inase ***K***inase
min	***min***ute
mRNA	***m***essenger ***RNA***
N. crassa	***N****eurospora* ***crassa***
NAD	***N***icotinamide ***a***denine ***d***inucleotide
nt	***n***ucleo***t***ide
N-terminal	Amino ***terminal***
OD	***O***ptical ***D***ensity
ORF	***O***pen ***R***eading ***F***rame
PBS	***P***hosphate-***b***uffered ***s***aline
PCR	***P***olymerase ***C***hain ***R***eaction
PPC	***P***hospho***p***antothenoyl***c***ysteine
PPCDC	**P**hospho***p***antothenoyl***c***ysteine ***d***e***c***arboxylase
PPM	***m***etal-dependent ***p***rotein ***p***hosphatase
PPP	***P***hospho-***p***rotein ***p***hosphatase

ABBREVIATIONS

PRPP	5-***p***hospho***r***ibosyl-1-***p***yro***p***hosphate
RNA	***R***ibo***n***ucleic ***a***cid
ROS	***R***eactive ***O***xygen ***S***pecies
s	***s***econd
S. cerevisiae	***S****accharomyces* ***cerevisiae***
S. pombe	***S****chizosaccharomyces* ***pombe***
SDS-PAGE	***S***odium ***d***odecyl ***s***ulfate ***P***oly***a***crylamide ***g***el ***e***lectrophoresis
SEM	***S***tandard ***E***rror of the ***M***ean
tRNA	***t***ransfer ***RNA***
TFIIF	***T***ranscription ***f***actors ***IIF***
TS	***T***hymidylate ***S***ynthase
U. maydis	***U****stilago* ***maydis***
UV	***U***ltra***v***iolet
WT	***W***ild ***T***ype
YPD	***Y***east extract ***p***eptone ***d***extrose
µg	***microg***ram
µM	***microm***olar concentration

ABBREVIATIONS

Abstract

ABSTRACT

Invasive fungal infections are an enormous threat, while only a limited number of antifungal drugs are currently available. The increasing incidence of fungal infections has aggravated the need for novel approaches for antifungal therapies. Our laboratory has discovered in *S. cerevisiae* the protein phosphatase (PPase) Ppz1, which is involved in multiple cellular processes and is important in the regulation of monovalent cation homeostasis. In budding yeast, Ppz1 is inhibited by two regulatory proteins, Hal3 and Vhs3. These two proteins have moonlighting properties, as they contribute to the formation of an atypical heterotrimeric PPC decarboxylase enzyme, crucial for CoA biosynthesis. Ppz1 is found only in fungi, including pathogenic ones, and has been found to be a virulence determinant in *Candida albicans* and *Aspergillus fumigatus*. In addition, when overexpressed, it appears to be the most toxic protein in budding yeast. These characteristics define Ppz1 as a possible target for antifungal therapies.

This project aims to elucidate the molecular basis of Ppz1 toxicity. First, by using a conditional Ppz1 overexpressing strain (ZCZ01, in which we replaced the *PPZ1* promoter by the *GAL1-10* promoter), we have confirmed that the toxic effect of Ppz1 occurs due to the increase in its phosphatase activity and not to depletion of Hal3/Vhs3. Besides, the growth defect caused by overexpression of Ppz1 was characterized by liquid growth assay, dot assay and flow cytometry. Since it is known that Ppz1 inhibits entry of potassium by regulating the Trk1/Trk2 high-affinity transporters, we also have confirmed that a potassium surplus does not rescue the conditional lethality caused by overexpression of Ppz1. In addition, we have defined the transcriptomic changes caused by overexpression of Ppz1 from the *GAL1-10* promoter, which revealed the development of an oxidative stress response.

Cryptococcus neoformans is a pathogenic fungus that produces meningoencephalitis in immunosuppressed patients (mainly HIV+) and is responsible for a high rate of mortality in invasive infections. Here we report the functional characterization of CnPpz1 and two possible Hal3-like proteins, CnHal3a and CnHal3b. CnPpz1 is a functional PPase and partially replaced endogenous ScPpz1. Both CnHal3a and CnHal3b interact with ScPpz1 and CnPpz1 *in vitro* but do not inhibit their phosphatase activity. Consistently, when expressed in *S. cerevisiae*, they poorly reproduced the Ppz1-regulatory properties of ScHal3. In contrast, both proteins were functional monogenic PPCDCs.

Ustilago maydis represents an important eukaryotic plant pathogen model system and has been considered one of the top ten plant fungal pathogens. Here we describe the functional characterization of UmPpz1 and UmHal3. We show that UmPpz1 is a functional PPase that partially mimics ScPpz1 *in vivo*. Both UmHal3 and its PPCDC domain interact with ScPpz1 and UmPpz1 *in vitro,* but the capacity to inhibit the phosphatase activity is not observed. In *S. cerevisiae* UmHal3 is not able to inhibit the ScPpz1 whereas is demonstrated as a functional PPCDC.

Overall, the results obtained in this work have established a basis of Ppz1 toxicity in *S. cerevisiae* and provide the foundations for understanding the regulation and functional role of the Ppz1-Hal3 system in the human pathogenic fungus *C. neoformans* and the plant pathogenic fungus *U. maydis*.

ABSTRACT

Las infecciones fúngicas invasivas son una amenaza enorme, pero actualmente solo hay un limitado número de medicamentos antifúngicos disponibles. El aumento de la incidencia de infecciones fúngicas ha agravado la necesidad de nuevos enfoques para las terapias antifúngicas. Nuestro laboratorio descubrió en *S. cerevisiae* la proteína fosfatasa (PPasa) Ppz1, que participa en múltiples procesos celulares y es importante en la regulación de la homeostasis de los cationes monovalentes. En la levadura, Ppz1 está inhibida por dos proteínas reguladoras, Hal3 y Vhs3. Estas dos proteínas tienen propiedades *moonlighting*, ya que contribuyen a la formación de una PPC descarboxilasa heterotrimérica atípica, crucial para la biosíntesis de CoA. Ppz1 se encuentra solo en hongos, incluidos los patógenos y se ha identificado como un determinante de virulencia en *Candida albicans* y *Aspergillus fumigatus*. Además, cuando se sobreexpresa, parece ser la proteína más tóxica en las levaduras. Estas características definen a Ppz1 como un posible objetivo para el desarrollo de terapias antifúngicas.

El primer objetivo de este proyecto es contribuir a dilucidar las bases moleculares de la toxicidad de Ppz1. Primero, mediante el uso de una cepa de sobreexpresión condicional de Ppz1 (ZCZ01, donde reemplazamos el promotor *PPZ1* por el promotor *GAL1-10*), hemos confirmado que el efecto tóxico de Ppz1 se produce debido al aumento en su actividad fosfatasa y no al agotamiento de Hal3/Vhs3. Además, el defecto de crecimiento causado por la sobreexpresión de Ppz1 se caracterizó por crecimiento en líquido y en sólido, y por citometría de flujo. Dado que se sabe que Ppz1 inhibe la entrada de potasio al regular los transportadores de alta afinidad Trk1/Trk2, también hemos confirmado que un exceso de potasio no rescata la letalidad condicional causada por la sobreexpresión de Ppz1. Además, hemos definido los cambios transcriptómicos causados por la sobreexpresión de Ppz1 bajo el promotor *GAL1-10*, que han revelado la aparición de una respuesta a estrés oxidativo.

Cryptococcus neoformans es un hongo patógeno que produce meningoencefalitis en pacientes inmunodeprimidos (principalmente HIV^{+}) y es responsable de una alta tasa de mortalidad en infecciones invasivas. Aquí presentamos la caracterización funcional de CnPpz1 y dos posibles proteínas similares a Hal3: CnHal3a y CnHal3b. CnPpz1 es una PPasa funcional y parcialmente reemplaza la ScPpz1 endógena. Tanto CnHal3a como CnHal3b interactúan con ScPpz1 y CnPpz1 *in vitro*, pero no inhiben su actividad fosfatasa. Consistentemente, cuando se expresan en *S. cerevisiae*, reproducen pobremente las propiedades reguladoras de Ppz1 típicas de ScHal3. Por el contrario, ambas proteínas son PPCDC monogénicas funcionales.

Ustilago maydis representa un importante organismo modelos eucariota de patógenos de plantas y se ha considerado como uno de los diez principales patógenos fúngicos de plantas. En este estudio mostramos la caracterización funcional de UmPpz1 y UmHal3. Hemos descubierto que UmPpz1 es una PPasa funcional y parcialmente imita a ScPpz1 *in vivo*. Tanto UmHal3 como su dominio PPCDC interactúan con ScPpz1 y UmPpz1 *in vitro*, mientras que no se observa la capacidad de inhibir la actividad de la fosfatasa. En *S. cerevisiae*, si bien UmHal3 no es capaz de inhibir la ScPpz1, se demuestra como una PPCDC funcional.

En conjunto, los resultados obtenidos en este trabajo permitenestablecer las bases de la toxicidad de Ppz1 en *S. cerevisiae* y proporcionan los fundamentos para comprender la regulación y el papel funcional del sistema Ppz1-Hal3 en el hongo patógeno humano *C. neoformans* y el hongo patógeno de plantas *U. maydis*.

Introduction

1. Protein Phosphorylation

In eukaryotic cells one of the most important and widespread regulatory mechanism to control intracellular events is the reversible phosphorylation of proteins, which plays a key role, for example, in signaling pathways, gene transcription and metabolism. This broad post-translational modification brings conformational structural changes in many enzymes and receptors, resulting in modification of their activities, interactions and localizations. Phosphoproteomics studies suggest that more than 70% of total eukaryotic cellular proteins, including humans, are regulated by phosphorylation (Kim *et al.* 2016). This mechanism is so important that aberrant alteration of protein phosphorylation state causes various diseases such as cancer, diabetes, rheumatoid arthritis and hypertension. In the case of the budding yeast *Saccharomyces cerevisiae* it has been demonstrated *in vitro* that at least 30% of the proteome could be phosphorylated (Ptacek *et al.* 2005). *In vivo*, diverse phosphoproteome studies have been performed on budding yeast and data from the diverse studies, available at the phosphoGRID database (https://thebiogrid.org/ (Sadowski *et al.* 2013), indicate that over 3100 proteins (~50% of the proteome) are phosphorylated in this organism.

The balance between protein kinases (PKase, transferring the γ-phosphate moiety from ATP to substrates) and phosphatases (PPase, removing the phosphate from substrates) define the protein phosphorylation status. Nine amino acid residues can be phosphorylated: tyrosine, serine, threonine, cysteine, arginine, aspartate, glutamate and histidine. In eukaryotic cells, serine, threonine and tyrosine residues are the most frequent choices (86.4%, 11.8% and 1.8% respectively in the human proteome) (Olsen *et al.* 2006; Moorhead *et al.* 2009).

Compared to the protein kinases, the functions of phosphatases are less understood, and the reasons are diverse. One of them is that phosphatases are often unselective. For example, one substrate could be recognized by different phosphatases at the same time, and one phosphatase could recognize different substrates. Besides, in contrast to kinases, there are no evident specific primary sequence signatures for phosphatases. As a general rule, the number of protein kinases is higher than the number of PPases. The genome of *S. cerevisiae* encodes 117 PKases while only 32 PPases have been found (Sakumoto *et al.* 2002).

1.1 Ser/Thr phosphatases

Based on biochemical assays the Ser/Thr phosphatases have been defined as type 1 (PP1) or type 2 (PP2). According to substrate specificities, requirement for divalent cations and sensitivity to certain inhibitors, the Ser/Thr phosphatases were further divided into four major classes: PP1, PP2A, PP2B and PP2C (Cohen 1989). The protein phosphatase type 1 (PP1) subfamily tends to dephosphorylate the β subunit of phosphorylase kinase and be inhibited by inhibitor-1 and inhibitor-2 (Foulkes *et al.* 1983). Moreover, Mn^{2+} is required to catalyze the dephosphorylation reaction (Foulkes *et al.* 1983). In contrast, the protein phosphatases type 2 (PP2) tend to dephosphorylate the α-subunit of phosphorylase kinase and be insensitive to inhibitor-1 and inhibitor-2. Based on the dependence on divalent cations, PP2 has been subclassified into PP2A, PP2B and PP2C. The divalent cations are not essential to PP2A, while Ca^{2+} is essential to PP2B and Mg^{2+} is necessary to PP2C activity (McGowan and Cohen 1988; Cohen 1989, 1997; Wera and Hemmings 1995).

In addition, on the basis of the sequence of catalytic core domains, the protein Ser/Thr phosphatases can be categorized into three families: the PPP (phospho-protein phosphatase) family, the PPM (metal-dependent protein phosphatase) family and the aspartate-based phosphatases (see Figure 1.1) (Shi 2009). Representative members of the PPP family include: PP1, PP2A, PP2B, PP4 (Bastians *et al.* 1997; Cohen *et al.* 2005), PP5 (Chen *et al.* 1994; Swingle *et al.* 2004; Zhi *et al.* 2015), PP6 (Bastians and Ponstingl 1996), and PP7 (Kutuzov *et al.* 1998). For the PPP family, the conserved catalytic subunit associates with one or more regulatory subunits. Instead of the regulatory subunits found in PPPs, members of the PPM family contain additional domains which may help determine substrate specificity (Tamura *et al.* 2004; Lammers and Lavi 2007). On the other hand, the phosphatases using the aspartate-based catalysis mechanism are represented by FCP/SCP proteins (TFIIF-associating component of RNA polymerase II CTD phosphatase/small CTD phosphatase) (Cho *et al.* 1999; Kobor *et al.* 1999). As shown in Figure 1.1, the FCP homology (FCPH) domain is the conserved structural core of FCP/SCP enzymes, whereas FCPs have an extra BRCT (BRCA1 C-terminal)-like domain (Ghosh *et al.* 2008).

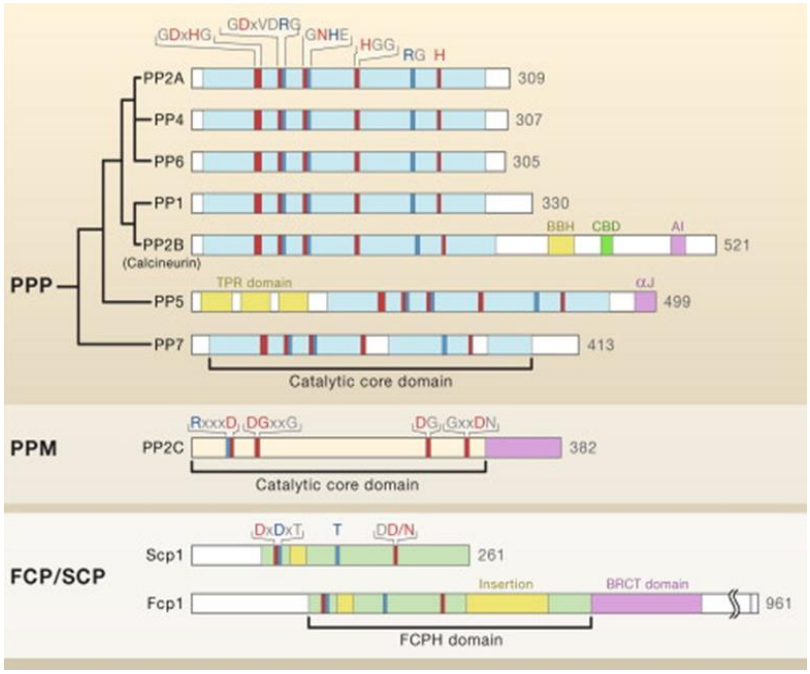

Figure 1.1 The three families of protein Serine/Threonine phosphatases.

The catalytic polypeptides corresponding to the three families of Ser/Thr PPases are shown. The catalytic core domains of each protein are indicated below the diagram. Signature sequence motifs are labeled above each diagram. Residues that contribute to metal coordination and phosphate binding are colored in red and blue, respectively. The PPP family contains three characteristic sequence motifs within the conserved 30 kDa catalytic domain: GDxHG, GDxVDRG, and GNHE (x, any amino acid). BBH, CNB-binding helix; CTD, carboxy-terminal domain; CBD, Ca^{2+}-calmodulin-binding motif; AI, autoinhibitory sequence; TPR, tetratricopeptide repeat; FCPH, FCP-homology domain (Shi 2009).

1.2 The Ser/Thr phosphatase type 1

Previous investigations have established that PP1 and PP2A together account for more than 90% of the protein phosphatase activity in eukaryotes (Moorhead *et al.* 2007; Virshup and Shenolikar 2009; Bollen *et al.* 2010). Recent data suggests that PP1 catalyzes most of the protein dephosphorylation events in eukaryotic cells, owing to the huge difference in the relative abundance of PP1 and PP2A (Janssens *et al.* 2008; Bollen *et al.* 2010). PP1 regulates various cellular processes such as protein synthesis, splicing of RNA, neuronal signaling, glycogen metabolism, muscle contraction, cell cycle progression, cell growth and differentiation (Gibbons *et al.* 2005; Rebelo *et al.* 2015).

The PP1 enzyme contains a catalytic subunit (PP1c), with a molecular mass ranging from 35 to 38 kDa, plus one or more regulatory subunits (Shi 2009). Variable regulatory subunits have been found to form stable complexes with this phosphatase. Distinct subunits convert PP1c into different forms (holoenzymes) which define the specific substrates, the subcellular locations and the phosphatase activities (Egloff *et al.* 1995; Zhao and Lee 1997; Cohen 2002). In all eukaryotes, PP1c is highly conserved with approximately 70% or greater protein sequence identity. The elucidation of the crystal structure of PP1c has established that this catalytic subunit adopts a compact α/β fold. The β sandwich is wedged between two α-helical domains (Goldberg *et al.* 1995; Egloff *et al.* 1995) (Figure 1.2). Additionally, Mn^{2+} and Fe^{2+} are in the three-way joint site of the β sandwich and two α-helical (small and large) domains. These two metal ions are coordinated with highly conserved residues, three histidines, two aspartic acids and one asparagine, indicating a common molecular mechanism of metal-catalyzed reaction. Besides, to initiate a nucleophilic attack on the phosphorus atom, Mn^{2+} and Fe^{2+} are believed to bind and activate a water molecule (Goldberg *et al.* 1995; Egloff *et al.* 1995). Furthermore, a Y-shaped surface feature is formed by three shallow surface grooves following the boundaries of the domains and the catalytic center (Figure 1.2) (Shi 2009).

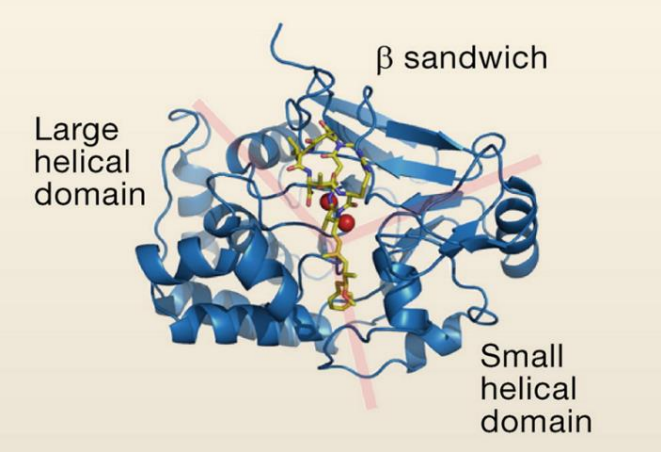

Figure 1.2 Structure of the catalytic subunit of protein phosphatase 1.

Structure of the catalytic subunit (blue) of protein phosphatase 1 (PP1) from rabbit muscle bound to okadaic acid (OA, yellow ball and stick). A Y-shaped surface groove (pink) is defined by the three domains of PP1. The two metal ions (red spheres) are Mn^{2+} and Fe^{2+}. (Shi 2009)

The catalytic domains of mammalian and fungal PP1s are 80-90% identical. When the mouse PP1c was expressed in the *Schizosaccharomyces pombe* mutant *dis2-11*, which

contains a conditional point mutation in the *dis*$^{2+}$ gene, one of the two genes encoding PP1 proteins, the phenotypes were partially complemented indicating that the functions of PP1s are also conserved (Sangrador *et al.* 1998). In *S. cerevisiae*, the single essential gene *GLC7* (*YER133W*), encoding a 312 residues protein with a 36 kDa molecular mass, has been identified as the catalytic subunit of PP1 (Ohkura *et al.* 1989; Clotet *et al.* 1991). Initially, *GLC7* attracted the attention because its important role in the accumulation of glycogen (Peng *et al.* 1990; Feng *et al.* 1991). As mammalian PP1c, Glc7 regulates a wide variety of intercellular events. For example, in G_2/M transition, Glc7 is essential for the control and the development of mitosis (Hisamoto *et al.* 1994; Zhang *et al.* 1995; Tu *et al.* 1996; Stark 1996). Besides, Glc7 participates in numerous functions related to the cytoskeleton, such as the spindle/kinetochore checkpoint activation and kinetochore formation (Bloecher and Tatchell 1999; Sassoon *et al.* 1999), the regulation of actin organization and endocytosis (Chang *et al.* 2002), polarization and filamentous growth, and pheromone responses (Cullen and Sprague 2002). Moreover, during sporulation, Glc7 also plays a critical role in the ascus formation (Tachikawa *et al.* 2001). Additionally, Andrew and Stark found that this protein was also involved in the maintenance of the cell wall integrity (Andrews and Stark 2000).

1.3 Ser/Thr phosphatases type Z in *S. cerevisiae* (Ppz1 and Ppz2)

Among the novel members of the PP1-related Ser/Thr phosphatase family in *S. cerevisiae* there are two closely related paralogs, Ppz1 and Ppz2, which show 67% full length identity (Hughes *et al.* 1993). In contrast to *GLC7*, *PPZ1* and *PPZ2* are not essential, indicating that these two phosphatases do not perform the same functions as yeast PP1c. Similar proteins have been discovered in other fungi, such as Pzh1 (*Schizosaccharomyces pombe*), Pzl1 (*Neurospora crassa*) and CaPpz1 (*Candida albicans*), which share structural and functional characteristics with ScPpz1 (Balcells *et al.* 1997, 1998; Szöőr *et al.* 1998; Vissi *et al.* 2001; Adam *et al.* 2012; Leiter *et al.* 2012). Up to now, homologues of *PPZ1* and *PPZ2* have not been detected in higher eukaryotes, suggesting that these phosphatases are restricted to fungi.

Structurally, Ppz1 and Ppz2 consist of two distinct domains. The catalytical domain in the C-terminal half (about 350 residues) presents over 60% sequence identity to PP1c from many species (even mammals). Several *in vitro* substrates for the Ppz1 catalytic domain have been reported, such as myelin basic protein, histone 2A, casein (Posas *et al.* 1995b) or myosin light chain (Petrényi *et al.* 2016). Besides, the presence of Mn^{2+} ions is

necessary for the activity of Ppz1, as it is for PP1c (Barford *et al.* 1998; Peti *et al.* 2013). Likewise, some PP1c inhibitory toxins (okadaic acid and microcystin-LR), which have been proved to bind to the PP1c active site, also have negative influence on Ppz1 (MacKintosh *et al.* 1990; Honkanen *et al.* 1990; Posas *et al.* 1995b). These similarities may come from the sequence GEFD present in the C-terminal domain of both PP1 and Ppz1 (Posas *et al.* 1995b). Moreover, Clotet and coworkers established that mutation of Arg^{451} in Ppz1 (equivalent to Arg^{95} in PP1c) largely leads to loss of the function and catalytic activity. (Clotet *et al.* 1996). On the other hand, the Ppz1 N-terminal half is rich in serine, threonine and asparagine residues, is predicted to be quite unstructured and appears unrelated to other phosphatase protein sequences (Posas *et al.*, 1992; Hughes *et al.*, 1993). It was also confirmed that Gly^2 in Ppz1 could be myristoylated *in vivo* (Clotet *et al.* 1996). Besides, different protein kinases such as PK-A, PK-C and Ck-2 can phosphorylate *in vitro* the N-terminal half of Ppz1 at multiple sites (Posas *et al.* 1995b). Till now the function of the N-terminal half is unclear. This region is possibility related to the specificity, and some residues (within the 241-317 region and Gly^2) have been reported to be necessary for full Ppz1 function. Additionally, it was proposed that the N-terminal half might regulate the phosphatase activity provided by the C-terminal half (Clotet *et al.* 1996). Although the N-terminal half is quite variable among different fungi, a serine and arginine-rich conserved motif (SxRSxRxxxS) has been discovered in the orthologs from various fungal species, suggesting that this motif participates in the function of the phosphatases, but the role is still unknown (Minhas *et al.* 2012; Szabó *et al.* 2019).

2. The cellular roles of Ppz1 in *S. cerevisiae*

Ppz1 plays an important role in the regulation of several important processes in *S. cerevisiae*, for example in osmotic and saline homeostasis (Posas *et al.* 1993, 1995a). It has been also established that Ppz1 influences protein translation and cell cycle at the G_1/S transition (Clotet *et al.* 1999; de Nadal *et al.* 2001). It was known for many years that overexpression of Ppz1 was highly toxic for the cell. Remarkably, a genome-wide study in *S. cerevisiae* overexpressing every single protein in high copy from the *GAL1-10* promoter reported that Ppz1 was one of the most toxic proteins, and that cells can only tolerate very low amounts of Ppz1 (Makanae *et al.* 2012).

2.1 The roles of Ppz1 in cation homeostasis

Extensive research has shown that the maintenance of cation homeostasis is essential to all living cells. These ions are present in many cellular environments, but cannot freely diffuse across cell membranes (Serrano, Kielland-Brandt and Fink, 1986; Rodríguez-Navarro, 2000; Sychrová, 2004; Ariño, Ramos and Sychrova, 2010; Jung *et al.*, 2012). For microorganisms such as *S. cerevisiae*, the intracellular concentrations of major monovalent cations (H^+, K^+, and Na^+) are tightly established (Serrano 1996). Thus, efficient systems have been developed to maintain homeostatic concentrations in response to changes in the external environment (Yenush 2016). Up to now, cation transport mechanisms in yeast have been well identified and characterized (Ariño *et al.* 2010; Merchan *et al.* 2011; Barreto *et al.* 2012; Cyert and Philpott 2013; Kahm and Kschischo 2016) (see figure 2.1) In the environment, sodium can be an abundant cation, while the intracelluar accumulation of sodium is actively avoided by yeast cells owing to its toxicity. Under normal growth conditions, the concentration of Na^+ is maintained low through the coordination of uptake and efflux systems. There are two classes of transport proteins playing fundamental roles in sodium efflux: Nha1 and the Ena family of ATPases (Yenush 2016). The Na^+/H^+ antiporter Nha1 is a plasma membrane protein that contributes to the intracellular homeostasis of Na^+ and pH (Prior *et al.* 1996; Kinclova-Zimmermannova *et al.* 2006). In addition, the gene *ENA1* encodes a P-type ATPase that contributes to sodium, lithium and potassium efflux in yeast cells. Up to five *ENA* genes have been identified in an unusual tandem repeat in some strains of *S. cerevisiae*. It has been reported that mutation of the *ENA* cluster results in sensitivity to high salinity and alkaline pH (Haro, Garciadeblas and Rodriguez-Navarro, 1991; Garciadeblas *et al.*, 1993; Rodríguez-Navarro, Quintero and Garciadeblás, 1994). The first member of the tandem, *ENA1,* encodes the most functionally relevant component of the cluster (Martinez *et al.* 1991; Haro *et al.* 1991; Wieland *et al.* 1995; Rodríguez-Navarro *et al.* 2002; Ruiz *et al.* 2003). Under standard growth conditions, the expression levels of the *ENA* genes are low. However, the expression of the *ENA1* gene is specifically and markedly increased in response to osmotic, saline and alkaline pH stress *via* activation of several signaling pathways (Yenush 2016). In addition, Alepuz and coworkers observed a transcriptional response of *ENA1* under conditions of glucose starvation, indicating that glucose exerts a repressor effect on *ENA1* expression (Alepuz *et al.* 1997).

It is now established that, at least in part, the way *S. cerevisiae* Ppz1 and Ppz2 determine salt tolerance is by affecting the expression level of *ENA1* (Posas, Camps and

Ariño, 1995; Ariño, 2002; Ruiz, Yenush and Ariño, 2003). The *ppz1* mutant strain is tolerant to sodium and lithium cations due to the increased efflux of these cations, which is accompanied by an increase in the expression of *ENA1* (Posas *et al.* 1995a). Additionally, the tolerance to sodium and lithium cations, as well as *ENA1* expression, are enhanced in the *ppz1 ppz2* double mutant (Posas *et al.* 1995a; Ruiz *et al.* 2003). It has been proposed that the Ppz phosphatases negatively regulate *ENA1* gene expresion to avoid the unnecesary expression of the ATPase under basal growth conditions (Posas *et al.* 1995a). The mechanism by which Ppz1 regulates *ENA1* expression is not fully solved. However, it seems to involve modulation of the calcineurin pathway (Ruiz *et al.* 2003).

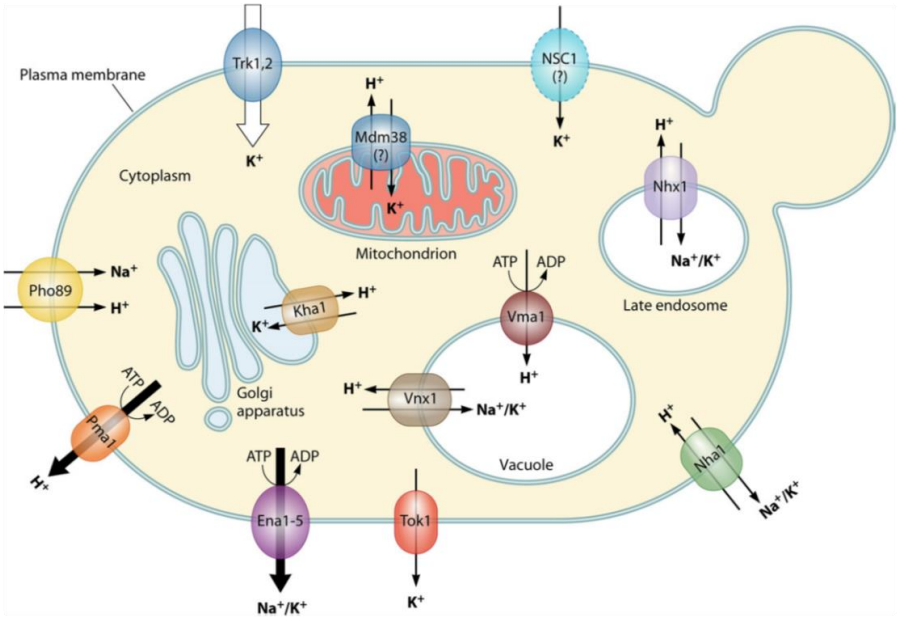

Figure 2.1 The major plasma membrane and intracellular cation transporters in the yeast *S. cerevisiae*.

The principal transporters involved in the homeostasis of monovalent cations in the yeast *S. cerevisiae* (Ariño *et al.* 2010).

Existing research recognize the essential role played by intracellular potassium in many processes, such as protein translation, pyruvate synthesis and regulation of the cell cycle (Ariño, Ramos and Sychrova, 2010; Rodríguez-Navarro and Benito, 2010; Cyert and Philpott, 2013). In yeast growing under normal conditions, the only alkali cation specifically transported is potassium. Potassium transport involves a high-affinity and a low-affinity system (Rodriguez-Navarro and Ramos 1984). The high-affinity potassium uptake is

mediated by the transporters Trk1 and Trk2 (Gaber *et al.* 1988; Ko *et al.* 1990; Ko and Gaber 1991), Trk1 being the most physiologically relevant. The *trk1 trk2* double mutant strain grows slowly under limiting potassium and addition of potassium to the media restores normal growth (Ko *et al.* 1990; Ko and Gaber 1991; Gómez *et al.* 1996; Madrid *et al.* 1998; Mulet *et al.* 1999).

The main regulatory mechanism of Trk transporters is performed at the protein level *via* phosphorylation (Yenush 2016). The activity and/or stability of Trk transporters are controlled by protein kinases and phosphatases such as Hal4 and Hal5 kinases. Previous studies have revealed that these protein kinases are required to stabilize the Trk transporters at the plasma membrane, especially under low potassium conditions (Mulet *et al.* 1999; Pérez-Valle *et al.* 2007). Although the nature of the direct phosphorylation of Trk transporters by Hal4 and Hal5 remains unclear, both *in vitro* and *in vivo* studies demonstrated that Trk1 could be phosphorylated by protein kinases, albeit the direct phosphorylation by Hal4 and Hal5 kinases has not been reported (Mulet *et al.* 1999; Yenush *et al.* 2005).

Ppz1 and Ppz2 have been described among the negative regulators of Trk transport activity. Massive potassium influx was reported in *ppz1 ppz2* double mutant cells, which resulted in the decrease of membrane potential and cytosolic alkalization, indicating that the Trk potassium transporters could be inhibited by Ppz phosphatases. The increased intracellular concentration of potassium leads to proton efflux to maintain electrical balance, and finally results in internal alkalinization. The inhibitory effect on the influx of toxic cations, due to reduced membrane potential, could account for the tolerance to saline stress of Ppz-deficient cells. Moreover, the abundant accumulation of intracellular potassium contributes to higher turgor pressure and increased cell size (Yenush *et al.* 2002; Merchan *et al.* 2004; Ruiz *et al.* 2004b). Yenush and coworkers have demonstrated that Trk1 physically interacts with Ppz1 in plasma membrane rafts as well as that the phosphorylated forms of Trk1 increase in Ppz mutant cells (Yenush *et al.* 2005), although no evidence for direct dephosphorylation has been obtained so far. As a brief conclusion, the regulation of Trk transporters by Ppz phosphatases plays an essential role in the maintenance of intracellular potassium and pH homeostasis.

2.2 The roles of Ppz1 in cell wall integrity maintenance

The cell wall of *S. cerevisiae* is fundamental for cell shape maintenance and acts as a shield against physical or chemical external stresses (Klis *et al.* 2006). This structure is so important for yeast cells survival that its integrity is tightly controlled by a well-known regulatory mechanism, the Cell Wall Integrity (CWI) pathway. This pathway is activated in response to the cell wall stress caused by chemical agents, such as congo red, calcofluor white, zymolyase and caffeine, or environmental conditions, such as heat shock, hypoosmotic shock and alkaline pH (Levin 2005). A group of cell wall sensors (Wsc1-3, Mid2, and Mtl1) and a small GTPase (Rho1) are upstream components of this important pathway. Rho1, a signal transducer, interacts with the protein kinase C (Pkc1), which leads to activation of the Mitogen Activated Protein (MAP) kinase cascade consisting of a MEKK(Bck1), two MEKs (Mkk1/Mkk2) and a MAPK (Slt2, also known as Mkk1) (Levin 2011). Once Slt2 is activated, several nuclear (as the transcriptional factor Rlm1) and cytosolic targets are phosphorylated, which leads to activation of specific transcription factors in response to cell wall aggressions (Levin 2005). The *slt2* mutant cells is prone to lysis when cells are exposed to salt or high temperature (37 °C). Moreover, these mutants are sensitive to caffeine or calcofluor white. Besides, when 1 M sorbitol is added as osmotic stabilizer, this lytic phenotype is abolished (Lee *et al.* 1993a).

Initially, the *PPZ2* gene was identified as a suppressor of the lysis defect related to the disruption of *SLT2*/*MPK1*, suggesting that Ppz phosphatases play a role in the maintenance of cell integrity in *S. cerevisiae* (Lee *et al.* 1993b). Then, it was observed that phenotypes such as sensitivity to temperature or caffeine, increased size and tendency to cell lysis were similar in Ppz phosphatase mutant cells and in cells lacking components of the Slt2/Mpk1 pathway (Posas *et al.* 1993; Hughes *et al.* 1993). An explanation for the link between Ppz phosphatases and the Slt2/Mpk1 pathway can be found in the Ppz-mediated regulation of potassium uptake (see above). Because the activity of Trk transporters in cells lacking Ppz phosphatases is increased, this leads to a high accumulation of intracellular potassium, and the resulting increased turgor pressure negatively affects the cell wall, which makes necessary for these cells to activate the Pkc1-Slt2/Mpk1 pathway (Yenush *et al.* 2002; Merchan *et al.* 2004).

2.3 The roles of Ppz1 in cell cycle progression

Progression through the cell cycle is a highly regulated process that is conserved all over eukaryotes (Cooper 2000). Therefore, in *S. cerevisiae*, the cell cycle consists in four tightly controlled phases: G_1 (G indicates gap), synthesis (S phase, DNA duplication), G_2 and mitosis (M phase, segregation). The regulation of the cell cycle is guaranteed by several control points (checkpoints). The cell cycle begins at "Start", a control point in the G_1/S transition which is controlled by the nutrients, mating factors and cell size (Cooper 2000; Johnson and Skotheim 2013). When their sizes are enough, DNA is not damaged, and nutrients are abundant, cells enter into S phase. At G_2/M, once DNA is fully replicated during the S phase, cells enter into mitosis (Tyson *et al.* 2002).

It has been established that the events that define different phases of the cell-division cycle are governed by distinct forms of the cyclin dependent kinase (CDK) (Wittenberg 2005). Cdc28 is the CDK responsible for the major cell cycle transitions through its association with different cyclins (Mendenhall and Hodge 1998; Andrews and Measday 1998; Miller and Cross 2001). For example, at the end of mitosis, Cdc28 and Cln3 (one of the G_1 cyclins) form the complex responsible to control the cell size. When the proper dimensions have been satisfied, several G_1 cyclins including Cln1, Cln2, Clb5 and Clb6, are induced by Cln3-Cdc28 through the activation of transcriptional complexes (Koch *et al.* 1996). In addition, some phosphatases, such as Sit4 (belongs to Ser/Thr phosphatase type 2A family), are involved in the regulation of the G_1/S transition (Jiang 2006). In contrast to wild type, cells lacking Sit4 grow slower and present defects in bud emergence, a characteristic feature of delayed G_1/S transition (Sutton *et al.* 1991). Further study demonstrated that Sit4 is necessary for the expression of *SWI4*, *CLN1* and *CLN2* which are involved in bud emergence during the late G_1 phase. Moreover, Sit4 and Cln3 were revealed to provide parallel pathways for the mRNA accumulations of *CLN1*, *CLN2* and *PCL1* (G_1 cyclin), which justifies the lethal phenotype of *sit4 cln3* double mutants (Fernandez-Sarabia *et al.* 1992). On the other hand, overexpression of the *HAL3* gene (encoding the regulatory subunit of Ppz1, for detailed information see section 4) largely overcome the growth defect of cells lacking Sit4, and this effect was dependent on the presence of Ppz1 (Di Como *et al.* 1995; Clotet *et al.* 1999). Several phenotypes of cells overexpressing Ppz1 are also ascribed to a delay in G_1/S transition, such as the blockage of cell growth, delayed expression of *CLN2* and *CLB5* and the increase in unbudded cells (Clotet *et al.*, 1999). The growth defect derived from Ppz1 excess was exaggerated in cells with low G_1 cyclin levels, while the mutation of

PPZ1 rescued the lethal phenotype of *sit4 cln3* mutants. Besides, *ppz1* mutant cells express *CNL2* and *CLB5* earlier resulting in advanced entry in S phase. Therefore, Ppz1 plays an important role in the G_1/S transition which is partially opposed to the Sit4. Additionally, Ppz1 negatively regulate G_1 cycle transcription, and this mechanism is not mediated by Sit4, Bck2, or Cln3. (Clotet *et al.* 1999).

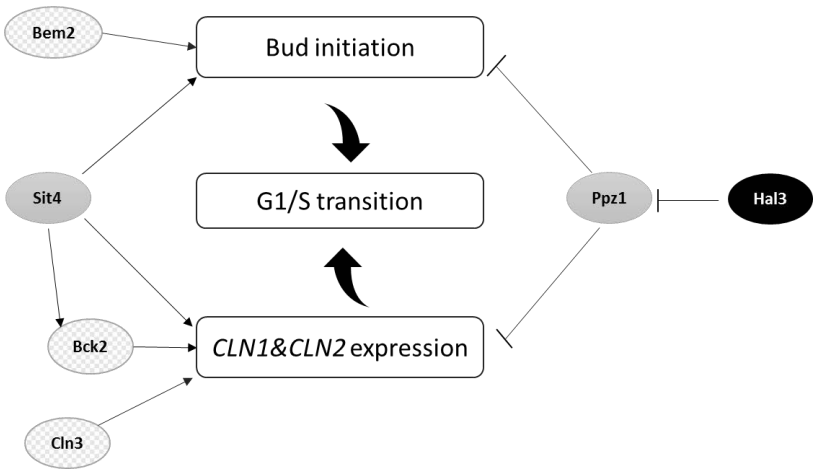

Figure 2.3 Schematic diagram of the roles of Ppz1 in cell cycle regulation.

(Clotet *et al.* 1999)

2.4 The roles of Ppz1 in protein translation

It is now well established that the mechanisms of translation elongation, termination, and recycling in *S. cerevisiae* are conserved in other eukaryotes (Dever and Green 2012; Dever *et al.* 2016). The structures of the elongation factors eEF1A and eEF2 are also conserved (Dever *et al.* 2016). As shown in Figure 2.4, at the beginning a peptidyl-tRNA is in the P site of the elongating ribosome meanwhile a deacylated tRNA occupies the A site. Then the eEF1A-GTP bound aa-tRNA deliver the aa-tRNA in the A site resulting in the release of eEF1A-GDP. Next the eEF1Bαγ complex catalyze the guanine nucleotide exchange on eEF1A. Then, eEF2-GTP move the peptidyl-tRNA from A site to P site and the deacylated tRNA from P site to E site. In addition, the fungal specific eEF3 component interacts with eEF1A and is proposed to assist in the release of tRNA in the E site (Dever *et al.* 2016).

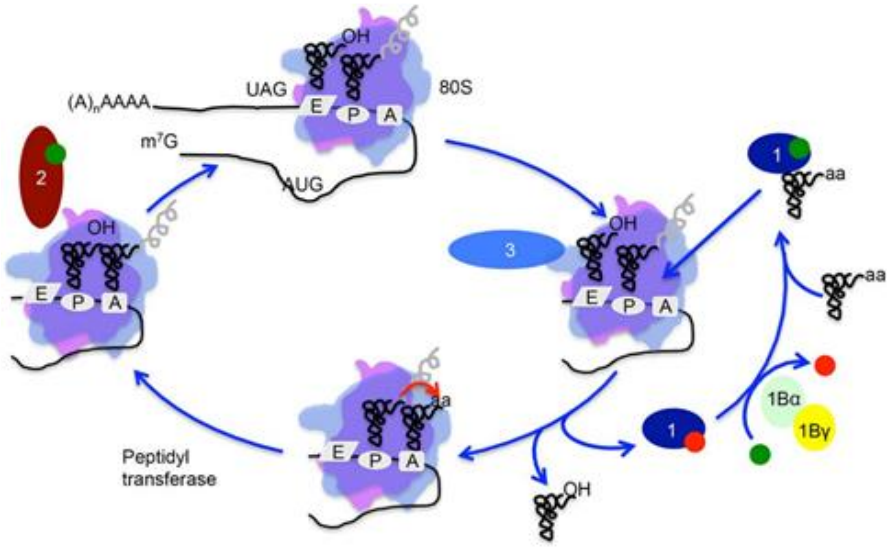

Figure 2.4 Model of yeast translation elongation.

Translation elongation stars with a peptidyl tRNA in the P site and a deacylated tRNA in the E site. The blue oval with the number 1 indicates eEF1A, the red oval with the number 2 indicates eEF2 and the fungal-specific essential factor eEF3 is indicated by the oval with number 3. The green and circles suggest GTP and GDP, respectively (Dever *et al.* 2016).

Previous research has suggested that the Ppz phosphatases influence protein translation. *In vivo*, Ppz1 was demonstrated to interact with eEF1Bα (Tef5). In addition, hyperphosphorylation of the conserved Ser^{86} of Tef5 was observed in cells lacking Ppz1 and Ppz2. Indeed, the read-through at all nonsense codons was enhanced in cells lacking Ppz phosphatases, indicating that the phosphatases might affect the translational fidelity (de Nadal *et al.* 2001). This view is reinforced by the reported influence of Ppz1 in read-through efficiency and manifestation of non-Mendelian anti-suppressor determinant [ISP(+)] (Aksenova *et al.* 2007; Rogoza *et al.* 2009; Ivanov *et al.* 2010; Nizhnikov *et al.* 2014).

3. The characteristics of ScPpz1 homologs in diverse fungi

The structures and functions of Ppz1 orthologs have been investigated in diverse fungal species, such as *Schizosaccharomyces pombe* (Balcells *et al.* 1997, 1998, 1999), *Neurospora crassa* (Vissi *et al.* 2001), *Debaryomyces hansenii* (Minhas *et al.*, 2012), and the pathogen fungi *Candida albicans* (Adam *et al.* 2012) and *Aspergillus fumigatus* (Leiter *et al.* 2012). In general, fungal Ppz1 enzymes share similar highly conserved C-terminal catalytic domain, while the N-terminal domains are varied in size and sequence. For example, the N-

terminal extension range from more than 300 residues in *S. cerevisiae* to around 150-180 residues in pathogenic fungi (see Figure 3). It has been estimated that the N-terminal extensions are unstructured. According to the structural conservation, these fungal Ppz1 enzymes, when expressed in other fungi, partially complement the deficiency in the endogenous phosphatase (Balcells *et al.* 1997; Vissi *et al.* 2001; Adam *et al.* 2012; Minhas *et al.* 2012; Leiter *et al.* 2012).

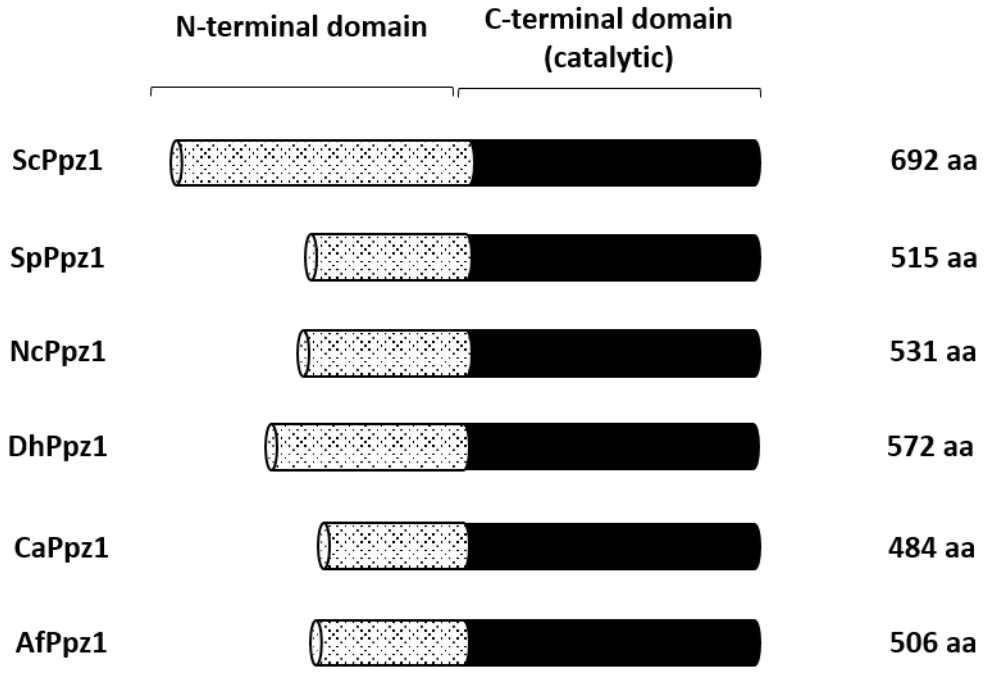

Figure 3 Structures of Ppz1 enzymes from different fungi

Schizosaccharomyces pombe can be usually isolated from habitats such as arak mash, molasses, apples, grape juice or palm wine (Wickerham 1953; Battley 1992). From a scientific point of view, the fission yeast, *S. pombe* is an attractive model system in the study of molecular genetics and cell biological processes such as cell cycle, metabolism or regulatory cascades (Zhao and Lieberman 1995; Calero and Ramos 2003; Giga-Hama *et al.* 2007). After the screening of a *S. pombe* genomic library with a C-terminal probe of the *S. cerevisiae* Ppz1, a 515-residue protein was detected and named as Pzh1 (phosphatase z homolog 1) (Balcells *et al.* 1997). The region from residue 193 to the end of the Pzh1 protein is 78% identical to the C-terminal half of *S. cerevisiae* proteins Ppz1 and Ppz2, while a lower level of identity (60-62%) is found when the same region is compared with the *S. cerevisiae*

Glc7 and the *S. pombe* PP1c Dis2 and Sds21 proteins. It has been demonstrated that the overexpression of *PZH1* can rescue the lytic defect induced by caffeine and slightly decrease the tolerance for Li^+ of *S. cerevisiae ppz1* mutant cells. Besides, the disruption of *PZH1* leads to increased Na^+ tolerance and K^+ hypersensitivity while has no effect on tolerance to caffeine or osmotic stress in *S. pombe* cells. It is well established that the Sod2 antiporter is an important determinant of salt tolerance in fission yeast (Jia *et al.* 1992; Dibrov *et al.* 1997). The *pzh1* mutation significantly increases salt tolerance in the absence of the *SOD2* gene indicating that Pzh1 could be involved in Sod2-independent regulatory pathways. Therefore, the *S. pombe* Pzh1 showed the capacity to regulate salt tolerance in fission yeast (Balcells *et al.* 1997).

Filamentous ascomycete fungi possess a specialized type of multicellularity uncommon in higher eukaryotic organisms, such as plants or animals. *Neurospora crassa*, a typical filamentous ascomycete fungus, has been used as a model organism for studying eukaryotic cell–cell communication, circadian rhythm, signal transduction and the mechanisms of environmental sensing (Borkovich *et al.* 2004; Herzog *et al.* 2015; Virgilio and Bertolini 2018). In *N. crassa* the gene *PZL-1* was found to encode a putative Ser/Thr protein phosphatase that is reminiscent of the Ppz1/Ppz2 and Pzh1 phosphatases from *S. cerevisiae* and *S. pombe* (Vissi *et al.* 2001). The expression of *PZL-1* controlled from the *PPZ1* promoter in a *S. cerevisiae ppz1* mutant was able to rescue the altered sensitivity to caffeine and Li^+. Moreover, the overexpression of *PZL-1* mitigated the lytic phenotype of a *S. cerevisiae slt2*/*mpk1* mitogen-activated protein (MAP) kinase mutant, suggesting that Pzl-1 mimicked the effects caused by overexpression of *PPZ1*. When *PZL-1* was expressed in *S. pombe,* controlled from the *nmt1* promoter (Basi *et al.* 1993), the growth defect of a *pzh1* mutation in high potassium was fully rescued, while the sodium-halotolerant phenotype was only partially complemented. Furthermore, the overexpression of *N. crassa PZL-1* in *S. pombe* was demonstrated to affect cell growth and morphology. Therefore, Pzl-1 was found to fulfill the known functions carried out by *S. cerevisiae* Ppz phosphatase proteins, despite the marked divergence in sequence within their N-terminal moieties (Vissi *et al.* 2001).

Debaryomyces hansenii is one of the most halotolerant yeast species and is considered as a model organism to understand halotolerance in yeast (Prista *et al.*, 2005; Aggarwal and Mondal, 2006). A single putative Ppz1-encoding gene was identified in *D. hansenii*, and this 572-amino acid-long hypothetical protein was called DhPpz1. The predicted amino acid sequence of DhPpz1 revealed 54.8 and 54.2% overall identity with Ppz1 and Ppz2 of *S. cerevisiae* (85.2 and 83.4% identity within the catalytic C-terminal

region), while in the N-terminal region, DhPpz1 exhibited only 25.0 and 35.4% identity with that of Ppz1 and Ppz2, even if this region is also rich in serine and asparagine residues. The *DhPPZ1* knock-out strain displayed increased tolerance to Li^+, Na^+, hygromycin and spermine. Besides, under salt stress, a 10-fold higher expression of *DhNHA1*, encoding a Na^+/H^+ antiporter, was detected in the *DhPPZ1* mutant compared with the wild type control, indicating that DhPpz1 regulates the expression of the Na^+/H^+ antiporter. In addition, the growth defect produced by the *dhmpk1* deletion could be abrogated by overexpressing DhPpz1. Besides, the conserved serine/arginine-rich motif in the N-terminal region was characterized to be essential for the cation tolerance. (Minhas *et al.*, 2012).

Candida albicans is an important human pathogen that is the most common cause of fungal infections in humans (Pappas *et al.* 2003). This organism contains a single *PPZ* candidate gene, termed *CaPPZ1*, which has at least four distinct alleles (Kovács *et al.* 2010). As other Ppz proteins (Ariño 2002), CaPpz1 consist of a short N-terminal regulatory domain and a C-terminal catalytic domain. It was demonstrated that the bacterially expressed CaPpz1 exhibited phosphatase activity which was inhibited by recombinant ScHal3, a known inhibitor of *S. cerevisiae* Ppz1 (see section 4) (Adam *et al.* 2012). The enzymatic properties of the full length CaPpz1 are similar to those of ScPpz1. It was well established that in *ppz1 S. cerevisiae* and *pzh1 S. pombe* mutant cells, the expression of *CaPPZ1* partially normalized the salt and caffeine phenotypes. Also, CaPpz1 showed the capacity to complement the *slt2* mutation in *S. cerevisiae*. Besides, deletion of *CaPPZ1* in *C. albicans* yielded cells sensitive to salts (Li^+ and K^+), caffeine and agents affecting cell wall biogenesis (calcofluor white and congo red), while they were tolerant to spermine and hygromycin B. Therefore, CaPpz1 plays an important role in cation homeostasis and cell wall integrity of *C. albicans* (Adam *et al.* 2012). In addition, CaPpz1 has been involved in the transition of *C. albicans* from the yeast to the hyphal form, associated with infectivity (Adam *et al.* 2012). This is also supported by the reduced rate of hyphal growth of the *CaPPZ1* mutant cells (Nagy *et al.* 2014). In agreement with these results, CaPpz1 has been found critical for *C. albicans* virulence (Noble *et al.* 2010; Adam *et al.* 2012).

Aspergillus fumigatus is a filamentous fungus that live in the soil and causes a wide variety of non-invasive and invasive diseases in mammalian hosts, termed aspergillosis (Dagenais and Keller 2009; Greenberger *et al.* 2014). The genome of *A. fumigatus* harbors the gene *PHZA* that encodes the catalytic subunit of protein phosphatase Z (PPZ), and the less harmful species *Aspergillus nidulans* encompasses a highly similar *PPZ* gene (*PPZA*) (Leiter *et al.* 2012). The structures of these homolog proteins (PpzA and PzhA) are highly

similar to each other. Both phosphatases are made by a C-terminal catalytic domain and a N-terminal domain which contains the conserved Arg/Ser rich segment and a myristylation site. The expression of *PPZA* and *PHZA* in *S. cerevisiae* or *S. pombe* partially complemented the changes in Na^+, K^+, and caffeine tolerance of the deletion mutants. Both *Aspergillus* phosphatase proteins also mimicked the effect of ScPpz1 overexpression on *slt2* MAP kinase deficient *S. cerevisiae* cells. However, it has been demonstrated in the *A. nidulans ppzA* mutant strain that PpzA is not necessary for the salt stress response and the cell wall integrity pathways (Leiter *et al.* 2012). On the other hand, it was found that inactivation of *ppzA* resulted in increased sensitivity to oxidizing agents like tert-butylhydroperoxide, menadione, and diamide. Such sensitivity was also observed in *S. cerevisiae ppz1* mutants, and PpzA and PhzA were able to rescue sensitivity to oxidants in *S. cerevisiae ppz1* cells (Leiter *et al.* 2012). Besides, due to the essential role of reactive oxygen species (ROS) in the killing of *A. fumigatus* following infection of the lung (Ben-Ami *et al.* 2010) and the cornea (Leal *et al.* 2012), the role of PzhA in the virulence of the opportunistic fungal pathogen was investigated. It was established that, in an experimental model of corneal infection in immunocompetent animals, the *phzA A. fumigatus* mutant showed attenuated virulence. In addition, PpzA was confirmed to be important for iron assimilation, secondary metabolite production and virulence (Manfiolli *et al.* 2017).

4. Regulations of Ppz1 by Hal3-like proteins in *S. cerevisiae*

In vertebrates, Ser/Thr protein phosphatase 1 (PP1) has nearly 200 validated interactors (Heroes *et al.* 2013), whereas for *S. cerevisiae* Ppz1 only two regulatory subunits, Hal3 and Vhs3, have been described.

In 1995, the *HAL3* gene was isolated independently by two research groups. Di Como and coworkers characterized *HAL3* (named *SIS2*) as a multicopy suppressor of the growth defect of a *sit4* mutant (Di Como *et al.* 1995). At the same time, Ferrando and coworkers revealed a phenotype of salt tolerance when the *HAL3* gene was overexpressed in wild type cells (Ferrando *et al.* 1995). It is established that *HAL3* is expressed constitutively and encodes a protein of 562 amino acids located in the cytoplasm (Ferrando *et al.* 1995). The protein Hal3 contains a characteristic C-terminal tail of around 80 amino acids which is very rich in acidic residues, especially in aspartic. Further studies demonstrated that *ENA1* expression was increased in cells overexpressing *HAL3,* which provided, at least in part, the basis for the observed tolerance to high concentrations of sodium and lithium (Ferrando *et*

al. 1995; de Nadal *et al.* 1998). Moreover, overexpression of *HAL3* increases the capacity for potassium influx via regulation of the Trk transporters, and in *slt2* mutant cells, the overexpression of *HAL3* induces cell lysis, which can be rescued by osmotic support. These phenotypes suggested that Hal3 could regulate Ppz1 in *S. cerevisiae* (de Nadal *et al.* 1998). The final evidence came from the demonstration that Hal3 interacts with and inhibits the catalytic C-terminal domain and the entire Ppz1 (de Nadal *et al.* 1998).

As mentioned above, the overexpression of *HAL3* improves growth of the *sit4* mutant, and this is due to the restoration of the normal expression of G_1 cyclins. (Di Como *et al.* 1995; Clotet *et al.* 1999; Simón *et al.* 2001). Additionally, the *sit4 hal3* double mutation is synthetically lethal, and the lethal phenotype could be suppressed by the deletion of *PPZ1* (Clotet *et al.* 1999). Besides, de Nadal and coworkers revealed that the phosphorylation of Tef5 (elongation factor 1Bα) increased in cells overexpressing Hal3 (de Nadal *et al.* 2001), in agreement with its proposed negative regulatory role on Ppz1. Thus, Hal3 have been

		PPZ1		***HAL3***	
Cellular Process	**Strain**	**Overexpression**	**Deletion**	**Overexpression**	**Deletion**
Saline Homeostasis	Wild Type	NA	Na^+/ Li^+ tolerance	Na^+/ Li^+ tolerance	Na^+/ Li^+ sensitivity
	ppz1	-	-	Na^+/ Li^+ tolerance	NP
	ppz1 ppz2	-	-	NP	NP
Cell Cycle Progression	Wild Type	No/slow Growth	NP	NP	NP
	sit4	Lethal	Improves Growth	Improves Growth	Lethal
Cell Integrity	Wild Type	NA	Caffeine sensitivity	NP	NP
	slt2	Improves Growth	Lethal	Lethal	Improves Growth

Table 4 Phenotypic comparison between the overexpression or deletion of Ppz1 and its negative regulate subunit Hal3.

The phenotypes are grouped according to the cell processes. NA: not analyzed; NP: no phenotype.

characterized as the negative regulator of Ppz1 in all-known cellular manifestations, as summarized in Table 4.

There is no significant similarity between Hal3 and the various regulatory subunits of PP1c. Also, Hal3 does not interact with Glc7 (de Nadal *et al.* 1998; García-Gimeno *et al.* 2003), although it contains a ^{263}KLHVLF^{268} sequence that resemble the RVxF motif present in most PP1c regulatory subunits (Bollen *et al.* 2010). Our laboratory previously showed that mutation of the ^{263}KLHVLF^{268} sequence did not affected the ability of Hal3 to inhibit and bind to Ppz1, indicating that the mechanism by which Hal3 and Ppz1 interact is different from those reported for PP1c regulatory subunits in mammals and yeasts (Muñoz *et al.* 2004). A random mutagenesis analysis revealed several important residues for Hal3 function on Ppz1 in a relatively small region spanning from amino acid 446 to 480. Whereas changes in Glu^{460} and Val^{462} did not alter Ppz1 binding capacity, they resulted in Hal3 versions unable to inhibit the phosphatase. Therefore, there are independent Hal3 structural elements required for Ppz1 binding and inhibition (Muñoz *et al.* 2004).

S. cerevisiae encodes a protein (Vhs3) structurally related to Hal3, which is another negative regulator of Ppz1 (Ruiz *et al.* 2004a). The *VHS3* gene was identified as a multicopy suppressor of the G_1/S cell cycle blockade of a conditional *sit4 hal3* mutant strain (Muñoz *et al.* 2003). Vhs3 is a 674-residues protein closely related to *S. cerevisiae* Hal3 (49% of identity) and maintains the typical acidic C-terminal tail (Ruiz *et al.* 2004a). It has been demonstrated that the overexpression or the deletion of *VHS3* results in several phenotypes that are reminiscent to those detected in cells that overexpress or lack *HAL3* (Ruiz *et al.* 2004a). The overexpression of *VHS3* is able to rescue the G_1/S cell cycle blockade of a *sit4* mutation and aggravates the lytic phenotype of the *slt2*/*mpk1* mutation; the overexpression of *VHS3* on a wild-type strain can improve salt tolerance and increase the expression level of *ENA1* although the effects are less noticeable than with *HAL3*. *In vitro,* Vhs3 binds to the full-length and the catalytic moiety of Ppz1 and inhibits the activity of the phosphatase almost as efficiently as Hal3 does. However, the mutation of *VHS3* did not increase salt tolerance. Therefore, Vhs3 is considered to be an inhibitory subunit of Ppz1 with lesser prominent biological role than Hal3. This lesser efficiency may be explained because *VHS3* mRNA levels are almost undetectable and clearly lower than those of *HAL3* (Ruiz *et al.* 2004a). Remarkably, the *vhs3 hal3* double mutation is synthetically lethal, and this phenotype could not be rescued even in the presence of the *ppz1*, *ppz2* or *ppz1 ppz2* mutations. This suggested that Vhs3 or/and Hal3 must have important, Ppz-independent functions (Ruiz *et al.* 2004a), as described below.

S. cerevisiae encode another structurally Hal3-related protein, called Cab3. Cab3 is characterized as an essential protein showing a 28% sequence identity to Hal3. Besides, Cab3 also contains a C-terminal acidic tail of similar size that of Hal3. However, it has been published that Cab3 is not able to inhibit the phosphatase activity of Ppz1 (Ruiz *et al.* 2009).

Even if Ppz phosphatases are fungal-specific, their inhibitor Hal3 is evolutionarily conserved. Homologs of Hal3 have been reported not only in other fungi but also in plants and animals, such as *Arabidopsis thaliana*, *Nicotiana tabacum*, rice, *Drosophila melanogaster*, mouse and human, indicating that Hal3 like proteins plays a key role in the physiology of the diverse kind of cells (Espinosa-Ruiz *et al.*, 1999; Daugherty *et al.*, 2002; Kupke, Hernández-Acosta and Culiáñez-Macià, 2003; Yonamine *et al.*, 2004; Takahashi *et al.*, 2006; Bosveld *et al.*, 2008).

In *A. thaliana* two genes encode similar homologs of ScHal3, which were named as AtHal3a and AtHal3b. AtHal3a is 52% identical with the central core of ScHal3 and further study confirmed that the overexpression of AtHal3a could slightly complement the salt sensitivity of *S. cerevisiae hal3* mutants (Espinosa-Ruiz *et al.* 1999). This phenotype indicated that there were conserved functions between AtHal3a and ScHal3. After resolution of the three-dimensional structure by X-ray, AtHal3a was demonstrated to be a

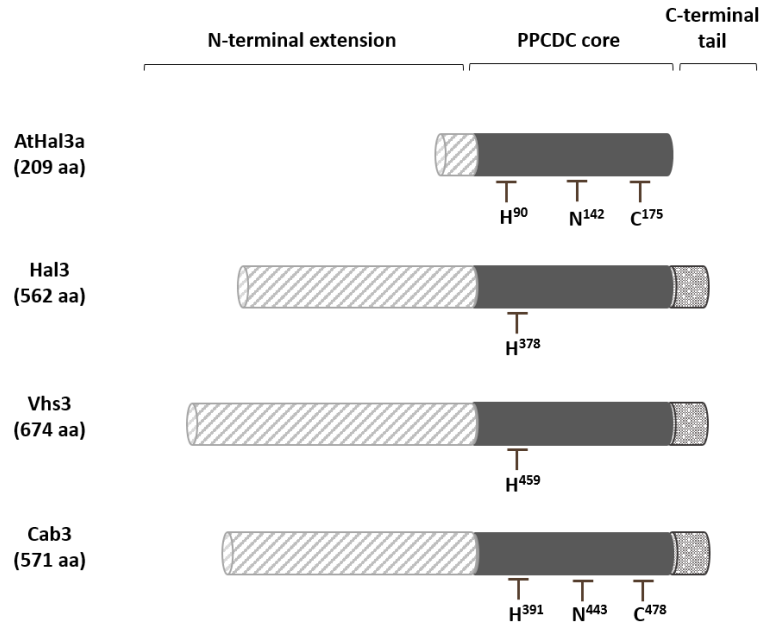

Figure 4 Structures of Hal3-like proteins from *S. cerevisiae* and *A. thaliana*

flavoprotein whose biological unit was a trimer (Albert *et al.* 2000). Shortly afterwards, Kupke and coworkers revealed that AtHal3 could catalyze *in vitro* the decarboxylation of phosphopantothenoylcysteine (PPC) to phosphopantetheine (PC), a reaction involved in coenzyme A biosynthesis (Kupke *et al.* 2001) (see section 5 and Figure 4). Besides, the essential catalytic active sites of AtHal3 were identified to be the residues His^{90}, Asn^{142} and Cys^{175}, which are provided by opposing monomers, so this enzyme has three identical active centers.

5. Moonlighting Hal3-like proteins form a heteromeric PPCDC in *S. cerevisiae*

Coenzyme A is characterized as a common cofactor of many enzymes and the flavoprotein phosphopantothenoylcysteine decarboxylase (PPCDC) is an essential component of its biosynthetic pathway. It has been established that the CoA biosynthetic pathway from pantothenate consist in five enzymatic reactions and the third one is performed by PPCDC (Begley *et al.* 2001; Ye *et al.* 2005). PPCDC catalyzes the decarboxylation of 4-phosphopantothenoylcysteine to form 4'-phosphopantotheine (PP) (Strauss *et al.* 2001; Hernández-Acosta *et al.* 2002). There are two steps in the PPCDC

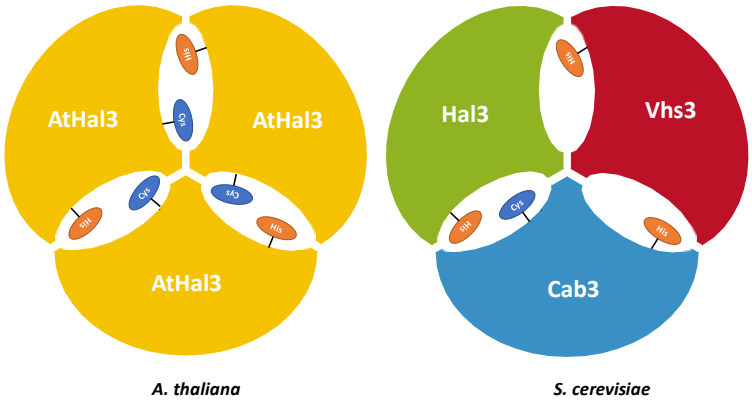

Figure 5.1 A model for functional *A. thaliana* and *S. cerevisiae* PPCDC

A cartoon of the homotrimeric *A. thaliana* PPCDC enzyme (AtHal3a), showing the conserved active sites histidine (His^{90}) and cysteine (Cys^{175}) residues. A cartoon of the proposed heterotrimeric structure of a potentially active *S. cerevisiae* PPCDC enzyme consisting of one protomer each of Hal3, Vhs3 and Cab3, with all three conserved histidine residues (His^{378} for Hal3, His^{459} for Vhs3, and His^{391} for Cab3) and the conserved cysteine residue (Cys^{478}) for Cab3 (Ruiz *et al.* 2009).

catalytic mechanism: in the first step, PPC is decarboxylated into a thioaldehyde generating an enediol intermediate, in which the histidine residue is essential; in the second step, in which the cysteine residue is essential, the enediol intermediate is reduced to PP and the FMN cofactor is reoxidized (Strauss *et al.* 2001).

It is now well established from a variety of studies that PPCDC is monogenic, encoded by a single gene in bacteria and eukaryotic organisms, such as *A. thaliana* and humans (Espinosa-Ruiz *et al.* 1999; Kupke 2001; Hernández-Acosta *et al.* 2002; Daugherty *et al.* 2002; Steinbacher *et al.* 2003). As shown in Figure 4, His, Cys and Asn are the essential residues in three identical protomers forming the enzymes. In budding yeast, PPCDC enzyme is a heterotrimer: one subunit of Cab3 is essential; the other two subunits are composed by Hal3, Vhs3, or one of each. In this heterotrimer, the catalytic Cys and Asn come from Cab3 (Cys^{478} and Asn^{443}) and the other catalytic residue His is provided by Hal3 or Vhs3 (His^{378} or His^{459}). Although Cab3 contains a potential catalytic His (His^{391}), this residue was reported to be non-functional (Ruiz *et al.* 2009). Thus, none of the three proteins individually are sufficient to construct the PPCDC enzyme. This structure explains well the lethal phenotype of cells lacking Hal3 and Vhs3 and the essential role played by Cab3.

In conclusion, Hal3 and Vh3 are able to perform two unrelated functions: they inhibit the Ppz1 phosphatase activity and contribute, with Cab3, to the PPCDC enzyme, which identify them as moonlighting proteins. A moonlighting protein is defined as a single protein that has multiple unrelated roles that are not due to gene fusions, multiple RNA splice variants or multiple proteolytic fragments (Jeffery 2003, 2009; Tompa *et al.* 2005). Moonlighting proteins have been reported in various species from prokaryotes to animals (Huberts and van der Klei 2010). In yeast several moonlighting proteins have been identified (Gancedo and Flores 2008; Huberts and van der Klei 2010; Gancedo *et al.* 2016), and it is believed that their presence is advantageous to the cells or organisms, allowing the expansion of functions without broadening the genome (Jeffery 1999, 2009).

A coarse functional mapping of Hal3 has been carried out (Abrie *et al.* 2012). As shown in Figure 5.2, the conserved central domain (PD), which shares structural similarity with PPCDC enzymes from other organisms, plays a key role in the PPCDC activity. In contrast, neither the N-terminal extension nor the acidic C-terminal tail appear necessary in PPCDC function. However, the stability of the interactions between Hal3 and Cab3 is influenced by the N-terminal extension. Besides, the Hal3 PD domain alone did not show the inhibitory capacity to the Ppz1 phosphatase activity although it is essential in Ppz1

binding and regulation. The acidic C-terminal tail of Hal3 is required for the Ppz1 phosphatase inhibition, indicating the potential existence of an interaction with Ppz1. In addition, a previous study showed that mutation of several amino acids at the PD domain affected the capacity to bind or inhibit Ppz1 without interference with the PPCDC activity (Muñoz *et al.* 2004). In conclusion, the Hal3 structural determinants required for Ppz1 regulation and PPCDC function are independent.

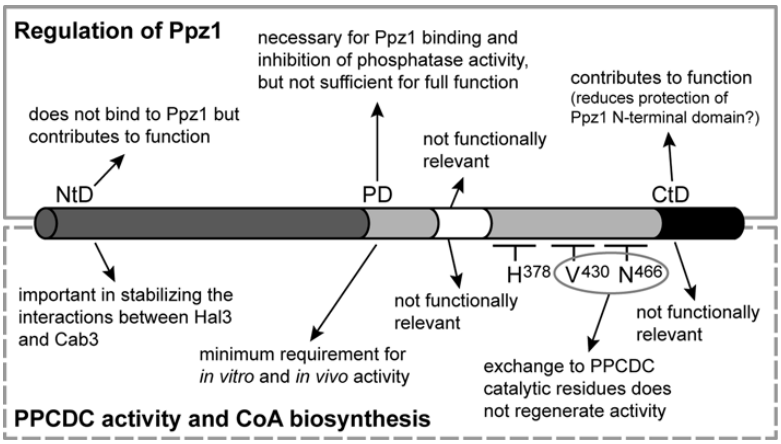

Figure 5.2 Schematic depiction of the functional domains of Hal3.

The upper panel refers to Hal3's Ppz1 phosphatase regulatory activity, whereas the lower panel refers to the role of the protein as a constituent part of the functional yeast PPCDC heterotrimer (Abrie *et al.* 2012).

6. Hal3-like proteins in diverse fungi

Unlike the homologs of Ppz enzymes in diverse fungi, the structures of the Hal3-like proteins are much more diverse. Extensive research has shown that PPCDC monomers are short proteins in plants and animals, similar to the AtHal3 polypeptide (see Figure 4 and Figure 6). As mentioned above, a long N-terminal extension and an acidic C-terminal tail flank the PPCDC core of Hal3 in *S. cerevisiae*. Moreover, all these elements has been revealed to be necessary for Ppz1 binding and inhibition (Abrie *et al.* 2012).

Recent work by our laboratory has established that the *S. pombe* ORF *SPAC15E1.04* (renamed as *SpHal3*) was identified as functional PPCDC (Molero *et al.* 2013). SpHal3 contains a Hal3-like N-terminal half and a C-terminal half related to thymidylate synthase (TS). Therefore, SpHal3 is likely the product of a gene fusion event. *In vitro*, SpHal3 and its N-terminal domain show the ability to bind to *S. cerevisiae* Ppz1 and the *S. pombe* homolog

Pzh1, as well as the capacity to inhibit the phosphatase activities of ScPpz1 C-terminal half and Pzh1. Besides, SpHal3 partially mimics *in vivo S. cerevisiae* Hal3 functions mediated by Ppz1, and both the entire SpHal3 and its N-terminal domain exhibit PPCDC function *in vitro* and *in vivo*, suggesting that SpHal3 is a monogenic PPCDC in fission yeast. In addition, the entire SpHal3 and its C-terminal domain have been found to have TS function in *S. cerevisiae*. Therefore, the *SpHAL3* gene is an essential gene that joins three different functional activities (Molero *et al.* 2013).

In the pathogenic fungus *C. albicans* two genes, *orf19.7378* and *orf19.3260,* were identified based on their similarity to *S. cerevisiae* ScHal3/ScVhs3 and ScCab3. These two genes were renamed as *CaHal3* and *CaCab3* (Petrényi *et al.* 2016) and encode proteins similar in size to *S. cerevisiae* Hal3 or Cab3 and retain their characteristic structural features as PPCDCs components (see Figure 6), including the typical active His in CaHal3 as well as the conserved Cys in CaCab3. *In vitro*, it was demonstrated that both CaHal3 and CaCab3 exhibited the capacity to bind and inhibit the entire CaPpz1 (which contains a shorter N-terminal domain than ScPpz1) as well as its C-terminal catalytic domain. However, when expressed in *S. cerevisiae*, only CaCab3 showed the ability to mimic the phenotypes related to ScHal3. In contrast, both CaCab3 and CaHal3 were established to maintain the PPCDC

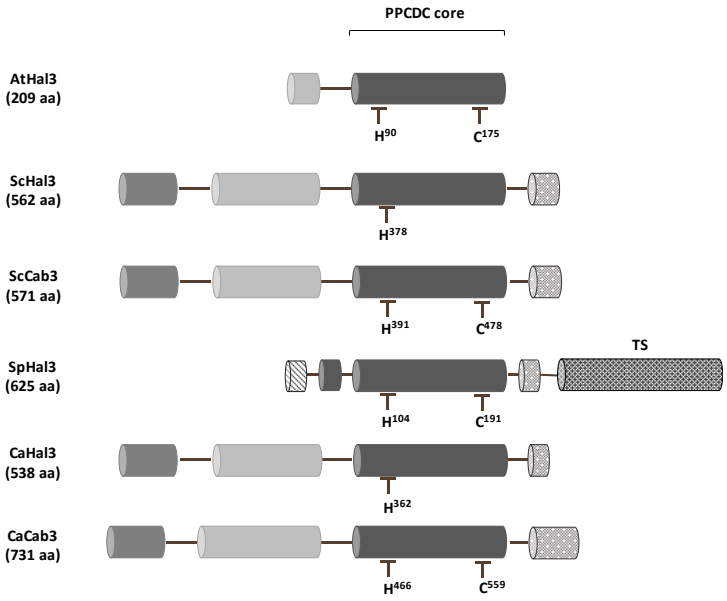

Figure 6 Structures of Hal3-proteins from diverse fungi

TS indicates thymidylate synthase domain.

functions. Since only CaCab3 was characterized as phosphatase regulator *in vivo*, it seems that CaCab3 (but not CaHal3) has the potential to act as a moonlighting protein in *C. albicans* (Petrényi *et al.* 2016).

7. Ppz1 enzymes are postulated as potential novel targets for antifungal therapy

Although fungi have made positive contributions to ecosystems, agroecosystems and human beings for centuries, they also generate devastating impacts as pathogens of plants and animals (Fones *et al.* 2017). In the past two decades, there is an unprecedented

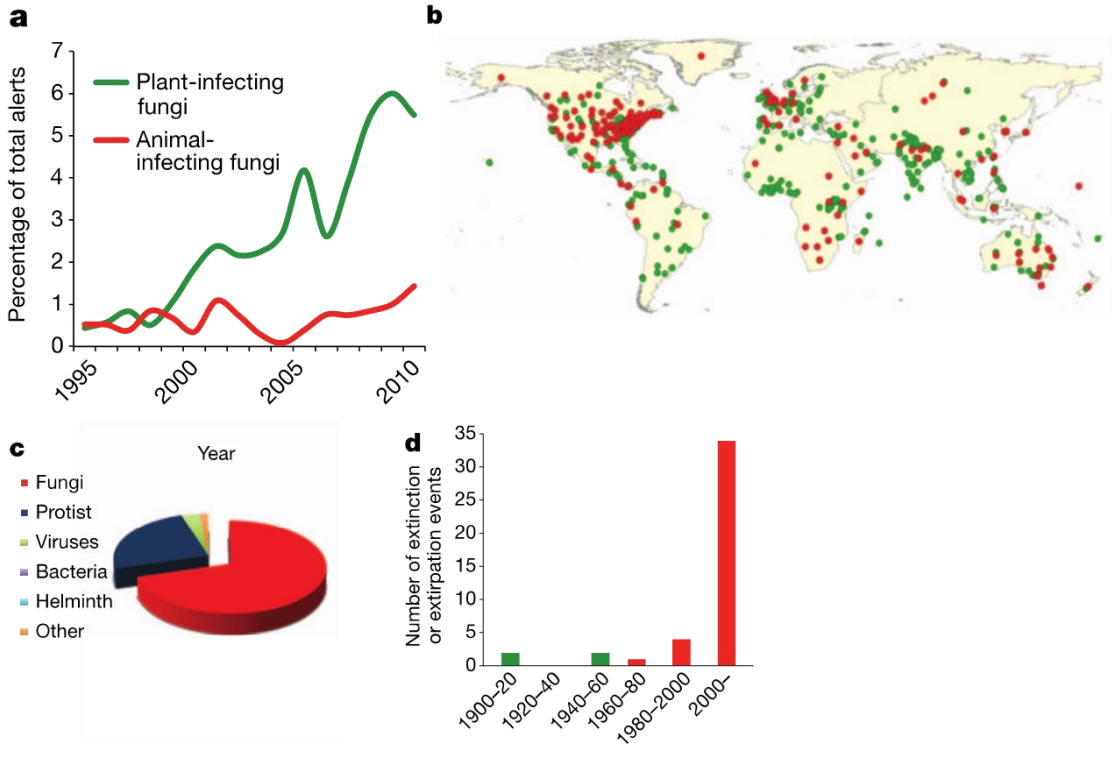

Figure 7 Worldwide reporting trends in fungal emerging infectious diseases (EIDs)

a, Disease alerts in the ProMED database for pathogenic fungi of animals and plants; **b**, the spatial location of the associated reports; **C**, Relative proportions of species extinction and/or extirpation events for major classes of infectious disease agents; **d**, the temporal trends for fungal pathogens (Fisher *et al.* 2012).

number of fungal and fungal-like diseases worldwide mainly owing to the human activities by modifying natural environments. The analyses based on the data from ProMED (the Program for Monitoring Emerging Diseases; http://www.promedmail.org) and HealthMap (http://healthmap.org) show increasing trends for fungal infections (see Figure 7)(Fisher *et al.* 2012).

Invasive fungal infections to human beings have been apparently rare over most of the history (Robert and Casadevall 2009). However, due to associations between fungal infections and the impaired immune function, it has been witnessed in recent decades a stark rise in fungal infections owing to medical interventions such as chemotherapy for cancer and immunosuppression such as HIV infection (Pfaller and Diekema 2010). For example, nearly one million cases of HIV-associated cryptococcal meningitis have been estimated per year, causing up to a third of all AIDS-related deaths (Simwami *et al.* 2011). In addition, fungi have been characterized among the dominant causal agents of plant diseases (Doehlemann *et al.* 2017). Thus, losses due to fungal infection in rice (rice blast caused by *Magnaporthe oryzae*), wheat (rust caused by *Puccinia graminis*), maize (smut caused by *Ustilago maydis*), and soybean (rust caused by *Phakospora pachyrizi*) vary regionally but pose a current and growing threat to food security (Pennisi 2010). It has been calculated that, if mitigated, the losses resulting from even low-level persistent crop disease would be sufficient to feed 8.5% of the 7 billion humans alive in 2011 (Fisher *et al.* 2012). Thus, it is important and necessary the development of antifungal therapies.

As mentioned above, Ppz1 has been characterized to be related to virulence in *C. albicans* and *A. fumigatus*. Besides, the regulatory mechanism appears to differ from that of the related type-1 protein phosphatase (an ubiquitous enzyme) (Chen *et al.* 2016; Molero *et al.* 2017). In addition, the three-dimensional structure revealed several novel elements present in the catalytic domain of CaPpz1. Further research has demonstrated that these structural differences create novel binding surfaces, suggesting that these unique structural elements are suitable for the development of CaPpz1-specific inhibitors (Chen *et al.* 2016). Therefore, given that their presence is restricted to fungi, Ppz1 enzymes are potential novel targets for antifungal therapy. In this study, the Ppz/Hal3 phosphatase systems from the human pathogenic fungus *Cryptococcus neoformans* and the plant pathogenic fungus *Ustilago maydis* have been characterized.

8. The human pathogenic fungus *Cryptococcus neoformans*

In the late 19th century, *Cryptococcus neoformans* was first identified as a human pathogen, but only until the late 1970s it was finally recognized as a common cause of human disease (Rocco 1992; Knoke and Schwesinger 1994). With one million new infections per year, it has been established that cryptococcal meningitis is an infection of global importance. *C. neoformans* significantly contributes to the morbidity and mortality especially among AIDS-related patients (Park *et al.* 2009). In the mid-1980s, the incidence of disease increased notably, with HIV/AIDS accounting for more than 80% of cryptococcosis cases worldwide (Hajjeh *et al.* 1999; Perfect and Casadevall 2002; Kwon-Chung *et al.* 2014). Furthermore, extensive research has shown an unacceptably high prevalence of morbidity and mortality associated with cryptococcal meningitis specifically in sub-Saharan Africa and parts of Asia. In fact, in the first decade of the 21st century, this mortality peaked at around 600,000 deaths per year; even today, approximately several hundred thousand cryptococcal meningitis-related deaths per year have been reported (Park *et al.* 2009).

In the environment *C. neoformans* is ubiquitous and is commonly isolated from avian excreta, soil and trees, where it can interact with wild animals (mammals, birds and reptiles) or microbial predators (nematodes and amoebae), maintaining its virulence (Idnurm *et al.* 2005). It has previously been observed that the infection by exposure to *Cryptococcus* early in life through inhalation of spores or desiccated yeast cells is asymptomatic (Sukroongreung *et al.* 1998). Then the cryptococcal infection is either cleared or develops to be dormant. However, in immunocompromised individuals such as AIDS-related patients, *C. neoformans* cells have the capacity to spread from the lungs to the central nervous system finally causing meningoencephalitis (Liu *et al.* 2002). *C. neoformans* has three well established virulence factors: a capsule, melanin and the ability to grow at human body temperature (Idnurm *et al.* 2005). In *C. neoformans* virulence, the capsule plays a vital role (Srikanta *et al.* 2014). It has been established that the capsule protects the fungus from the host immune system acting as a "shield" (O'Meara and Alspaugh 2012). Additionally, capsule enlargement occurs in a specific phase of the cell cycle, particularly the G_1 phase, and in response to environmental changes (García-Rodas *et al.* 2014). The cell cycle of *C. neoformans* isolated from patients and the environment is the same as of budding yeast. However, this organism is also able to dimorphic switch to a filamentous growth form by two distinct pathways: mating and monokaryotic fruiting. Filamentation enables nutrient

scavenging beyond the confines of the colony and the production of spores, which are thought to be infectious particles (Idnurm *et al.* 2005).

The limitation of molecular tools and the challenges presented by the cell wall, an extensive capsule, and a propensity for non-homologous recombination, hampered the early studies of *C. neoformans* (Heitman *et al.* 1999). Owing to the rapid development of biotechnology tools and the accomplishment of the *C. neoformans* 19-Mbp genome sequencing (Loftus *et al.* 2005; D'Souza *et al.* 2011; Janbon *et al.* 2014), these obstacles have been largely overcome. *C. neoformans* belongs to the most intron-rich fungal species and these introns have been showed to be important for regulation of gene expression (Csuros *et al.* 2011; Goebels *et al.* 2013). For example, genome-wide analysis revealed that a typical average *C. neoformans* gene contains 5.7 introns (Janbon *et al.* 2014). The study of *C. neoformans* genome has provide insights into the genetic basis of processes such as stress responses, mating efficiency and virulence. Nowadays, *C. neoformans* is being used as a model organism contributing to the knowledge on basic physiology and fungal pathogenesis (Srikanta *et al.* 2014).

9. The plant pathogenic fungus *Ustilago maydis*

Up to now, the fungus *Ustilago maydis* represents one of the limited number of eukaryotic plant pathogen model systems in which the pathogen effectors can be studied considering both the pathogen and its respective host plant (Dean *et al.* 2012; Giraldo and Valent 2013; Stotz *et al.* 2014; Rovenich *et al.* 2014; Lanver *et al.* 2017). *U. maydis* belongs to the smut fungi which is a large group of biotrophic parasites infecting mostly *Poaceae* such as maize, wheat, barley and sugar cane (Agrios 2005; Lanver *et al.* 2017). Instead of killing their hosts, biotrophic pathogens tend to keep their hosts alive and enable metabolic reprogramming to support the infection process. *U. maydis* is able to cause disease symptoms in all the green parts of infected maize plants, while the disease symptoms induced by the other smut fungi are restricted to the reproductive organs of the plants. The infection of *U. maydis* remains locally confined and has been characterized by the induction of anthocyanin biosynthesis and the formation of large tumors where spores develop (Lanver *et al.* 2017). Under field conditions, yield losses due to *U. maydis* are generally mild (*circa* 2 %) (Silva-Rojas *et al.* 2017). However, the commercial value is significant, owing to the especially high productions which could reach to 313 and 192 million tons in the USA and China (FAOSTAT 2013; Silva-Rojas *et al.* 2017). Thus, maize smut is a worldwide disease

causing an enormous economic impact on corn sector (Djamei and Kahmann 2012). Nowadays *U. maydis* has been considered as one of the top ten fungal pathogens in plant pathology (Dean *et al.* 2012).

When the diploid spores are exposed in appropriate conditions, it is the opportunity for the spores to germinate and form a promycelium where the four haploid nuclei migrate. Then, the compartments containing one haploid nucleus are produced by septation. After mitosis, haploid cells sprout from the promycelium and then the vegetative life cycle begin. On the leaf surface, haploid cells of different mating types meet and fuse. Next a filamentous cell cycle-arrested dikaryon is formed, which is the pathogenic form (García-Muse *et al.* 2003). When cells enter the early infective stage, the cell cycle arrest is released, hyphae star to branch and clamp-like structures shape up to guarantee the two nuclei are segregated correctly in the growing dikaryotic hyphae (Scherer *et al.* 2006). During these intracellular stages, hyphae are completely encased by the host plasma membrane (Brefort *et al.* 2009). Thus, the host pathogen interaction zone has been established in endomembrane structures (Bauer *et al.* 1997). During the plant tumor formation, fungal hyphae are mainly detected intercellularly (Doehlemann *et al.* 2008). Furthermore, the two nuclei of the dikaryon fuse forming huge aggregates in apoplastic cavities (Doehlemann *et al.* 2008; Tollot *et al.* 2016). Aggregated hyphae become embedded in a gelatinous polysaccharide matrix (Snetselaar and Mims 1994). Finally, hyphal fragment and dark colored ornamented spores develop (Banuett and Herskowitz 1996).

The sequencing of the 25 Mbp *U. maydis* genome was accomplished and predicted to contain 6902 protein-encoding genes. However, expected pathogenicity signatures, such as plant cell wall degrading enzymes, were not identified (Kämper *et al.* 2006). Genome analysis detected unexpected clusters of genes encoding small secreted proteins with unknown functions. However, expression analysis has showed that most of these proteins are regulated together and induced in infected tissue (Kämper *et al.* 2006). Furthermore, the average number of introns per gene in *U. maydis* genome is 0.46, with 70% of genes lacking introns. Apparently, the *U. maydis* genome has been shaped by massive, lineage-specific intron loss, as it has been observed in the ascomycetous yeasts *S. cerevisiae* and *S. pombe* (Roy and Gilbert 2006; Kämper *et al.* 2006).

Due to its unique infective features, and the rich molecular toolbox including reverse genetics, cell biology, comparative genomics and completed genome sequencing, *U. maydis* is of value as a model system for the study of biotrophic fungal pathogens (Lanver *et al.* 2017).

Objectives

The objectives of this work have been:

1.- To generate the relevant tools and to initiate the study of the molecular basis for the toxicity of high levels of the protein phosphatase Ppz1

2.- To characterize structurally and functionally the Ppz/Hal3 system in the human pathogenic fungus *Cryptococcus neoformans*.

3.- To characterize structurally and functionally the Ppz/Hal3 system in the plant pathogenic fungus *Ustilago maydis*.

Experimental Procedures

1. Strains and media

S. cerevisiae cells were grown at 28 °C unless otherwise stated in YPD medium (10 g/L yeast extract, 20 g/L peptone and 20 g/L dextrose). When carrying plasmids, the cells were grown in synthetic medium lacking the appropriate selection requirements for the plasmids (Adams *et al.* 1997). For the sporulation of *S. cerevisiae* diploid strains, the sporulation medium (10 g/L potassium acetate, 1 g/L yeast extract and 0.5 g/L glucose) was used. Tetrad analysis followed the procedure used in (Ruiz *et al.* 2009; Petrényi *et al.* 2016).

Escherichia coli DH5α (plasmids host), BL21(DE3) RIL (GST-fused recombinant proteins expression host) and GM2163 (a dam^- *E. coli* strain) were grown at 37 °C unless otherwise stated in LB (Lysogeny Broth) medium with antibiotics corresponding to the plasmid-conferred resistance (100 μg/ml ampicillin or 34.5 μg/ml chloramphenicol). *E. coli* strain BW369, carrying the *dfp*-707^{ts} mutation, is defective in PPCDC function in a temperature-sensitive way, so cells cannot grow at 37°C (Spitzer and Weiss 1985; Spitzer *et al.* 1988). Therefore, BW369 was grown in LB at 30°C unless otherwise stated.

All yeast strains used in this work are listed in Supplementary Table 1.

2. Recombinant DNA techniques

Recombinant DNA techniques and transformations of *S. cerevisiae* and *E. coli* followed the standard procedures (Adams *et al.* 1997; Sambrook *et al.* 2012). In particular, when the *slt2* mutant strain was transformed with high-copy number plasmids bearing Hal3, 1 M sorbitol was added to the selection medium to avoid cell lysis.

2.1 Constructions of *S. cerevisiae* strains

To elucidate the basis for Ppz1 toxicity, a yeast strain overexpressing *PPZ1* controlled by the *GAL1-10* promoter was constructed. The DNA fragment containing the *GAL1-10* promoter, the kanMX6 marker, and 5'-end sequences (40 nucleotides) of the target *PPZ1* gene was amplified using oligonucleotides PPZ1-F4 and PPZ1-R2 and the template plasmid pFA6a-KanMx6-pGAL1 (Longtine *et al.* 1998). The amplified DNA fragment was introduced into strain BY4741 and the homologous recombinants carrying the marker module were

identified by resistance to G418 (Jimenez and Davies 1980; Hadfield *et al.* 1990) and subsequently were confirmed by PCR using oligonucleotides E1_kpnI and K3. This galactose-induced Ppz1 overexpressing strain was name as ZCZ01. The *NHA1* deletion was introduced in the BY4741 and ZCZ01 background as follows. The cassette *NHA1::LEU2* from the plasmid pCRII-NHA::LEU2 (a gift from Prof. Alonso Rodríguez-Navarro) was linearized by SacI and XbaI digestion and used to transform competent cells. The clones able to grow in the absence of leucine were tested for the disruption by PCR using oligonucleotides NHA1 anl disr 3' and leu2-3´. The resulting strains were named as *nha1* and ZCZ06, respectively.

2.2 Constructions of plasmids used in this study

For overexpression of the PPZ1^{R451L} version, which lacks catalytic function, pYES2-PPZ1^{R451L} was constructed by replacing the KspAI and SacI fragment in pYES2-PPZ1 by the equivalent fragment from YCp-PPZ1^{R451L} (Clotet *et al.* 1996).

The attempts to amplify the entire CnPpz1 ORF directly from the *C. neoformans* cDNA library (a generous gift from Dr. Oscar Zaragoza) were unsuccessful, likely because of the very high G/C rich (82%) region expanding more than 150 nt at the 5' region of the ORF. This problem was overcome by creation of two modules (see Figure 2.3). The high G/C rich part was generated by PCR from genomic DNA using oligonucleotides PPZ1-RI-L (P1) and FUS-RV (P3). The other part was made by PCR using oligonucleotides FUS-FW (P2) and Cryp_PPZ1_XhoI_L_1 (P4) from the cDNA library. Then, a fusion PCR amplification using Takara PrimeSTAR HS DNA Polymerase (this source of DNA polymerase was essential) and oligonucleotides PPZ1-RI-L and Cryp_PPZ1_XhoI_L_1 was carried out to merge both modules and generate the CnPpz1 ORF fragment.

This DNA fragment was digested with EcoRI and XhoI and then inserted into the plasmid pGEX-6P-1 (GE Healthcare) linearized at the same sites to yield pGEX-CnPpz1. This plasmid allows expression in *E. coli* of CnPpz1 with a GST tag at the N-terminus. To express the predicted catalytic region of CnPpz1 in *E. coli*, the relevant region from residue 346 to the last codon was amplified using oligonucleotides CnPPZ1_5'_cat_EcoRI and Cryp_PPZ1_XhoI_L_1 from the cDNA library and cloned into pGEX-6P-1 as for pGEX-CnPpz1 to yield vector pGEX-CnPpz1-Cter.

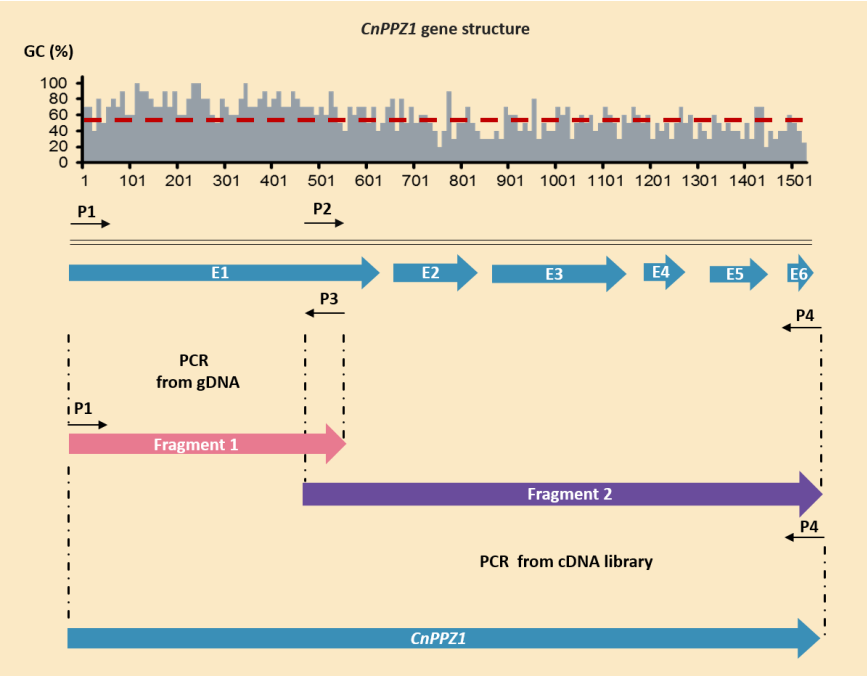

Figure 2.3 Modules for amplification of CnPpz1 cDNA for expression in *E. coli* and in *S. cerevisiae*.

The grey histogram shows that exon 1 region is highly GC-rich (discontinuous line represents the average level of GC% in *C. neoformans*). Generation of CnPpz1 cDNA was accomplished by a combination of PCR from cDNA library (a part of exon1 and exons 2-6) and genomic PCR (most of exon 1) followed by fusion PCR using Takara PrimeSTAR HS DNA Polymerase. The small arrows represent the primers mentioned above.

For the purpose of expression in *S. cerevisiae*, CnPpz1 was cloned into several vectors. Expression controlled from the native *PPZ1* promoter was gained using high-copy (YEplac181) and low-copy (YCplac111) vectors. YEp-CnPpz1 was constructed as follows. Plasmid YEplac181-ScPPZ1 (Clotet *et al.* 1996) was transferred into the strain GM2163 (a *dam*$^{-}$ *E. coli* strain), and the plasmid was then recovered and gapped by XbaI and SphI digestion. Meanwhile the fusion PCR CnPpz1 fragment described above was amplified using primers Cryp_PPZ1prom_XbaI and Cryp_PPZ1prom_SphI, digested with the same restriction enzymes, and cloned into the gapped plasmid. Once the sequence of CnPpz1 was confirmed to be correct, XbaI and SphI were used to release the ORF and introduce it into the YCplac111 vector to yield YCp-CnPpz1. Overexpression controlled by the *GAL1-10* promoter was accomplished in a similar way. The oligonucleotides CnPPZ1-RI-L-ATG and Cryp_PPZ1prom_SphI were used to amplify the CnPpz1 ORF, then the fragment was inserted into the vector pYES2 at restriction sites EcoRI and SphI to generate pYES-CnPpz1.

The CnHal3a and CnHal3b ORFs were directly amplified from the cDNA library by using oligonucleotide pairs Cn00909_EcoRI / Cn00909_SalI and Cn07348_EcoRI / Cn07348_SalI, respectively. To express CnHal3a and CnHal3b with an N-terminal 3x-HA tag from the strong *ADH1* promoter in *S. cerevisiae*, the high-copy number vector pWS93 (Song and Carlson 1998) was linearized by EcoRI and SalI digestion, and then the CnHal3a and CnHal3b ORFs were cloned at these same sites to yield pWS-CnHal3a and pWS-CnHal3b. To express CnHal3a and CnHal3b as GST-fusion proteins, the same DNA fragments were cloned into the vector pGEX-6P-1 at the EcoRI and SalI sites to generate pGEX-CnHal3a and pGEX-CnHal3b.

To exchange the sequence ^{204}QGAGRLAC^{211} present in the catalytic loop of CnHal3b by the sequence ^{458}SEKVMDIN^{466} of ScHal3, the following steps were taken. Firstly, the sequence containing the upstream region (from nt +4 to +609) of the catalytic loop was amplified using oligonucleotides Cn_07348_EcoRI and 3_insert_Sc_Cn07348 from the plasmid pGEX-CnHal3b. Meanwhile the sequence containing the downstream fragment (from nt +632 to +993) was amplified using oligonucleotides Cn07348_SalI and 5_insert_Sc_Cn07348. Then a fusion PCR was performed using oligonucleotides Cn_07348_EcoRI and Cn07348_SalI to amplify the merged fragment. Finally, the plasmids carrying CnHal3b with the ScHal3 loop (pWS-Cn0Hal3b_ScL and pGEX-CnHal3b_ScL) were made by inserting the EcoRI-SalI-digested amplification product into pWS93 and pGEX-6P-1 at EcoRI and SalI sites

To replace the C-terminal tail of CnHal3b by the acidic tail of ScHal3, the fragment containing the upstream sequence (from nt +4 to +690) of CnHal3b was amplified using oligonucleotides Cn_07348_EcoRI and Cn07348_ScCtD_RV from the templates pGEX-CnHal3b or pGEX-CnHal3b_ScL; the fragment containing the *S. cerevisiae* C-terminal tail was amplified using oligonucleotides Cn07348ScCtD_FW and Reverse HAL3-XhoI from the template pWS-ScHal3 (Ruiz *et al.* 2009). The merged fragment was achieved by fusion PCR with oligonucleotides Cn_07348_EcoRI and Reverse HAL3-XhoI, digested with EcoRI and XhoI, and then inserted into the EcoRI/SalI-digested vectors pWS93 and pGEX-6P-1, to generate plasmids pWS-CnHal3b_ScL_Cter and pGEX- CnHal3b_ScL_Cter.

For expression in *S. cerevisiae*, UmPpz1 was cloned into different vectors. To clone into YCplac111 and YEplac181, plasmid YCp-CaPpz1 (Adam *et al.* 2012) was introduced into GM2163 *E. coli* cells, recovered, and digested with XbaI and HindIII to remove the CaPpz1 ORF (leaving the Sc*PPZ1* promoter). Meanwhile, the UmPpz1 ORF was amplified with oligonucleotides UmPpz1_XbaI and UmPpz1_HindIII from *U. maydis* genomic DNA (a generous gift from Dr. José Pérez-Martín). The fragment was then digested with XbaI and

HindIII and cloned into the digested YCp-CaPpz1 vector. After the inserted fragment was confirmed by sequencing, the UmPpz1 ORF was released and introduced into EcoRI /HindIII-digested YEp-CaPpz1 to yield YEp-UmPpz1. To obtain plasmid YCp-UmPpz1-HA the oligonucleotides UmPpz1_XbaI and UmPpz1_HA_HindIII were used to amplify the ORF (plus a C-terminal HA tag encoded in the oligonucleotides) from YCp-UmPpz1 and then the fragment was inserted between the restriction sites XbaI and HindIII of YCp-CaPpz1 vector to replace the CaPpz1 ORF.

For overexpression from the *GAL1-10* promoter with an HA tag at the C-terminus, the UmPpz1 ORF was amplified with oligonucleotides UmPpz1_ATG_BamHI and UmPpz1_HA_EcoRI using YCp-UmPpz1-HA as the template, digested with BamHI and EcoRI and inserted into the pYES2 vector at the same restriction sites. To overexpress ScPpz1 with a C-terminal HA tag under the control of the *GAL1-10* promoter, the ScPpz1-HA ORF was amplified with oligonucleotides ScPpz1-HA-NotI and ScPpz1_in_PacI from pCM190-PPZ1-HA (our laboratory, unpublished data) and then inserted into the pYES2 vector at the restriction sites NotI and PacI to yield pYES-ScPpz1-HA

For overexpression of *Saccharomyces* and *Ustilago* phosphatase proteins in *S. cerevisiae* under the control of the *ADH1* promoter, the ScPpz1 ORF was amplified with primers OMLM3 and ScPpz1_SalI Rv from pCM190-PPZ1-HA and then inserted into the pWS93 vector using BamHI and SalI sites, to yield pWS-ScPpz1. The UmPpz1 ORF was amplified with oligonucleotides UmPpz1_BamHI and UmPpz1_SalI from YEp-UmPpz1 and was inserted into the same restriction sites as in pWS-ScPpz1.

To overexpress *Ustilago* Ha3-like proteins in *S. cerevisiae* from the *ADH1* promoter with an N-terminal 3x-HA tag, the UmHal3 ORF was amplified with oligonucleotides UmHal3_EcoRI and UmHal3_BamHI from genomic DNA and then inserted into the pWS93 vector after EcoRI and BamHI digestion to generate pWS-UmHal3. The C-terminal region (UmHal3_PD, corresponding to the putative PPCDC domain) was amplified with oligonucleotides UmHal3_PD_EcoRI and UmHal3_BamHI, and subsequently inserted into pWS93 as it was done for UmHal3 ORF, to yield pWS-UmHal3_PD. The pWS-UmPD_ScCter version was obtained from plasmid pGEX-UmHal3_ScCter (described in the next paragraph) by digestion with EcoRI and XhoI, and then cloned into plasmid pWS93 linearized by EcoRI and SalI.

For expression in *E. coli*, the UmPpz1 ORF was amplified with oligonucleotides UmPpz1_BamHI and UmPpz1_EcoRI from genomic DNA. Then, the fragment was digested with BamHI and EcoRI and inserted into the pGEX-6P-1 vector at the same restriction sites.

The UmHal3 and UmHal3_PD ORFs were amplified with oligonucleotides UmHal3_EcoRI or UmHal3_PD_EcoRI, respectively, and UmHal3_NotI, and were then inserted into pGEX-6P-1 at restriction sites EcoRI and NotI. The acidic tail of ScHal3 was added to UmHal3_PD by amplifying the upstream region from UmHal3_PD with oligonucleotides UmHal3_EcoRI and UmHal3_ScCtD_RV, using pWS-UmHal3 as template, and the downstream C-terminal tail with oligonucleotides UmHal3_ScCtD_FW and Reverse HAL3-XhoI, using pWS-ScHal3 as template. The merged fragment was obtained by amplification with oligonucleotides UmHal3_EcoRI and Reverse HAL3-XhoI and was inserted into pGEX-6P-1 upon digestion with EcoRI and XhoI to yield pGEX-UmPD_ScCter.

The vectors described above, together with other plasmids used in this work, are listed in Supplementary Table 2.

3. Phenotypic analysis of yeast cells

3.1 Characterization by microscopy and flow cytometry

Cells expressing *PPZ1* from the powerful *GAL1-10* promoter, which is switched off when in glucose and switched on when in galactose, were gown in YPD medium overnight. Then cultures were diluted to OD_{600} of 0.2 and transferred to medium containing raffinose (a nearly neutral carbon source). When OD_{600} reached around 0.6, galactose was added to the appropriate concentration. Samples were taken at the appropriate times and processed for microscopic observation (E800 Microscope, Nikon) and flow cytometry (FACSCalibur, Becton Dickinson).

For microscopic observation, one ml of each culture was collected by centrifugation at 3000 xg for 5 minutes and resuspended in 1 ml of PBS containing formaldehyde (Merck) at a final concentration of 2%. After 5 minutes at room temperature, cells were washed with PBS and resuspended in fifty µl of PBS. Finally, three µl of each sample was placed on a slide for microscopic observation.

For flow cytometry analysis, cultures were made 2% galactose. Immediately, one ml of culture was taken and centrifuged at 1800 xg for 2 minutes. Then, the supernatant was removed, and the pellet was resuspended with 1 ml of 70% ethanol (AR grade). These samples were stored at 4°C. Cells taken at different time-points were treated in the same way. When all samples were collected, cells were washed twice with one ml of 50 mM Tris-

HCl (pH 7.8) buffer and resuspended in the same buffer with RNAse A (200 µg/ml). After incubation for 2 hours at 37°C, cells were spun down and resuspended with 0.5 ml of pepsin solution (5 mg/ml pepsin dissolved in 50 mM HCl) and then incubated for additional 30 minutes at 37°C. Next, cells were washed with 1 ml of FACS buffer (200 mM Tris-HCl pH 7.5, 211 mM NaCl, 78 mM $MgCl_2$) and resuspended with 0.5 ml of FACS buffer containing 55 µl of propidium iodide (0.5 mg/ml). Fifty µl of each sample was transferred to FACS tubes containing 1 ml of 50 mM Tris-HCl (pH7.8) buffer and then sonicated at 10% amplitude for 10 seconds using a Digital Sonifier (Branson). Finally, the samples were analyzed in a FACSCalibur (Becton Dickinson) and the FlowJo X10 software

3.2 Liquid growth assays

Growth of cells overexpressing Ppz1 upon galactose induction was evaluated in 96-well plates. Wild type BY4741 and ZCZ01 strains were grown in YPD medium overnight, and then transferred to YP raffinose containing 0.5%, 1% and 2% galactose at initial OD_{600} of 0.004. Cells containing pYES2-based vectors were grown overnight in synthetic medium (lacking uracil) using glucose as carbon source, then transferred to medium with raffinose as carbon source, with and without 2% galactose, at an initial OD_{600} of 0.008. After 24 hours of growth at 28°C, the OD_{600} of the plates was measured by a Multiskan Ascent plate reader (Thermo Electron Corporation).

3.3 Dot assays

To evaluate the sensitivity of *S. cerevisiae* cells to LiCl, NaCl, KCl, spermine and caffeine, starting cultures at OD_{600} of 0.05 were spotted after serial dilutions on SD medium lacking uracil (for pWS93-based, YEplac195-based and pRS699-based vectors) or leucine (for YCplac111-and YEplac181-based vectors). Cultures of cells for overexpression of Ppz1 from the *GAL1-10* promoter were spotted in a similar way on YP medium (ZCZ01 background) or SD medium lacking uracil (pYES2-based vectors) and containing 2% galactose as carbon source. After 2 to 4 days of incubation at 28°C, the growth was monitored.

4. Phenotypic analysis of *E. coli* cells

To evaluate the PPCDC functions of Hal3-like proteins from *C. neoformans* and *U.*

maydis, the empty pGEX-6P-1 plasmid and the same vectors bearing the plant AtHal3, ScHal3, CnHal3a, CnHal3b, the CnHal3b variants, UmHal3 and the UmHal3 variants were introduced into the *E. coli* strain BW369 (*dfp*-707^{ts}) carrying a mutation that eliminates PPCDC activity at 37°C. At first, transformants were grown in LB medium with 100 µg/ml ampicillin at 30°C overnight. Next, the overnight cultures were diluted till OD_{600} of 0.05 and transferred to 30°C or 37°C (permissive and non-permissive temperatures respectively) for 6 hours. Then, the cultures were plated at the indicated temperatures. In some cases, IPTG (0.2 mM) was added to cells (both liquid cultures for 6 h and plates) prior incubation at 37°C as indicated. After overnight incubation, the growth of plates was monitored.

5. Spore analysis

For sporulation, diploid cells containing pWS93-based vectors carrying ScHal3, ScCab3, CnHal3 and UmHal3 proteins were incubated in SD medium lacking uracil at 28°C. Then, cells were centrifuged at 3000 xg for 5 minutes, washed twice with H_2O and transferred to sporulation medium. After 5-7 days of incubation, the percentage of asci in the cultures was investigated by optical microscopy (cultures with >60% of tetrads were considered suitable for further analysis). Tetrad analysis was performed as the standard protocol (Sherman and Hicks 1991). Firstly, 15 µl of sporulated cultures was collected and washed with H_2O. Then cells were resuspended in 250 µl H_2O and 12 µl Zymolyase (10 U/ml, MP biomedicals) was added. After 10 minutes at room temperature, around 20 µl of the culture was spread as a line on a fresh YPD-agar plate. The MSM300 Yeast Dissection Microscopy (Singer Instruments) was used to dissect asci on the same plate. Then, plates were incubated at 28°C for 3 days. The genotype of each spore was finally detected by replicating haploid clones to appropriate selective plates.

6. RNA purification and transcriptomic analysis by RNA-seq

For the analysis of the transcriptional response to Ppz1 overexpression induced by galactose, wild type BY4741 and ZCZ01 strains were grown on YPD medium, and then cells were transferred to medium with raffinose as carbon source at starting OD_{600} of 0.2. When the OD_{600} of the cultures reached around 0.6, galactose was added to a final concentration of 2%. Samples (10 ml) were taken after half hour, 2 hours and 4 hours by quick filtration through GN-6 Metricel filters (Pall Corp.) and immediately frozen. Total RNA was extracted by the Ribo Pure™-Yeast kit (Ambion) following the manufacturer's instructions. The

quantity was assessed by electrophoresis in denaturing 0.8% agarose gels (Lonza) and quantified by measuring the A_{260} in a Nanodrop ND-1000 Spectrophotometer.

Libraries were prepared with the QuantSeq 3' mRNA kit (Lexogen, Greenland, NH, USA) using 0.5 µg of total RNA purified as above. Sequencing was performed in an Illumina MiSeq machine with Reagent Kit v3 (single end, 75 nt/read). Three replicates were sequenced, obtaining a total number of 3.7–8.3 million reads per condition. Mapping of fastq files to generate SAM files was carried out with the Bowtie2 software in local / sensitive mode (97.2–98.6% mapped reads). The SAM files were analyzed with the SeqMonk software (www.bioinformatics.bbsrc.ac.uk/projects/seqmonk). Mapped reads were counted using CDS probes (extended 100 nt downstream the open reading frame because the library is biased towards the 3' -end of mRNAs) and corrected for the largest dataset. Raw data was subjected to diverse filters to remove sequences with too low number of reads.

7. Protein immunodetection

7.1 Protein extraction

To evaluate Ppz1 expression level at different induction strengths, BY4741 (WT) and ZCZ01 cells were grown first in YPD medium overnight. Then, these cultures were diluted to OD_{600} of 0.2 and transferred to medium containing raffinose as carbon source. Samples (10 ml) were taken after growing 20 hours with galactose at final concentrations ranging from 0.01% to 2%. Cells were collected by centrifugation for 5 min at 3000 xg and 4°C and immediately frozen at -80°C for further use. Samples were then resuspended in 100 µl of lysis buffer (50 mM Tris-HCl (pH 7.5), 150 mM NaCl, 0.1% Triton X-100, 1 mM DTT, 10% glycerol and Complete™ protease inhibitor mixture (Roche Applied Science)). One hundred µl of acid-washed glass beads (Sigma) was added to break the cells using a Fast Prep cell breaker (Bio 101) at setting 5.5 for 45 s, three times in total. After centrifugation at 500 xg for 10 minutes at 4°C, the clear supernatant was recovered, and the protein concentration was quantified by a Bradford assay. Finally, 25 µg of protein were loaded in 10% SDS-PAGE for protein immunodetection. When both ScPpz1 and UmPpz1 were overexpressed with a C-terminal HA tag from pYES2-based vectors, samples were collected and extracted in the same way except that 80 µg of proteins were loaded.

For the evaluation of the expression levels of Hal3-like proteins, yeast cells carrying the pWS93-based vectors bearing the relevant proteins were inoculated at an initial OD_{600} of 0.2 and collected after 6 hours of growth. The method for proteins extraction was the same as above and 40 µg samples were loaded for protein immunodetection (due to the high molecular weight of UmHal3, 6% SDS-PAGE was used in this case).

To investigate the interactions of Hal3 proteins with phosphatase proteins, *S. cerevisiae* strain IM21 (*ppz1Δ hal3Δ*) was transformed with pWS93-based plasmids containing ScHal3 and different CnHal3 and UmHal3 versions. Yeast protein extracts were prepared as described (Abrie *et al.* 2012), except that cells were collected when the OD_{600} of the culture was around 1.0 and Fast Prep cell breaker was set 45 s for each shaking cycle.

To characterize CnHal3 proteins in the *E. coli* strain BW369 (*dfp*-707^{ts}), the strain was transformed with pGEX-6p-1 based plasmids containing AtHal3, ScHal3, CnHal3a, CnHal3b and the CnHal3b variants. Transformants were grown at 30°C first, then diluted till OD_{600} of 0.05 and transferred to 30 or 37°C for 6 hours. When indicated, IPTG 0.2 mM was added at this point to cultures incubated at 37°C. Finally, samples (10 ml) were collected and protein extracts prepared as in (Abrie *et al.* 2012). Due to the largely dissimilar levels of expression of the relevant proteins, different amounts of whole extracts were loaded in the gel. In all cases, 12 µg of AtHal3 extracts and 60 µg of ScHal3 and CnHal3a extracts were used; for the samples incubated at 30°C, 20 µg of extracts of CnHal3b and the CnHal3b variants; only 6 µg of extracts of CnHal3b and CnHal3b_ScL from incubations at 37°C with IPTG, and 60 µg of extracts of the other CnHal3b samples from incubation at 37°C were loaded.

7.2 Immunoblot analysis

After electrophoresis, protein extracts were transferred to Immobilon-P membranes (Millipore), the membranes were blocked by 5% defatted milk and then incubated with primary antibodies corresponding to the proteins or protein tags. To evaluate the expression level of Ppz1, anti-Ppz1 antibody (1:250 dilution) was used (Posas *et al.* 1992). To assess the expression levels of proteins with HA tag and 3x-HA tag, anti-HA antibodies (1:1000 dilution) from two companies were used (Abrie *et al.*, 2012). The anti-HA antibodies from Roche (catalog number 11 666 606 001) were used for all studies of CnHal3 proteins, while the studies related to UmHal3 and UmPpz1 proteins employed antibodies from Covance (catalog MMS-101P). The level of expression of Hal3 proteins in the *E. coli* strain BW369 were confirmed by using anti-GST antibodies (Santa Cruz Biotechnology) at 1:1000 dilution.

When anti-Ppz1 and anti-GST antibodies were employed as primary antibody, anti-rabbit peroxidase antibodies (1:10000 dilution, GE Healthcare) worked as secondary antibody. When anti-HA antibodies were used, anti-mouse peroxidase antibodies (1:10000 dilution, GE Healthcare) were employed. The immunocomplexes were visualized by ECL western blotting detection kit (GE Healthcare). Chemiluminescence was detected with a Versadoc Image System 4000 MP (Bio-Rad).

8 Expression and purification of GST-fused recombinant proteins

All GST-fused recombinant proteins were expressed in *E. coli* BL21(DE3) RIL and purified as previously reported (Abrie *et al.* 2012), except that induction was accomplished with 0.1 mM IPTG at 20°C overnight. To detect the phosphatase activity, the expression media for the phosphatase proteins contained 0.5 mM $MnCl_2$ and the lysis buffer was made also 2 mM $MnCl_2$. When it was necessary to remove the GST tag, the PreScission protease (GE Healthcare) was used as described in (Abrie *et al.* 2012). In all cases, to calculate the concentrations of the proteins, samples were run on the 10% SDS-PAGE with Coomassie Blue-staining, images were taken, and scanned in an Epson Perfection V500 Photo scanner. The concentration of the protein of interest was estimated in comparison with BSA standards in the same gel by means of the Gel Analyze 2010a software.

9. Pull-down experiments

To assess the interactions between the phosphatase proteins and various Hal3 versions from *S. cerevisiae, C. neoformans* and *U. maydis*, the binding assays were performed as previously described (Abrie *et al.* 2012). For evaluating the interactions between proteins from *S. cerevisiae* and *C. neoformans*, aliquots of 50 µl of the glutathione agarose beads containing 4 µg of bound GST-ScPpz1, GST-ScPpz1-Cter, GST-CnPpz1 and GST-CnPpz1-Cter were incubated with around 600 µg of protein extracts prepared from strain IM021 (*ppz1Δ hal3Δ*) expressing the different 3xHA-tagged Hal3 versions. For evaluating the interactions between *S. cerevisiae* and *U. maydis* proteins, aliquots of glutathione agarose beads containing 4 µg of the GST-tagged UmPpz1 or 8 µg of ScPpz1 and ScPpz1-Cter were incubated with protein extracts (0.6-1.0 mg of proteins). The amount of protein extracts used was determined after detection and quantification by immunoblot of the expression

levels of the relevant proteins. The beads were finally resuspended in 100 µl of 2xSDS sample buffer and, after boiling for 5 min, 25 to 50 µl of the samples were analyzed by SDS-PAGE (10%, except 6% in the case of UmHal3) and immunodetection. Samples were transferred to Immobilon-P membranes (Millipore), and processed for immunoblotting as described in section 7.

10. *In vitro* enzyme assays

The phosphatase activities of *S. cerevisiae*, *C. neoformans* and *U. maydis* Ppz1 and the inhibitory capacity of the diverse Hal3-like proteins were determined as previously described (Abrie *et al.* 2012).

Increasing amounts of the inhibitors were incubated with the corresponding amount of phosphatase for 5 min at 30°C in reaction buffer (50 mM Tris-HCl (pH 7.5), 2 mM $MnCl_2$ and 1 mM DTT). In the study of *C. neoformans*, 6 pmol/assay of ScPpz1 and Ppz1-Cter, and 7.5 to 15 pmol/assay of CnPpz1 were used, whereas in the study of *U. maydis*, 10 pmol/assay of UmPpz1 and 5 to 10 pmol/assay of ScPpz1 and Ppz1-Cter were employed. The reaction was started by the addition of the substrate (10 mM *p*-nitrophenylphosphate, Sigma) and the activity was measured at 405 nm and 30°C in a Multiskan Ascent plate reader (Thermo Electron Corporation). When the optical densities of the reactions were around one, the data was recorded and analyzed. The final reaction time depends on the phosphatase activities of the enzymes.

Results

1. Deciphering the molecular basis of Ppz1 toxicity in *S. cerevisiae*

1.1 Construction of the galactose-induced Ppz1 strain ZCZ01

Although the blockage in cell proliferation caused by Ppz1 overexpression seems to be related to alteration in the cell cycle, the specific basis for this effect is unknown. Due to the multifunctional role of Hal3 and Vhs3 in CoA synthesis (Ruiz *et al.* 2009), there are at least two main explanation for the toxicity of Ppz1 overexpression:

-It could be caused by an excessive increase in Ppz1 catalytic activity;

-It could be caused by the excess of Ppz1 protein, which would titrate down available Hal3 and/or Vhs3, thus avoiding the formation of the essential PPCDC decarboxylase (the "titration" hypothesis).

To distinguish between these two possibilities, we constructed a galactose-induced Ppz1 strain ZCZ01 (see Figure 1.1.1 and experimental procedures 2.1).

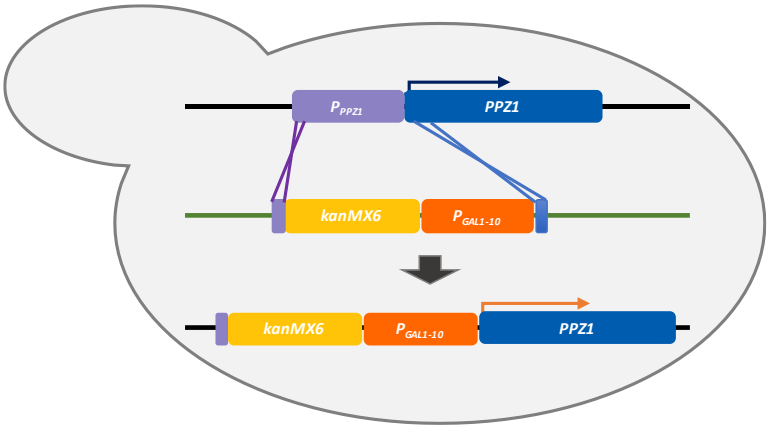

Figure 1.1.1 Modules for construction of strain ZCZ01.

Purple boxes: the *PPZ1* promoter; blue boxes: *PPZ1* ORF in the genome; yellow boxes: selectable markers including the *kanMX6* module (Wach *et al.*, 1994); orange boxes: the *GAL1-10* promoter. Arrows upon the boxes indicate the direction of transcription. The black lines indicate genome localization; the green line indicates that the modules were amplified from plasmid pFA6a-kanMX6-pGAL1 (Longtine *et al.* 1998).

Once the galactose-induced promoter *GAL1-10* was confirmed to be inserted at the right location into the genome, the expression level of Ppz1 in strain ZCZ01 grown on raffinose was initially evaluated at both 0.5% and 2% galactose. After 2.5, 4, 6, 9 and 24 hours of galactose induction, the expression levels of Ppz1 were detected by immunoblot. The protein immunodetection revealed that the expression levels of Ppz1 were similar in both galactose concentrations after 2.5 hours induction (Figure 1.1.2A). The expression profile was investigated at shorter times using 0.5%, 1% and 2% galactose. The immunoblot analysis showed that the Ppz1 expression levels were alike in all conditions used (Figure 1.1.2B), even at the shortest induction time. Taken together, these results indicate that in strain ZCZ01 the expressing level of Ppz1 quickly increases upon addition of galactose (within half hour) and the accumulation of Ppz1 is maintained at least for 24 hours upon induction. Because the lowest galactose concentration used did provide full response, even lower concentrations ranging from 0.01% to 0.5% were used to induce Ppz1 and the expression levels were investigated after 20 hours induction. As observed in Figure 1.1.2C expression of Pppz1 can be detected even at 0.01% galactose, and expression levels increased in parallel with the concentration of the inductor.

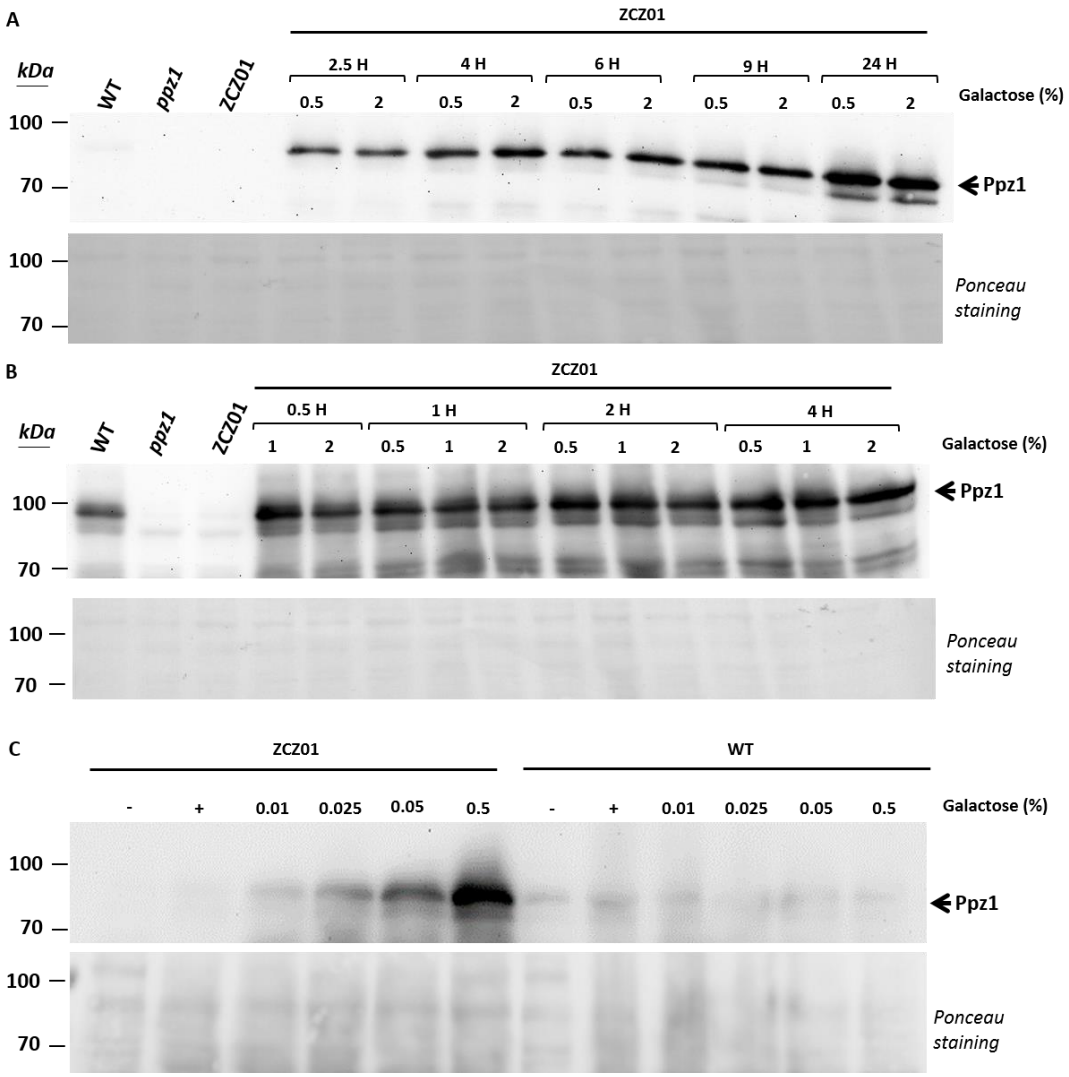

Figure 1.1.2 Evaluation of expression levels of Ppz1 in strain ZCZ01 in various conditions

Panel A, Time-course of the overexpression of Ppz1 in raffinose-grown strain ZCZ01, using low concentration (0.5%) and high concentration (2%) of galactose. Panel B, Overexpression of Ppz1 in strain ZCZ01, using different concentrations of galactose (0.5%, 1% and 2%) after 30 min and 1, 2 and 4 hours. Panel C, Overexpression of Ppz1 using galactose concentrations from 0.01% to 0.5% after 20 hours induction. The symbol "-" indicates that the samples were taken before adding galactose and the symbol "+" indicates the samples that were taken immediately after adding galactose. All the samples contained 25 µg of protein. The Ppz1 protein was detected with anti Ppz1-antibodies (indicated by arrowheads). Ponceau staining of the membranes is shown.

1.2 Phenotypic characterization of the strain ZCZ01

To evaluate the effect on growth of the accumulation of Ppz1, the OD_{600} of cultures of cells overexpressing Ppz1 after 24 hours of galactose induction were recorded. Growth of the strains overexpressing *PPZ1* is largely blocked even at 0.5% galactose and becomes virtually null at higher galactose concentrations. (Figure 1.2.1A). Next, the budding index of the cultures was determined after 4 h of Ppz1 induction. It is apparent from Figure 1.2.1B that the percentages of cells containing either small or large buds decreased significantly in the ZCZ01 strain after galactose induction, while the percentage of unbudded cells increased up to 88%, suggesting that the accumulation of Ppz1 plays animportant and detrimental role in cell growth progression.

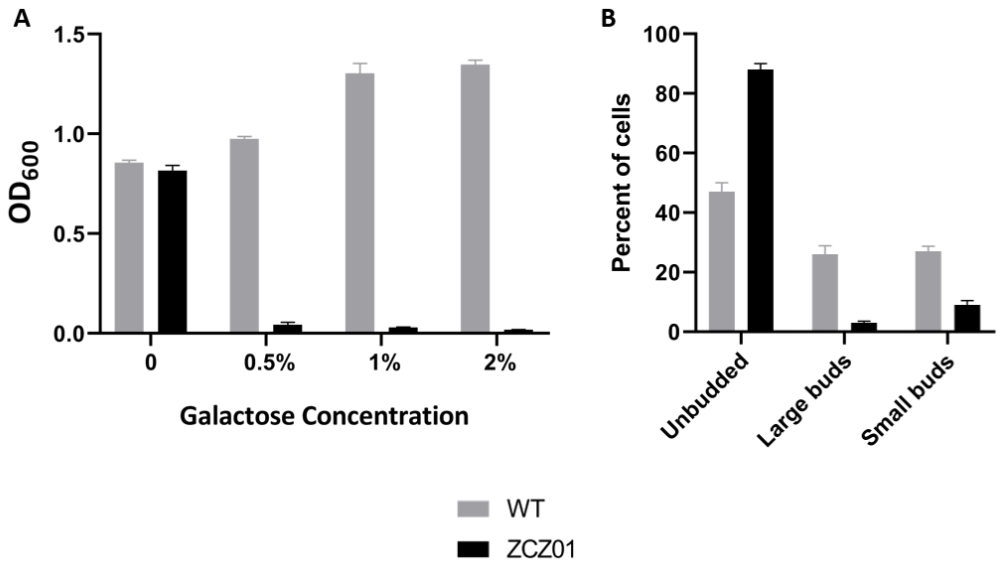

Figure 1.2.1 Phenotypic effects of the overexpression of Ppz1 in strain ZCZ01.

Panel A, Ppz1 was induced in strain ZCZ01 by using 0.5%, 1% and 2% of galactose. Cultures were started at OD_{600} = 0.04 and after 24 hours of galactose induction, the OD_{600} of each sample were recorded and the mean calculated. The error bars (SEM) stem from three independent experiments and each experiment contains three repeats. Panel B, the cultures of wild type BY4741 and ZCZ01 strains were grown from OD_{600} = 0.2 using raffinose as carbon source. When OD_{600} of both cultures was around 0.6, a final concentration of 2% galactose was used to overexpress Ppz1. After 4 hours of induction, samples were collected, and the budding index determined under the microscope. Cells were allocated to three possible groups: unbudded, small buds, and large buds. The numbers of counted cells ranged from 129 to 359 per experiment and the SEM were calculated from three independent experiments.

Cells overexpressing *PPZ1* were collected after 1, 2, 3 and 4 hours of 2% galactose induction and then the state of cell cycle of these cells was analyzed by propidium iodine staining and flow cytometry. As shown in Figure 1.2.2, *PPZ1* overexpression decreased the amounts of cells in G_2/M phase, with accumulation of cells with 1 DNA content, likely arrested in G_1. Taken together, these results suggest that overexpression of Ppz1 in strain ZCZ01 reproduces the previously characterized toxic effects identified upon overexpression of Ppz1 from the pYES2 (2-micron, *GAL1* promoter) plasmid vector (Clotet *et al.* 1996), with impact on cell cycle progression. Therefore, this strain is a useful tool to decipher the molecular basis of Ppz1 toxicity.

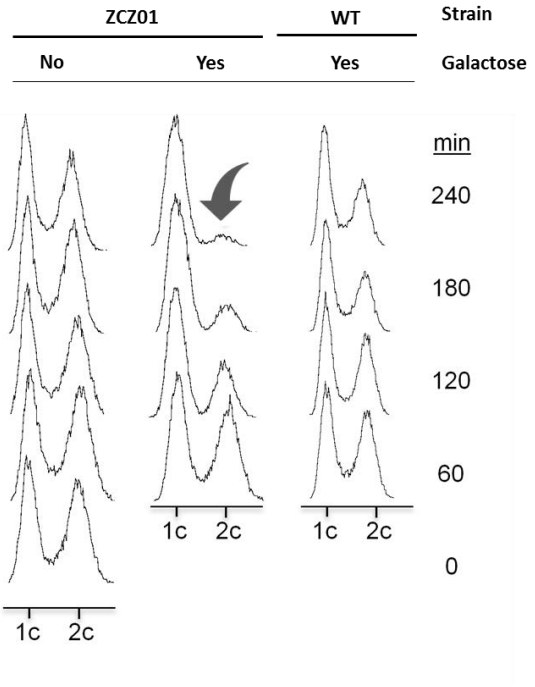

Figure 1.2.2 Effects of overexpression *PPZ1* on cell cycle progression.

PPZ1 was overexpressed in asynchronous cultures and cell cycle distribution was monitored by flow cytometry upon propidium iodine staining of DNA at different times upon addition of 2% galactose.

1.3 The catalytic activity of Ppz1 is essential to toxicity

1.3.1 A catalytically impaired version of Ppz1 is not toxic when overexpressed

To evaluate the requirement for Ppz1 activity in the toxic phenotype due to overexpression of the phosphatase, the inactive version $Ppz1^{R451L}$ was cloned in the high-copy plasmids pYES2 and introduced into the wild type BY4741 strain and the *ppz1* derivative. This inactive version was shown to have almost null phosphatase activity and to be unable to restore the wild type phenotype either under salt or caffeine stress, even when expressed from a high copy number plasmid in a *ppz1* mutant (Clotet *et al.* 1996). After 24 hours of induction with 2% galactose, a clear growth defect was observed in cells overexpressing native *PPZ1*, whereas the growth defect was largely relieved in cells overexpressing the inactive version (Figure 1.3.1A). The same effect was observed when cells well cultured on agar plates (figure 1.3.1B). These results indicate that the catalytic activity is essential to Ppz1 toxicity.

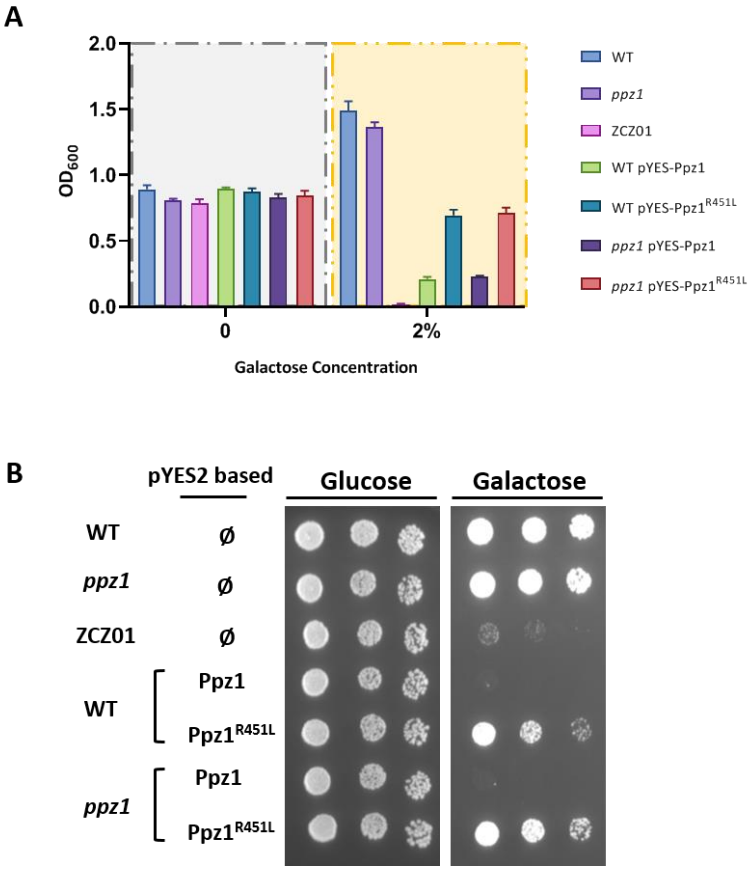

Figure 1.3.1 Growth effects of the overexpression of a WT and a catalytically inactive version of Ppz1.

Panel A, Ppz1 was overexpressed in strain ZCZ01 by using 2% of galactose as positive reference for toxicity. The catalytically inactive version of Ppz1 ($Ppz1^{R451L}$) was expressed from the high-copy *GAL1-10* promoter (plasmid pYES2) in BY4741 (wild type) and *ppz1* mutant cells. Cells harboring pYES2 plasmids grew in synthetic medium lacking uracil and raffinose was used as carbon source in all cases. Cultures were grown from OD_{600} = 0.08 and after 24 hours galactose induction, optical densities were recorded. The error bars (SEM) stem from the three independent experiments, and each experiment contains three technical repeats. The grey background indicates data from cultures without galactose and the yellow background indicates data from cultures with galactose. Panel B, both active and inactive versions of Ppz1 were expressed from plasmid pYES2 in wild type and *ppz1* strains. Empty plasmids were used as controls. Cultures were spotted at OD_{600} = 0.05 and at 1/5 dilutions in synthetic medium lacking uracil and using glucose or galactose as carbon source. Growth was recorded after 4 days.

1.3.2 Human PPCDC does not counteract Ppz1 toxicity

In order to test the "titration" hypothesis, the two reported negative regulators of Ppz1, Hal3 and Vhs3, as well as the human PPCDC (HsHal3), were overexpressed in galactose-induced ZCZ01 cells. Hal3 and Vhs3 have been characterized as moonlighting proteins form a heteromeric PPCDC with Cab3 in yeast CoA biosynthesis (Ruiz *et al.* 2009).

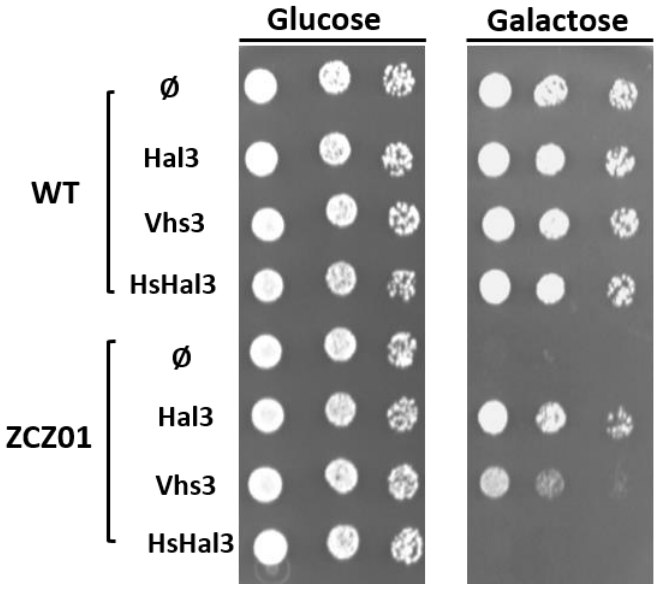

Figure 1.3.2 Phenotypic effects of the expression of the native regulators and the human PPCDC on Ppz1 toxicity.

The negative regulators of Ppz1, Hal3 and Vhs3, and the human PPCDC protein, HsHal3, were introduced as high-copy plasmids in wild type and ZCZ01 strains. Cultures were spotted at OD_{600} = 0.05 and at 1/5 dilutions on synthetic medium lacking uracil and using glucose or galactose as carbon source. Growth was recorded after 2 days.

As shown in Figure 1.3.2, overexpression of Hal3 fully rescued the toxic effect of the overproduction of Ppz1. Overexpression of Vhs3 also allowed growth of the ZCZ01 strain, although the effect was less prominent than that of Hal3 (Muñoz *et al.* 2004). In contrast, human PPCDC was completely ineffective in counteracting Ppz1 toxicity. These results support the notion that the toxicity due to overexpression of Ppz1 is not due to down-titration of necessary *S. cerevisiae* PPCDC subunits.

1.3.3 Functional evaluation of different versions of Hal3 on Ppz1 toxicity.

A previous study revealed that a Hal3^{Y313D} version has a relatively weak loss of both Ppz1 inhibitory and binding abilities; Hal3^{V390G} and Hal3^{W452G} show substantially decreased binding while partially retain the capability to inhibit the Ppz1 phosphatase activity; Hal3^{E460G} and Hal3^{V462A} maintain in part the ability to bind to Ppz1, but they inhibit the phosphatase very poorly (Muñoz *et al.* 2004). Therefore, these Hal3 versions represent a useful tool to test the correlation between Ppz1 inhibitory capacity and the ability to counteract the toxic effects of Ppz1 overexpression. As observed in Figure 1.3.2B, Hal3^{Y313D} rescued growth of the ZCZ01 strain similarly to native Hal3, whereas Hal3^{W452G} and Hal3^{E460G} where completely ineffective. Hal3^{V390G} and Hal3^{V462A} exhibited intermediate phenotypes. Therefore, the ability of Hal3 in suppressing the toxic effects of Ppz1 overexpression is markedly related to its ability to bind to and inhibit the phosphatase. Taking together, these results demonstrate that the toxicity of higher-than-normal levels for Ppz1 is not due to

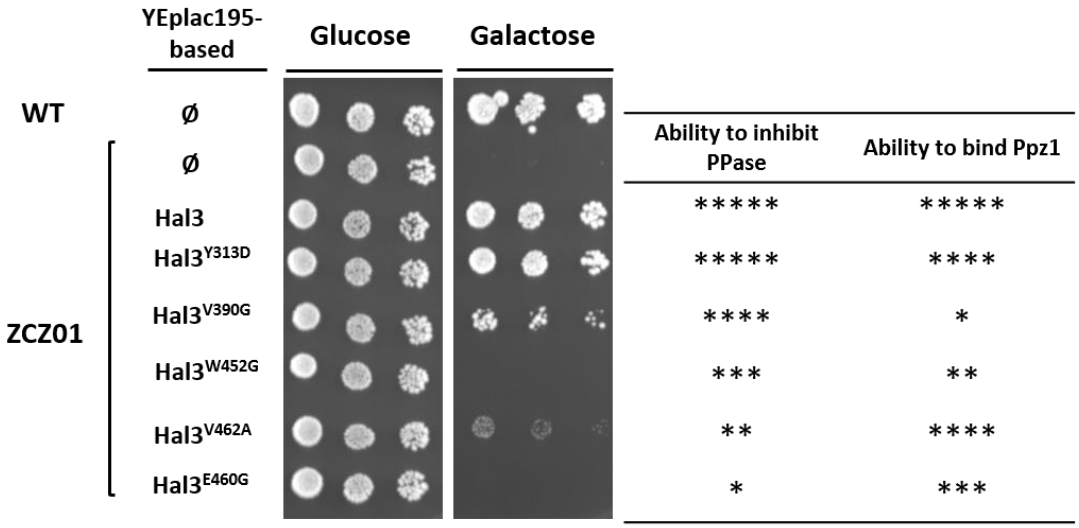

Figure 1.3.3 Phenotypic effects of the expression of different mutated versions of Hal3 on Ppz1 toxicity.

The indicated versions of Hal3 were introduced as high-copy (YEp) plasmids in strain ZCZ01. Cultures were spotted at OD_{600} = 0.05 and at 1/5 dilutions on synthetic medium lacking uracil and using glucose or galactose as carbon source. Growth was recorded after 4 days. The relative abilities of the different Hal3 versions to bind to and inhibit Ppz1 are indicated (5*, WT; *, virtually lost) (Muñoz *et al.* 2004).

interferences with PPCDC activity and CoA biosynthesis, but to an excessive cellular phosphatase activity.

1.4 Addition of exogenous K^+ does not rescue the slow-growth phenotype of strain ZCZ01

Since it is known that Ppz1 inhibits entry of potassium by regulating Trk1/Trk2 high affinity transporters (Ariño *et al.* 2010), it was plausible that the deleterious effect of Ppz1 overexpression could be due to strong blockage of potassium influx. It was revealed that *trk1 trk2* mutant strain grew as wild type cells on media supplemented with potassium (Bertl *et al.* 2003; Navarrete *et al.* 2010). Therefore, we tested if a surplus of potassium could counteract the toxicity due to Ppz1 overexpression. In parallel, the *NHA1* gene encoding the K^+,Na^+/H^+ antiporter was mutated in wild type and ZCZ01 in order to help keeping the intracellular concentration of potassium (Ariño *et al.* 2010). As shown in Figure 1.4, the growth of the *trk1 trk2* mutant strain on media supplemented with 200 mM KCl was as that of the wild type. However, only a vestigial increase in growth was detected in

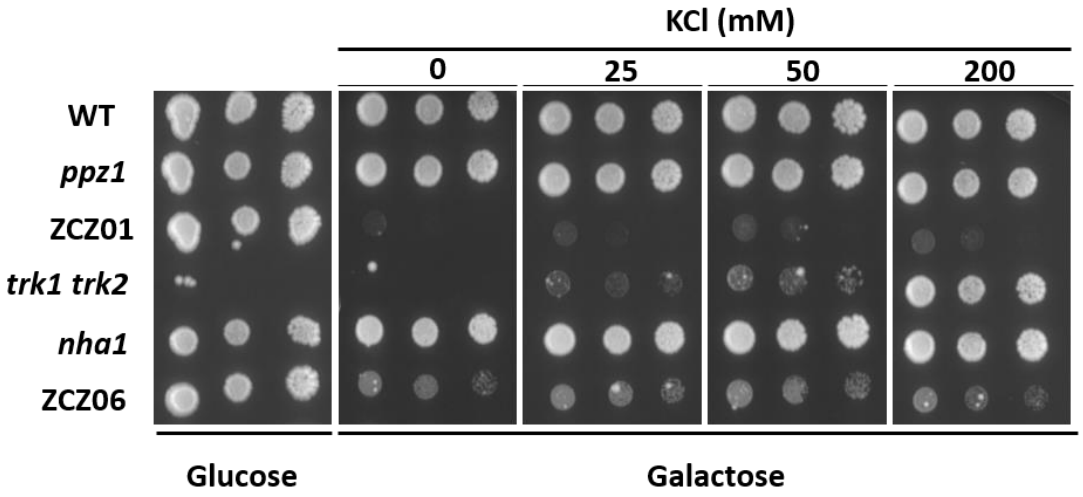

Figure 1.4 Phenotypic effects of surplus of potassium on the Ppz1 overexpressing strain

The indicated strains (ZCZ06 is a *nha1Δ* derivative of ZCZ01) were grown in synthetic medium and then cultures were spotted at OD_{600} = 0.05 and at 1/5 dilutions on plates containing the synthetic medium with the indicated amounts of potassium. The carbon source, glucose or galactose, is shown below the pictures. Growth was recorded after 7 days.

ZCZ01 cells overexpressing *PPZ1* with the surplus of potassium. On the other hand, the *nha1Δ* derivative allowed weak growth of galactose-induced Ppz1 cells, although the grown increase was not in parallel with the concentration of the potassium supplement. These results indicate that the growth defect in strain ZcZ01 cannot be rescued by a surplus of potassium and suggest that the targets of the excess of Ppz1 are not Trk transporters.

1.5 Changes in transcriptomic profile induced by overexpression of Ppz1

To evaluate the impact of high levels of Ppz1 on genome-wide mRNA levels, wild type BY4741 strain and its derivative ZCZ01 were grown on raffinose and *PPZ1* expression induced by addition of galactose. Total RNA was prepared from samples taken at 30 min, 2 h and 4 h upon induction and subjected to RNA-seq. Data from three experiments was combined and evaluated. As shown in Figure 1.5.1A, the expression of 94 genes was induced at least 2-fold after 30 min of addition of galactose, whereas only 19 were down-regulated. Induced genes increased up to 356 after 2 h and even further (625) at 4 h. In contrast, the peak of repressed genes was found at 2 h (356) and decreased to 135 at 4 h (Figure 1.5.1B). Altogether, 890 genes were induced and 420 were repressed at least at one time-point.

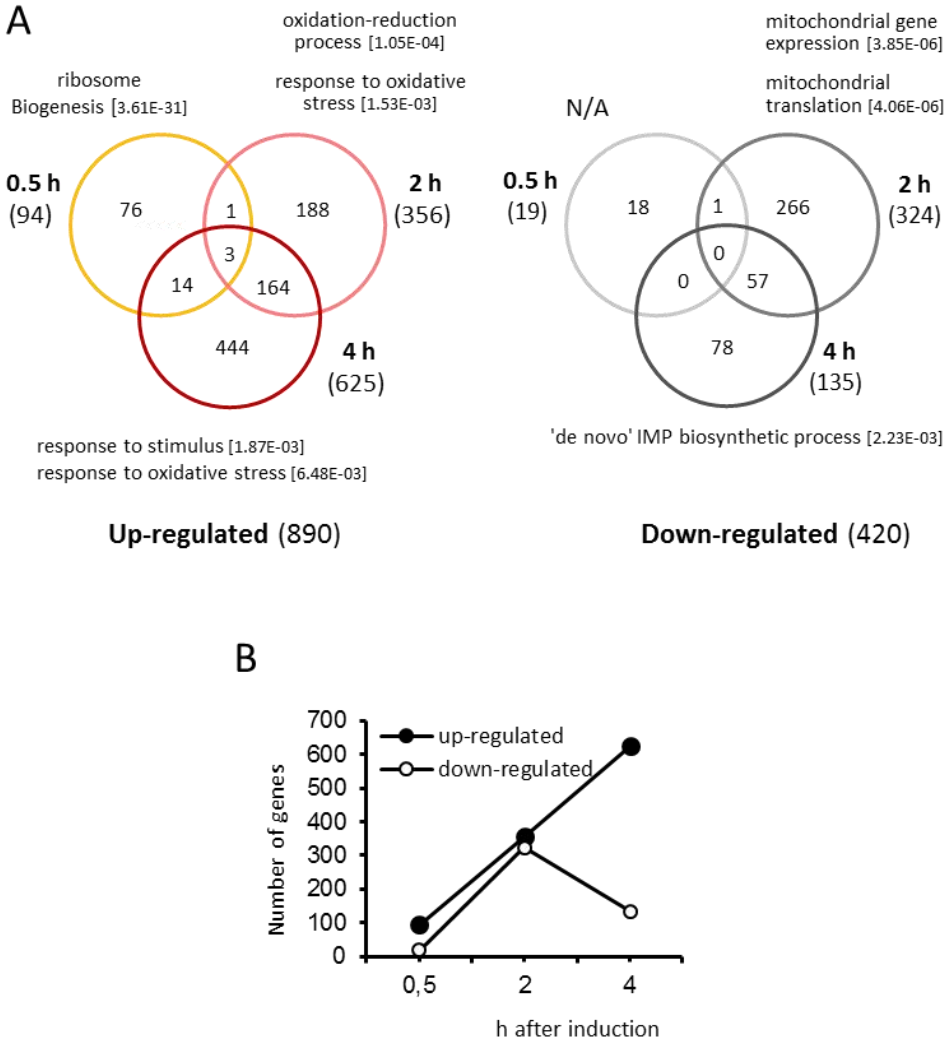

Figure 1.5.1 Transcriptional changes associated with overexpressing Ppz1

Panel A Venn diagrams showing the number of genes whose expression was induced or repressed (>=2-fold, p<0.05) at different times upon overexpression of *PPZ1*. Total numbers of genes in each category are in parentheses. Gene Ontology annotations are also shown (*p*-values are in brackets). N/A, not specific enrichment. Panel B, Time-course distribution of up- and down-regulated genes.

Gene Ontology analysis revealed specific traits for gene expression along the experiment. As shown in Figure 1.5.1A, early response (0.5 h) was characterized by a consistent increase in the expression of genes related to ribosome biogenesis. Further analysis revealed that most of these genes were involved rRNA processing. The pattern changed drastically after 2 and 4 h, when many genes related to the response to oxidative

stress emerged (such as *GRE1*, *CTT1*, *TSA2*, *SRX1*, *AHP1*, *GPX1* or *GTT2*). Analysis of the set of repressed genes did not show any specific enrichment after 0.5 h. However, at 2 h it was enriched in genes required for mitochondrial translation, most of them encoding proteins that are components of both the large and small ribosomal subunits. The profile changed after 4 h and, in this case, we found repressed many of the genes involved in the synthesis of IMP from 5-phosphoribosyl-1-pyrophosphate (PRPP), such as *ADE8*, plus *ADE2*, *ADE1*, *ADE13*, and *ADE17* (these last four genes are responsible for the last five reactions of the pathway). In fact, examination of the entire pathway revealed that other genes, such as *ADE4*, *ADE5*,7 and *ADE6* were also repressed (although they were not included in the analysis because the *p*-value was around 0.1 and did not pass the $p < 0.05$ the threshold). In fact, *ADE12*, necessary for the transformation of IMP into AMP was also repressed. Therefore, the entire pathway from PRPP to AMP appears down-regulated upon over-expression of *PPZ1*. An overall view of the expression changes is presented in Figure 1.5.2 as a heat-map generated from the results of gene clustering.

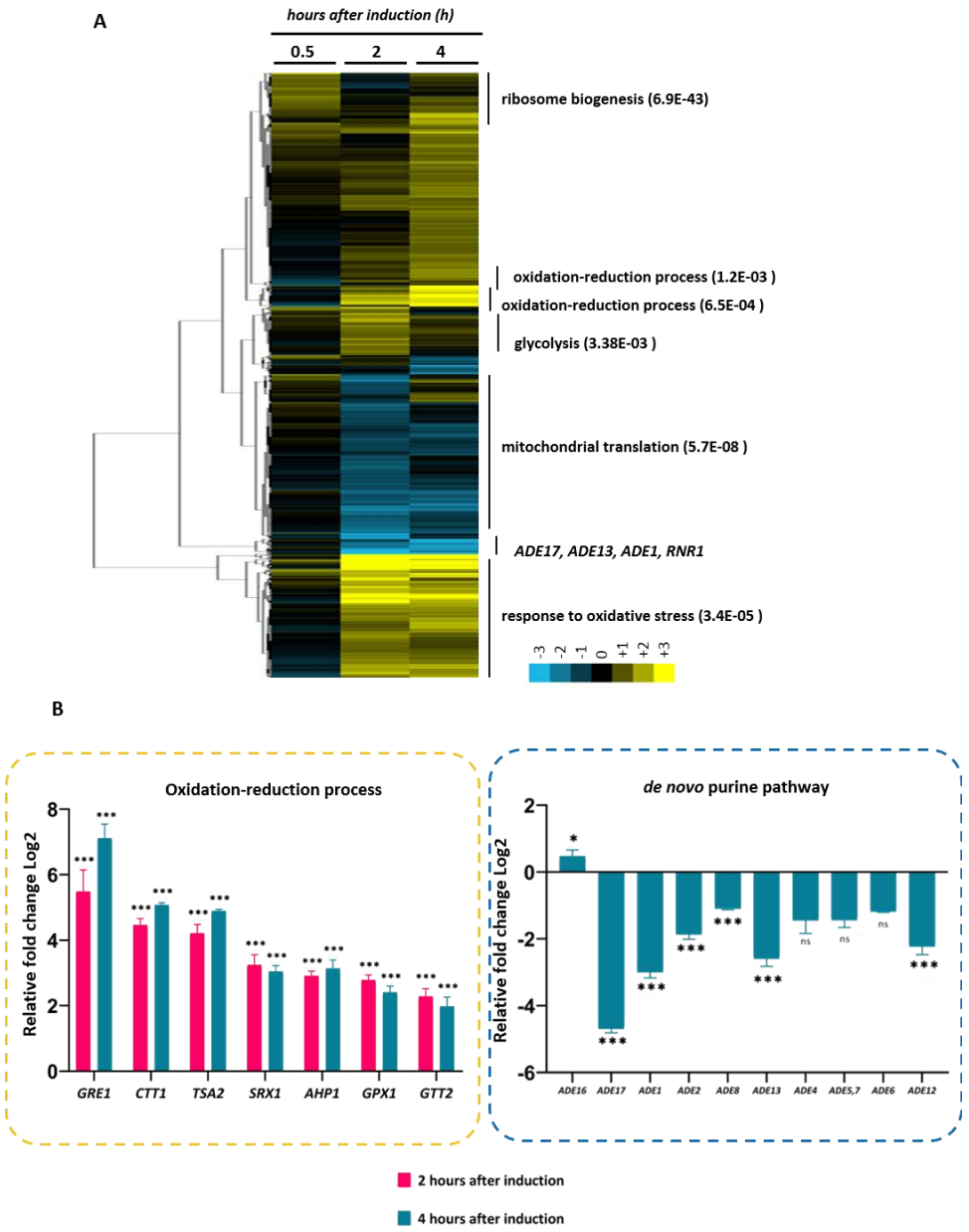

Figure 1.5.2 Clustering of genes induced or repressed after overexpressing Ppz1.

Panel A, Data for expression changes for 1294 genes showing induction or repression at least at one time-point were subjected to hierarchic clustering (Euclidean distance / complete linkage) using the Cluster software (v. 3.0). The result was visualized with Java Tree View (v. 1.145). The intensity of the expression change can be inferred by comparison with the enclosed scale (log(2) values). Panel B, Gene expression differences detected by RNAseq for the indicated GO categories are shown as mean ± SEMs, and the *p*-values are ns>0.05, *≤0.05, and ***≤0.001, compared to the expression in the control wild type strain. Only data at 4 h is shown in the right panel because no significant changes were observed at earlier times.

2. Characterization of the atypical Ppz/Hal3 phosphatase system from the pathogenic fungus *C. neoformans*

2.1 Identification of Ppz1 and Hal3-like proteins in *C. neoformans*

BLAST analysis of the *C. neoformans* H99 genome using the *S. cerevisiae* Ppz1 sequence allowed the identification of a single gene (CNAG_03673) encoding a 507-residue protein with a characteristic C-terminal region of 327 residues, highly similar to the C-terminus of ScPpz1 (74.5% identity, > 85% similarity, Figure 2.1).

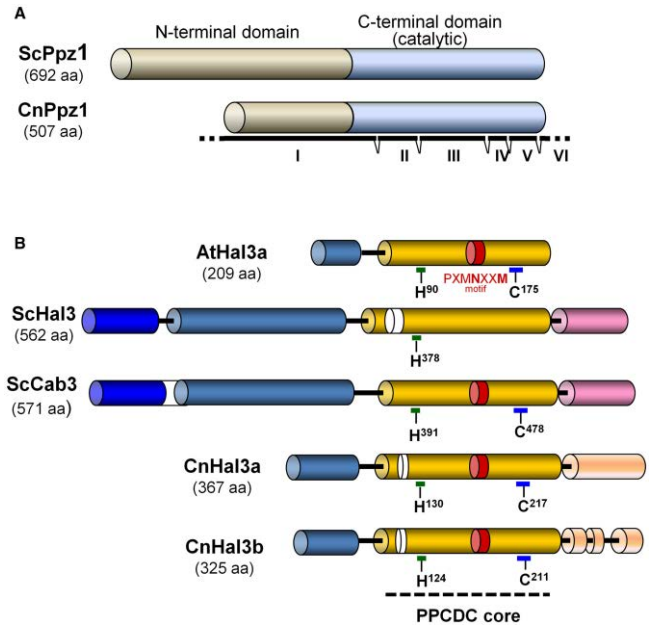

Figure 2.1 Schematic comparison of *S. cerevisiae* and *C. neoformans* Ppz1 and Hal3-like proteins.

Panel A. comparison of ScPpz1 and CnPpz1. The lines at the bottom of CnPpz1 define the exon-intron structure of the encoding gene. Note the shorter N-terminal extension in CnPpz1, similar in size to that found in *C. albicans*, *S. pombe* and other fungi. Panel B. Comparison of *A. thaliana* Hal3a, *S. cerevisiae* Hal3 and Cab3, and *C. neoformans* Hal3a and Hal3b. The His and Cys residues relevant for PPCDC activity are indicated in each case. The PXMNXXM motif is denoted by a red section. The color of the C-tail in the *S. cerevisiae* proteins is different from that of the *C. neoformans* ones to symbolize that the former is highly acidic whereas the latter is not. The exon-intron structure of the Hal3-like *C. neoformans* proteins is not depicted for simplicity. Length of each protein is indicated in parentheses.

The N-terminal extension (186 residues) of CnPpz1 has low identity to *S. cerevisiae* Ppz1 (26%, 45% similarity). The ORF (here after, CnPpz1) is interrupted by five short introns, all of them located at the region of the gene encoding the C-terminal half of the protein. The same analysis was carried out with *S. cerevisiae* Hal3 and Cab3 proteins and yielded two cryptococcal genes, CNAG_00909 (CnHal3a) and CNAG_07348 (CnHal3b), encoding related proteins of 367 residues and 325 residues respectively. In both genes the ORF was interrupted by five introns. These proteins are mainly composed of a conserved PPCDC domain, similar to that found in *A. thaliana* AtHal3a, flanked by a short N-terminal segment and a C-terminal segment (~100 residues), somewhat longer in CnHal3a. This C-terminal tail, in contrast to ScHal3 or ScCab3, is not enriched in acidic residues. Both gene products include the characteristic His and Cys residues (His^{130} and Cys^{217} in CnHal3a; His^{124} and Cys^{211} in CnHal3b), together with the PAMNTXM motif (PAMN^{182}THM and PAMN^{176}TYM respectively) found in AtHal3a. These features are compatible with both proteins being putative homotrimeric (and, therefore, monogenic) PPCDCs.

2.2 Functional characterization of CnPpz1 in *S. cerevisiae*

In order to characterize CnPpz1 we tried to generate the cDNA from total RNA. However, the numerous attempts were unsuccessful. We attributed this failure to the presence in CNAG_03673 of a very G/C rich (80%) N-terminal region segment expanding from nt 80 to 260 from the initiating ATG, with two stretches of > 40 nt in which the G/C content was > 90%. Therefore, the full-length intron-less ORF was obtained by generating two modules, the 3' region by PCR from a cDNA library and the 5' region by genomic PCR amplification, that were then combined by fusion PCR (see experimental procedures for details). This ORF was cloned downstream of the ScPPZ1 gene promoter in both centromeric (low-copy number, nearly mimicking chromosomal expression) and episomal (high-copy) vectors, and then introduced into different *S. cerevisiae* strains.

Deletion of *PPZ1* in *S. cerevisiae* increases tolerance to the toxic cation Li^+, and this phenotype is revered by re-introducing *ScPPZ1* both in low or high-copy number [Figure 2.2 and (Posas *et al.* 1995a)]. When CnPpz1 was expressed in a *ppz1* strain from the centromeric plasmid, the decrease in tolerance was hardly noticeable. However, expression from the episomal plasmid decreased lithium tolerance, although not as much as the native phosphatase. Lack of Ppz1 makes *S. cerevisiae* cells sensitive to certain cell wall stressors, such as caffeine (Posas *et al.* 1993). We observed that low-copy number expression of

CnPpz1 was nearly as effective as that of ScPpz1 in increasing caffeine tolerance in *ppz1* cells (Figure 2.2B). Similarly, episomal expression of CnPpz1 substantially improved growth of the *slt2* strain, in the presence of caffeine. The same effect was observed when the *slt2* strain was challenged with Calcofluor White, a compound that causes cell wall stress by interfering with the synthesis of chitin (Figure 2.2B). Interestingly, cells expressing CnPpz1 from the episomal vector appeared to be more tolerant to caffeine than the equivalent cells

expressing ScPpz1 (Figure 2.2B). However,

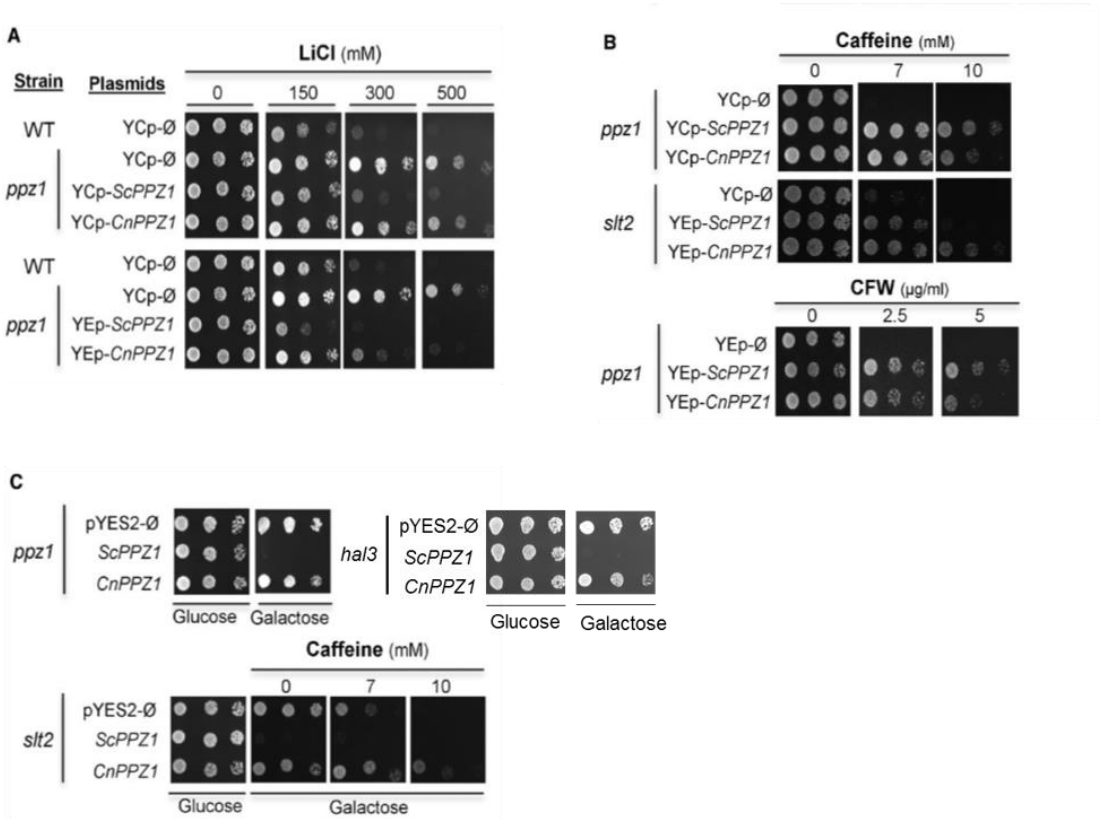

Figure 2.2 Phenotypic characterization of CnPpz1 expression in *S. cerevisiae*.

The indicated strains were transformed with YCplac111 (centromeric, *LEU2* marker), or YEplac181 (episomal, *LEU2* marker)-based constructs bearing *S. cerevisiae* (ScPpz1) or *C. neoformans* (CnPpz1) phosphatases. Cultures were spotted at OD_{600} = 0.05 and at 1/5 dilutions on synthetic medium plates lacking leucine and containing the indicated amounts of LiCl (panel A), caffeine or Calcofluor White (panel B). Plates were grown for 48 h. WT, wild type BY4741 strain; Ø, empty plasmid. Panel C. The *ppz1* strain and *hal3* strain was transformed with empty pYES2 plasmid (pYES2-Ø) or the same plasmid expressing ScPpz1 or CnPpz1 from the *GAL1* promoter. Cells were grown on SD medium lacking uracil and spotted on plates containing the same medium or synthetic medium with 2% galactose. The *slt2* strain was transformed and spotted as above, including the indicated amounts of caffeine in the plates containing galactose as carbon source. Growth was monitored after 3 days.

the difference could be explained by the detrimental effect on cell growth caused by high copy expression of ScPpz1. If this is the case, it could be assumed that strong overexpression of CnPpz1 in *S. cerevisiae*, contrary to that of the native enzyme, might have no negative effects on cell growth. To test this, we cloned the CnPpz1 ORF in the plasmid pYES2, to allow

expression of the phosphatase in high-copy number from the powerful *GAL1-10* promoter. As observed in Figure 2.2C, growth was completely blocked when cells were spotted on galactose to allow expression of ScPpz1 but, under the same conditions, cells overexpressing CnPpz1 showed robust growth. This lack of toxicity was not due to the inability to express CnPpz1 from the vector, because CnPpz1 was able to improve tolerance to caffeine when introduced in *slt2* cells (Figure 2.2C)

2.3 Characterization of CnHal3a and CnHal3b for Ppz1-related functions in *S. cerevisiae*

For functional testing in *S. cerevisiae*, both ORFs encoding putative CnPpz1 regulators were cloned in plasmid pWS93, which allows high-copy number expression from the *ADH1* promoter of N-terminally 3xHA epitope-tagged proteins. Introduction of these constructs in wild type cells led to a slight increase in tolerance to LiCl (Figure 2.3A). Interestingly, when the proteins were expressed in Hal3-deficient cells a different effect was observed: expression of CnHal3b was more effective in improving tolerance to the toxic cation (although with lesser potency than overexpression of ScHal3). We then tested the tolerance to caffeine of wild type and *slt2* cells expressing both *C. neoformans* proteins. As showed in Figure 2.3A, whereas expression of ScHal3 in wild type cells decreased tolerance to caffeine, that of CnHal3a or CnHal3b did not. When the same test was performed using *slt2* cells, which cannot tolerate Hal3 overexpression unless osmotically supported (e.g. by the presence of 1 M sorbitol), cells overexpressing CnHal3a behaved like those carrying the empty plasmid, whereas those carrying CnHal3b displayed slightly higher tolerance (Figure 2.3A). The rather weak complementation produced by the *Cryptococcus* proteins cannot be attributed to lower levels of expression, since immunoblot analysis of protein extracts from *S. cerevisiae* wild type and *slt2* cells expressing native Hal3 as well as both *C. neoformans* proteins (Figure 2.3B) indicated that the amounts of cellular CnHal3a, CnHal3b and ScHal3 were comparable. Therefore, the differences observed may be due to the intrinsic properties of the proteins

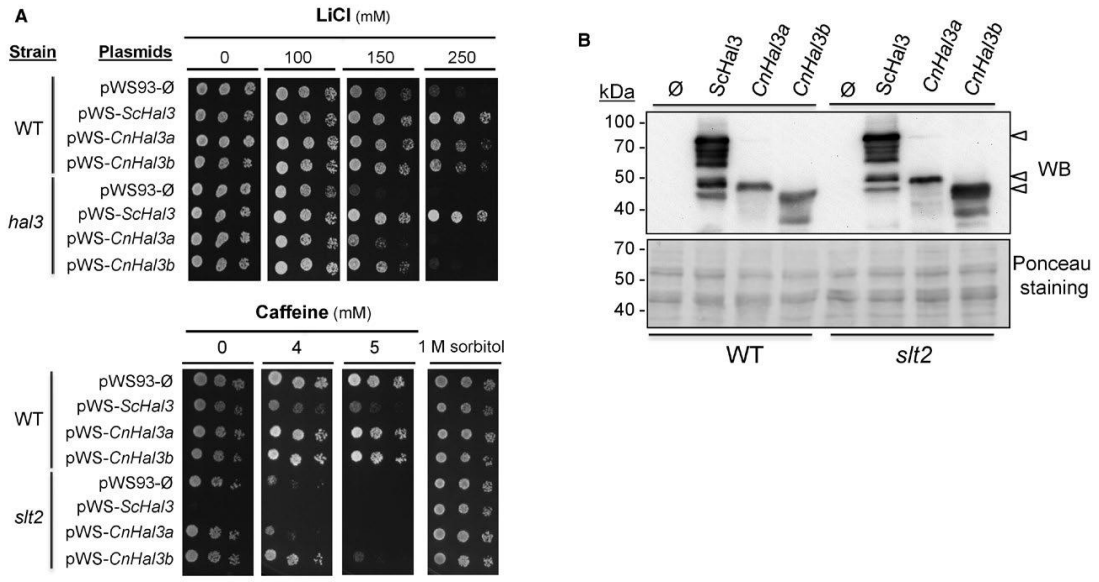

Figure 2.3 Effects of CnHal3a and CnHal3b on tolerance to LiCl and caffeine in *S. cerevisiae* and evaluation of expression levels.

Panel A. Wild type BY4741 (WT) and its *hal3* and *slt2* derivatives were transformed with plasmid pWS93 (episomal, *URA3* marker) and the same plasmid expressing ScHal3, CnHal3a, and CnHal3b. Cells were spotted on synthetic medium plates lacking uracil (without 1 M sorbitol except otherwise stated) and containing different concentrations of LiCl or caffeine. Growth was recorded after 48 h. Panel B. Protein extracts from cultures of the strains described above were prepared and subjected to SDS-PAGE. Proteins were transferred to membranes and the different 3xHA-tagged proteins detected with anti-HA antibodies (WB, indicated by empty arrows). Ponceau staining of the membranes is shown for comparison of loading and transfer efficiency. Cultures of the *slt2* strain included 1 M sorbitol to avoid lysis of cells expressing ScHal3.

2.4 *In vitro* characterization of *C. neoformans* CnPpz1, CnHal3a and CnHal3b proteins

In vitro characterization of CnPpz1 was accomplished by expression in *E. coli* of the full-length and C-terminal phosphatase domain (from residue 346 to the stop codon) as fusion proteins with a glutathione S-transferase (GST) tag. The proteins were then purified by glutathione agarose affinity chromatography and, while bound to the resin, they were used as baits for binding assays with *S. cerevisiae* extracts containing equivalent amounts of HA-tagged ScHal3, CnHal3a or CnHal3b.

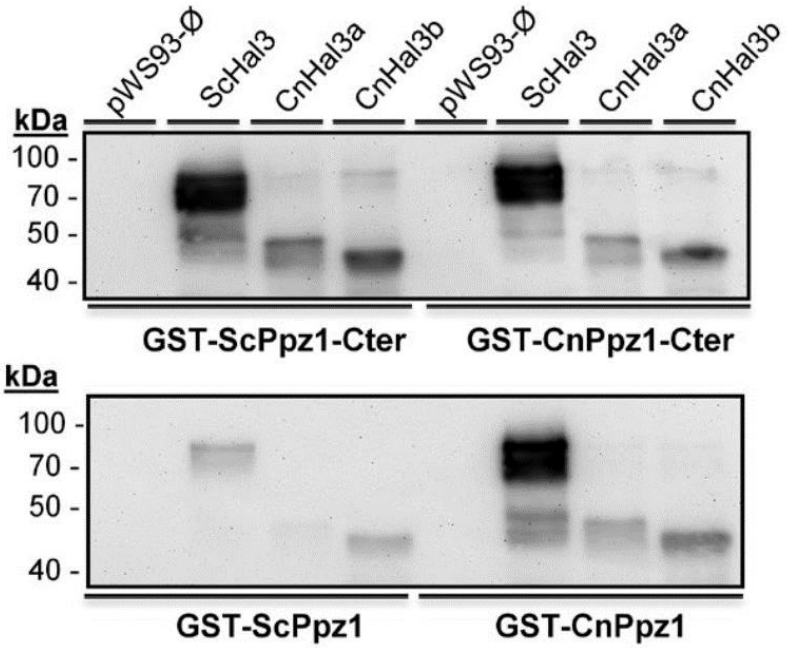

Figure 2.4.1 Interaction of CnHal3a and CnHal3b Hal3 with ScPpz1 and CnPpz1.

Equal amounts of the indicated versions of GST-tagged phosphatases were immobilized on glutathione beads and used as an affinity system to recover HA-tagged ScHal3, CnHal3a or CnHal3b expressed from the pWS93 plasmid in IM021 (*ppz1 hal3*) cells. Beads were washed and processed for SDS-PAGE (10% gels) and immunoblotting using anti-HA antibodies as described in Methods.

As shown in Figure 2.4.1, and it was previously known, the interaction of the full length ScPpz1 with ScHal3 is relatively weak, and it is greatly enhanced by removal of the N-terminal region (ScPpz1-Cter bait). Remarkably, the strength of the interaction of both full length and the catalytic C-terminal domain of CnPpz1 with ScHal3 was comparable with that of the C-terminal domain of ScPpz1. ScPpz1-Cter interacted with both CnHal3a and CnHal3b with similar efficiency (although less than with ScHal3). Full length ScPpz1 only showed a slight interaction with CnHal3b, but none with CnHal3a (Figure 2.4.1). Both versions of CnPpz1 interacted similarly with CnHal3b and CnHal3a, at levels equivalent to that of ScPpz1-Cter. *In vitro* assays confirmed the phosphatase activity of CnPpz1, although the recombinant enzyme showed a specific activity 3-to 5-fold lower than that of ScPpz1 (not shown). Interestingly, while CnPpz1 was strongly inhibited by recombinant ScHal3, it was not inhibited by CnHal3b or CnHal3a (Figure 2.4.2). Likewise, the *C. neoformans* Hal3-like proteins were completely ineffective as inhibitors of either the full-length or the catalytically active C-terminal domain of the *S. cerevisiae* phosphatase.

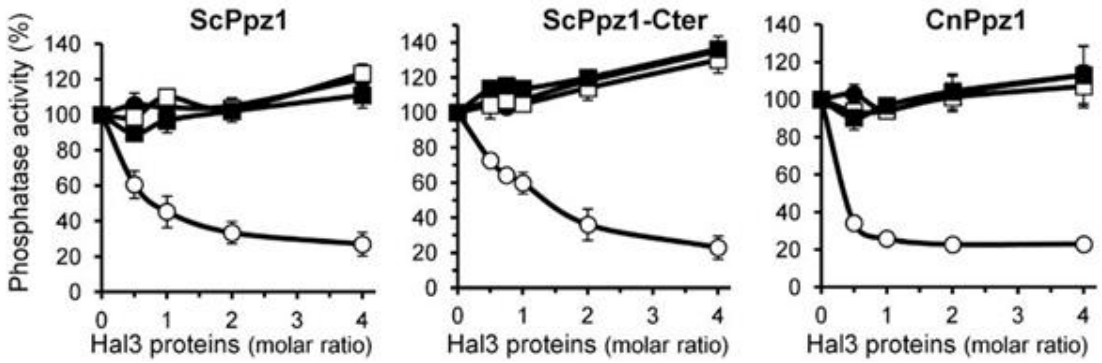

Figure 2.4.2 inhibitory capacity of CnHal3a and CnHal3b with ScPpz1 and CnPpz1.

Dephosphorylation assays were carried out as described under Methods. Six pmols of ScPpz1 or ScPpz1-Cter, and 7.5 to 15 pmols of CnPpz1 were pre-incubated for 5 min at 30°C with increasing amounts of ScHal3 (–○–), CnHal3a (–●–), CnHal3b (–□–) or CnHal3b-ScL (–■–), prior initiating the assay by addition of the substrate. Values are means ± SEM from 4 different assays and are expressed as the percentage of phosphatase activity relative to control without inhibitor. At least two different preparations of the phosphatases and the inhibitors were tested.

2.5 Characterization of hybrid ScHal3/CnHal3b proteins

The inability of *Cryptococcus* Hal3-like proteins to inhibit ScPpz1 and CnPpz1 *in vitro* was surprising, particularly in the case of CnHal3b, which exhibited some (albeit limited) Hal3-like behavior when tested for Li^+ tolerance in *S. cerevisiae*. Comparison of its sequence with that of the minimal version of ScHal3 that retains the ability to inhibit Ppz1 (Abrie *et al.* 2012) showed two major differences: one is the sequence ^{458}SEKVMDIN^{466} in ScHal3, which correspond to a likely flexible loop containing residues relevant for Ppz1 inhibition but not for binding (Muñoz *et al.* 2004), and that is very different in CnHal3b (as ^{204}QGAGRLAC^{211}, forming part of the PPCDC catalytic loop); the other is the characteristic ~80-residues highly acidic C-tail of ScHal3, which appears in CnHal3b as a ~100-residues long non-acidic tail of unrelated sequence. Therefore, we decided to create hybrid versions of CnHal3b by replacing one or both features by the ones from ScHal3.

Our results show that replacement of the ^{204}QGAGRLAC^{211} loop by the equivalent *S. cerevisiae* sequence did not increase tolerance to LiCl nor affected sensitivity to caffeine (Figure 2.5.1). Consistent with this, the recombinant modified protein was unable to inhibit

ScPpz1 or CnPpz1 enzymes *in vitro* (Figure 2.4.2). In contrast, expression of versions of CnHal3b carrying the modified C-terminal tail conferred a significant increase in tolerance to LiCl that was noticeable in wild type and, particularly, in Hal3-deficient strains (Figure 2.5.1). However, sensitivity to caffeine was not affected by expression of these modified

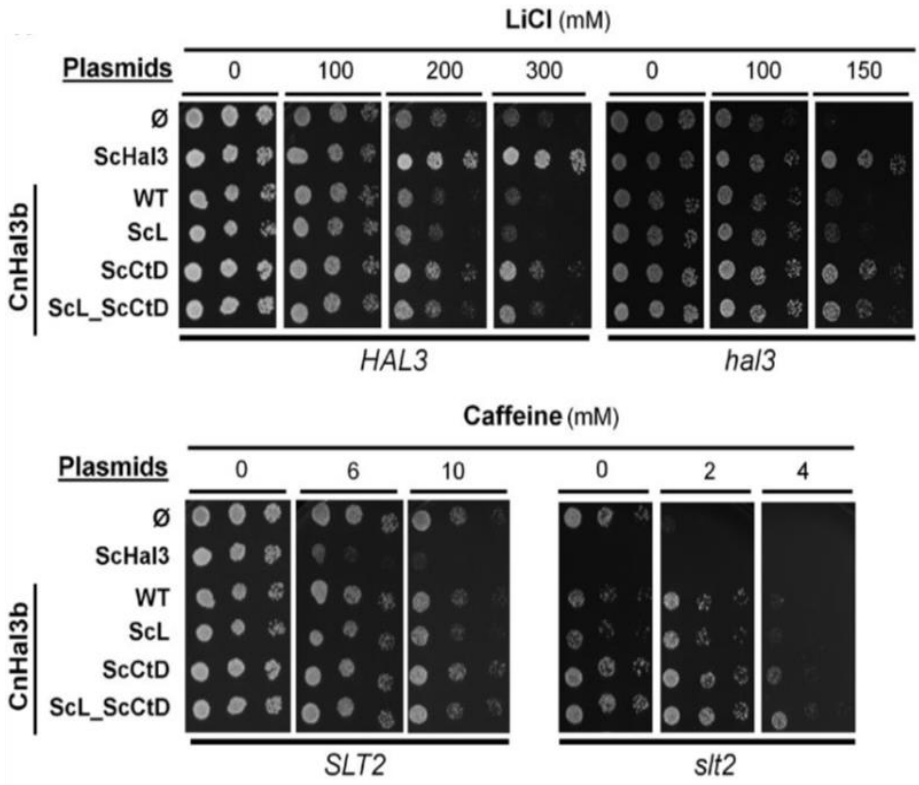

Figure 2.5.1 Functional evaluation of hybrid versions of the CnHal3b protein.

The indicated strains in the BY4741 background were transformed with empty pWS93 plasmid (Ø), *S. cerevisiae* Hal3 (ScHal3) or the different variants of the CnHal3b protein. ScL (ScLoop), ScCtD (Sc acidic C-terminal tail). Cultures were spotted as in Figs 2.2 and 2.3. All pictures were taken after 60 h of growth except plates containing 300 mM LiCl, which was recorded after 4 days.

versions.

Evaluation by immunoblot (Figure 2.5.2) of the *in vivo* expression of the different variants revealed that the versions carrying the C-terminal acidic tail were present at even lower levels than the native protein, indicating that the observed phenotypic effects were due to changes in the intrinsic functional abilities of the proteins.

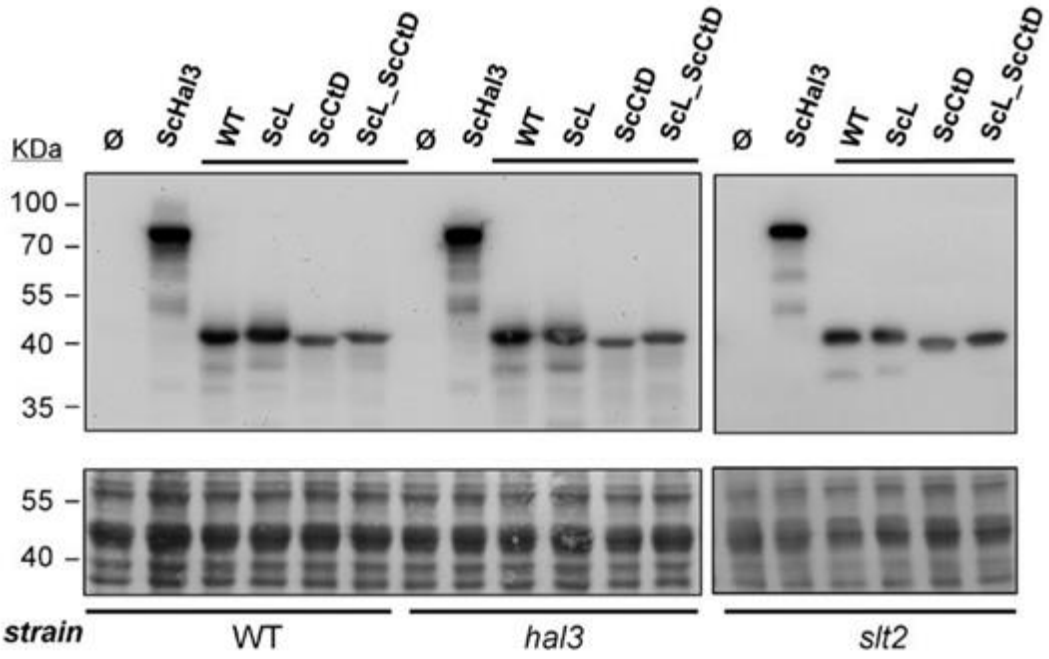

Figure 2.5.2 Evaluation of expression levels of hybrid versions of the CnHal3b protein.

Protein extracts from cultures of the indicated strains were obtained and processed as described in the Figure 2.3. Designation of the constructs used for transformation is the same as in Figure 2.5.1.

2.6 Functional analysis of CnHal3a and CnHal3b as PPCDC enzymes

2.6.1 UV-visible scanning of preparations of purified recombinant CnHal3a and CnHal3b

As mentioned above, both CnHal3a and CnHal3b proteins contain key determinants necessary for PPCDC activity, such as the catalytic His, Asn and Cys residues. In addition, UV-visible scanning of preparations of purified recombinant CnHal3a and CnHal3b showed characteristic peaks at 382 and 452 nm, compatible with the presence of an oxidized flavin, a molecule involved in the PPCDC catalytic process (Figure 2.6.1). In addition, treatment of the recombinant CnHal3b protein, lacking the GST-moiety, with the cross-linking agent glutaraldehyde, a, resulted in the formation of high molecular weight aggregates, compatible with a trimeric structure, as expected for an active PPCDC enzyme.

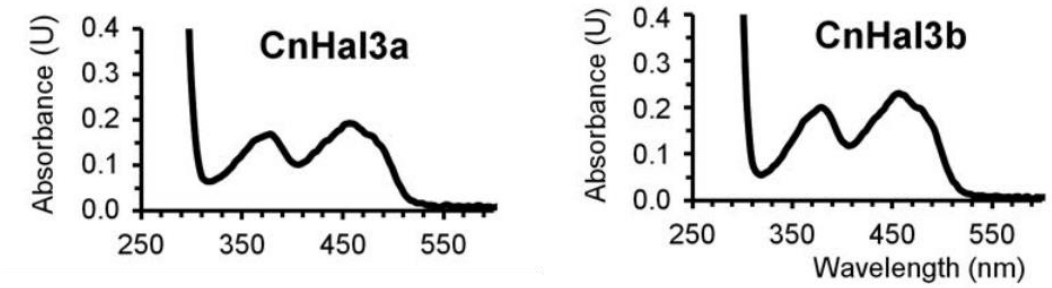

Figure 2.6.1 UV-spectrum of the CnHal3a and CnHal3b

GST-CnHal3a and GST-CnHal3b were expressed in *E. coli* and, after removal of the GST moiety, the visible-UV absorption profile was recorded. Note the appearance in both proteins of two peaks characteristic of flavin-containing proteins

2.6.2 Functional evaluation of CnHal3 proteins as PPCDC in *S. cerevisiae*

To test if these proteins were able to act as PPCDC enzymes *in vivo* we carried out the expression of each protein in diploid *S. cerevisiae* strains heterozygous for the *hal3 vhs3* or the *cab3* mutations, and we evaluated, by random spore analysis and/or tetrad analysis, the ability of the *Cryptococcus* proteins to rescue the deletion mutants. As shown in Fig. 2.6.2, transformation of strain MAR25 (*CAB3/cab3Δ*) with either pWS93-CnHal3a or pWS93-CnHal3b vectors allowed recovering four viable spores, similarly as it happens when ScCab3 is expressed, indicating that the *Cryptococcus* proteins are able to replace endogenous Cab3 in *S. cerevisiae*. Similarly, when either CnHal3a or CnHal3b were introduced into strain AGS04 (*HAL3/hal3 VHS3/vhs3*) and sporulation was induced, haploid double mutants bearing the vector were recovered with similar efficiency as when ScHal3 was used for transformation. These results demonstrate that both cryptococcal proteins can efficiently replace Hal3 or Cab3 when expressed in *S. cerevisiae*, indicating that both could work as homomeric PPCDC enzymes.

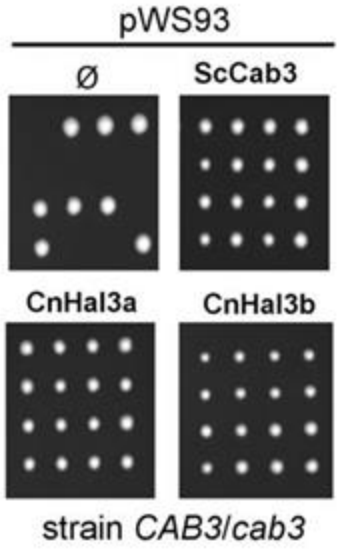

Figure 2.6.2 Evaluation of CnHal3a and CnHal3b PPCDC function in *S. cerevisiae*.

Strain MAR25 (*CAB3/cab3Δ*) was transformed with the indicated plasmids and sporulation was induced. Spores from diverse asci were separated with a micromanipulator and incubated up to the formation of colonies. Note that the presence of the *C. neoformans* proteins allowed germination and growth of all four spores in the tetrad, indicating that they complement the lethal *cab3* mutation.

2.6.3 Functional evaluation of CnHal3 proteins as PPCDC in *E. coli*

To further confirm the statement above, we expressed both *C. neoformans* proteins in the *E. coli* strain BW369 that carries the *dfp*-707^{ts} mutation. Such mutation affects PPCDC function in a temperature-sensitive way, so cells cannot grow at 37°C (Spitzer and Weiss 1985; Spitzer *et al.* 1988).

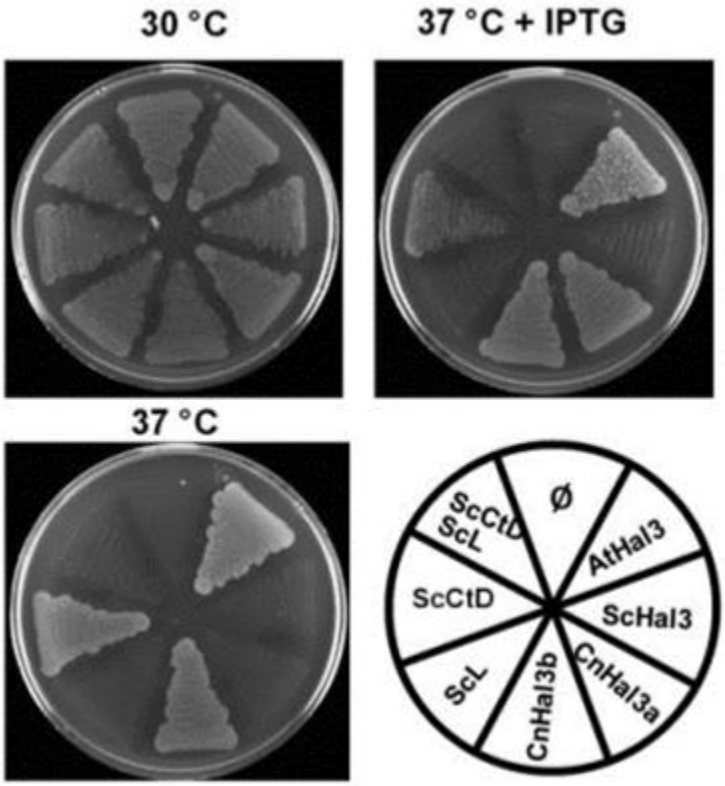

Figure 2.6.3 Evaluation of CnHal3a and CnHal3b PPCDC function in *E. coli.*

The *E. coli* strain BW369 (*dfp*-707^{ts}), which carries a mutation that abolishes PPCDC activity at 37 ˚C, was transformed with the empty pGEX6P-1 plasmid (Ø) and the same plasmids bearing the plant AtHal3 (as positive control), ScHal3 (as negative control), CnHal3a, CnHal3b and the CnHal3b variants. Transformants were grown at 30 ˚C, diluted till OD_{600} = 0.05, transferred to 30 or 37 ˚C (permissive and non-permissive temperatures respectively) for 6 h and then plated at the indicated temperatures. Where indicated, IPTG 0.2 mM was added to cells just prior incubation at 37 ˚C. Growth at 37 ˚C denotes complementation of the ts PPCDC mutation.

Surprisingly, only CnHal3b was able to support growth of the *E. coli* mutant at the restrictive temperature, while expression of CnHal3a failed to do so (Figure 2.6.3). To assess the possibility that such failure could be due to a deficient expression level, we included 0.2 mM IPTG in the plates to enhance expression from the plasmid-borne *tac* hybrid promoter. In this case, cells expressing the CnHal3a protein were able to grow. Immunoblot analysis of the expressed proteins under the different growth conditions showed (Figure 2.6.4) that, indeed, CnHal3a was expressed at much lower amounts, so the protein was undetectable at 37°C in the absence of the inducer. Therefore, the different behavior of CnHal3a and

CnHal3b in complementing the *dfp*-707^{ts} mutation was likely due to uneven expression levels and not necessarily to different catalytic capacities. Addition of the *S. cerevisiae* acidic tail to CnHal3b (CnHal3b_ScCtD construct) did not impair the ability of the protein to complement the *dfp*-707^{ts} mutation but, as expected, replacement of the ^{204}QGAGRLAC^{211} region did.

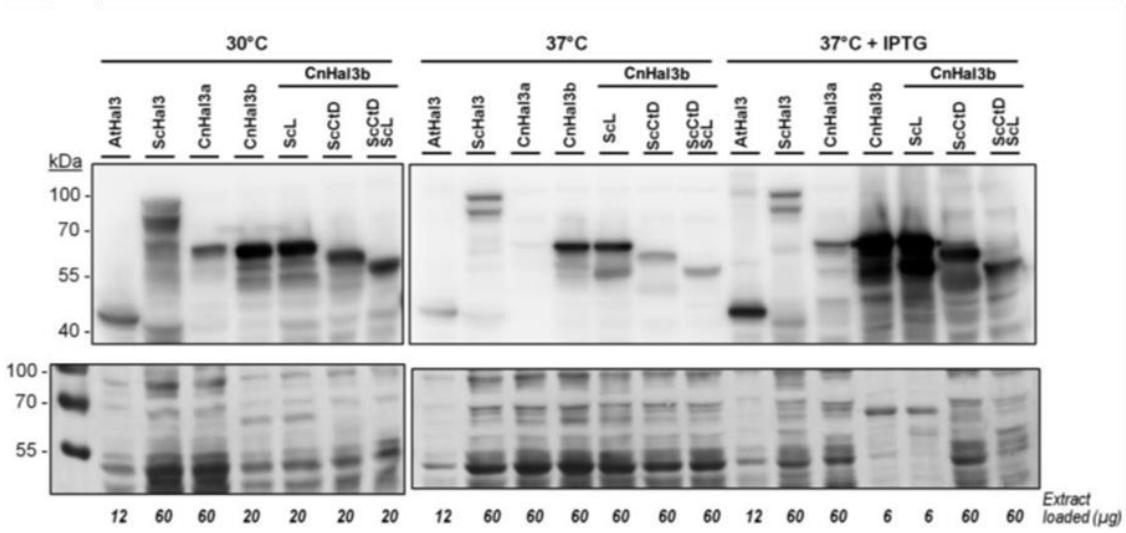

Figure 2.6.4 Evaluation of expression levels of CnHal3 proteins in *E. coli* BW369

Aliquots (10 ml) of the cultures used in Figure 2.6.3 were collected just prior plating, protein extracts prepared as in (Abrie *et al.* 2012), and samples analyzed by SDS-PAGE (10%) followed by immunoblot with anti-GST antibodies. Note that due to the largely dissimilar levels of expression of the relevant proteins, to facilitate comparison different amounts of whole extracts (denoted at the bottom of the Ponceau staining) were loaded in the gel.

3. Characterization of the Ppz/Hal3 phosphatase system from *Ustilago maydis*

3.1 Identification of Ppz1 and Hal3-like protein in *U. maydis*

BLAST analysis of fungal databases using the *S. cerevisiae* Ppz1, Hal3 and Cab3 protein sequences revealed a putative ortholog for *PPZ1* in *Ustilago maydis*, encoding the hypothetical protein UM04827.1, and a single putative ortholog for Hal3 and Cab3 (hypothetical protein UM05916.1).

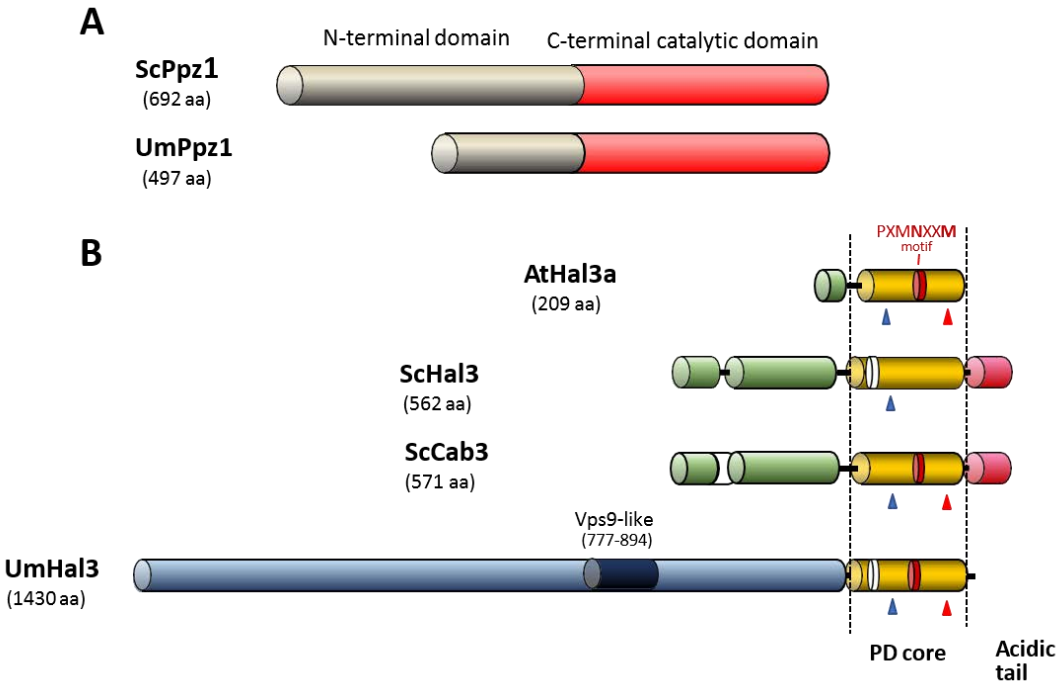

Figure 3.1 Comparison of the structures of *S. cerevisiae* and *U. maydis* Ppz1 and Hal3 proteins.

Panel A. ScPpz1 and UmPpz1 structures. Note the shorter N-terminal extension in UmPpz1. Panel B. Comparison of *A. thaliana* Hal3a, *S. cerevisiae* Hal3 and Cab3, and *U. maydis* Hal3 (UmHal3). The His and Cys residues required for PPCDC activity are indicated as blue and red arrowheads, respectively. The red section corresponds to the PXMNXXM motif. To note the absence in UmHal3 of the acidic C-tail found in both *S. cerevisiae* proteins. The length of each protein is indicated in parentheses. Scales in panel A and B are different.

As shown in Figure 3.1, UM04827.1 (UmPpz1) is a 497-residue protein that shows an overall 38.2% identity (46.5% similarity) with ScPpz1. The C-terminal section of UmPpz1, containing the characteristic traits of a Ser/Thr protein phosphatase, shows high identity with the C-terminal phosphatase domain of ScPpz1 (67.9%, 77.6% similarity from residue 151 to the C-terminal residues). Therefore, the N-terminal extension of UmPpz1 is about half the size than that of ScPpz1 (Figure 3.1). The UM05916.1 protein (UmHal3), is a very large polypeptide of 1430 residue. The last 240 amino acids show significant identity with known PPCDCs, such as AtHal3a (34.2% identity, 48.9% similarity), as well as with the PPCDC core of both ScHal3 (24.1% / 39.7%) and ScCab3 (26.8% / 40.5%), although the *Ustilago* protein lacks the characteristic C-terminal acidic tail found in *S. cerevisiae* (Figure 3.1) and *C. albicans*. Therefore, UmHal3 has a very long N-terminal extension whose similarity to the one present in Hal3 or Cab3 is only marginal. To note, UmHal3 presents at positions 777-894 a Vps9-like sequence. In fact, the entire Vps9 protein can be aligned with UmHal3 (from residue 570 to 1096) albeit with relatively low identity (19.4%, 35.5% similarity %). In *S. cerevisiae*, Vps9 is acts as a GEF for Vps21 and is needed for the transport of proteins from biosynthetic and endocytic pathways into the vacuole.

3.2 Functional characterization of UmPpz1 in *S. cerevisiae*

3.2.1 UmPpz1 partially mimicked the ScPpz1 function in *S. cerevisiae*

To this end, the UmPpz1 ORF was expressed from the *ScPPZ1* promoter in both centromeric and episomal vectors. As it can be observed in Figure 3.2.1, expression of UmPpz1 from low or high-copy number vectors was unable to decrease the abnormally high tolerance of the *ppz1* mutant to LiCl. The mutation of *PPZ1* yields *S. cerevisiae* cells hypersensitive to caffeine, and the sensitivity to the drug is normalized when a centromeric copy of ScPpz1 is reintroduced in the cells. Transformation of *ppz1* cells with centromeric UmPpz1 increased only marginally the tolerance to caffeine, but high-copy expression of UmPpz1 restored wild-type tolerance (Figure 3.2.1). The fact that cells expressing UmPpz1 from the episomal vector grow better in the presence of caffeine than cells expressing ScPpz1 can be explained by previous observations that high-copy expression of ScPpz1 from its own promoter has a negative effect on cell growth (de Nadal *et al.* 1998). A modest beneficial effect of the expression of UmPpz1 was also observed when the experiment was carried out in a *slt2* mutant, which is defective in cell wall remodeling and highly sensitive to caffeine.

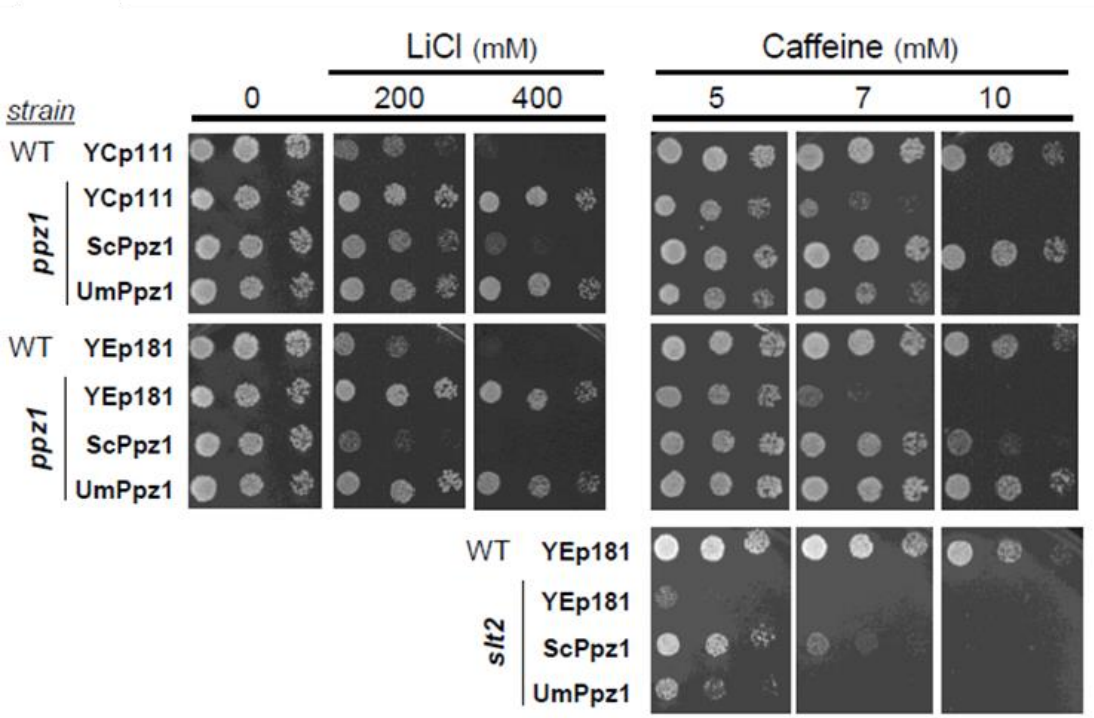

Figure 3.2.1 Phenotypic analysis of the expression of UmPpz1 in *S. cerevisiae*.

The wild type BY4741 strain (WT) and its *ppz1* and *slt2* derivatives were transformed with YCplac111, or YEplac181 plasmids carrying *S. cerevisiae* (ScPpz1) or *U. maydis* (UmPpz1) phosphatases. Cultures were spotted at OD_{600}=0.05 and at 1/5 dilutions on synthetic medium plates lacking leucine and containing the indicated amounts of LiCl or caffeine. Plates were grown for 4 days. Ø, empty plasmid.

3.2.2 Functional evaluation of overexpression of UmPpz1 in *S. cerevisiae*

In contrast to ScPpz1, expression of UmPpz1 under the same conditions did not affect growth (Figure 3.2.2A). The absence of effect was not due to insufficient expression levels, since immunoblots experiments showed that HA-tagged UmPpz1 accumulates even more abundantly than ScPpz1 (Figure 3.2.2B). Therefore, UmPpz1 does not reproduce the toxic effects of ScPpz1.

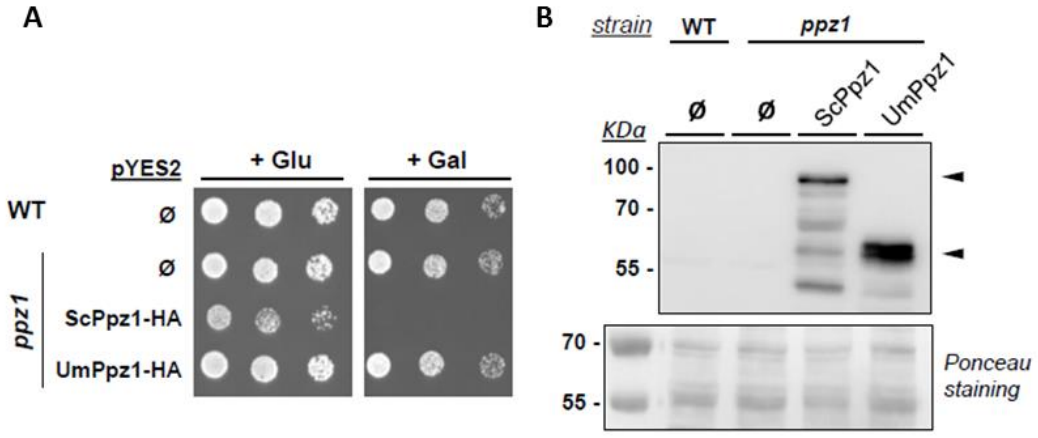

Figure 3.2.2 Phenotypic analysis of the overexpression of UmPpz1 in *S. cerevisiae*.

Panel A, wild type and *ppz1* strains were transformed with empty pYES2 plasmid (pYES2-Ø) or the same plasmid expressing ScPpz1-HA or UmPpz1-HA from the *GAL1-10* promoter. Cells were grown on synthetic medium lacking uracil supplemented with 2% glucose and spotted on the same plates containing either 2% glucose or 2% galactose. Growth was monitored after 2 days. Panel B, the same strains were grown in liquid medium with 2% galactose. Samples were taken after 6 hours and processed for SDS-PAGE as described. Eighty µg of protein were electrophoresed in 10% SDS-polyacrylamide gels, transferred to membranes and probed with anti-HA antibodies to detect the tagged proteins (arrowheads). Ponceau staining of the membranes was carried out (lower panel) to monitor for correct loading and transfer.

3.3 Functional characterization of UmHal3 in *S. cerevisiae*

Expression of UmHal3 in *S. cerevisiae* was accomplished by cloning the entire ORF in the high-copy plasmid pWS93. In this way, the protein is expressed from the *ADH1* promoter as a N-terminally 3xHA epitope-tagged polypeptide. In addition, we cloned in the same vector the C-terminal region of UmHal3, corresponding to the PPCDC domain (UmHal3 PD region) and this same region followed by the highly acidic C-terminal tail found in ScHal3 (UmPD_ScCter).

As shown in Figure 3.3.1, expression of UmHal3 or its PD region in a *hal3* strain did not improve tolerance to LiCl or NaCl, which are typical effects of ScHal3 overexpression. Interestingly, expression of UmPD_ScCter increased somewhat tolerance to LiCl. In contrast, none of the versions restored wild-type tolerance to the toxic cation spermine or to caffeine.

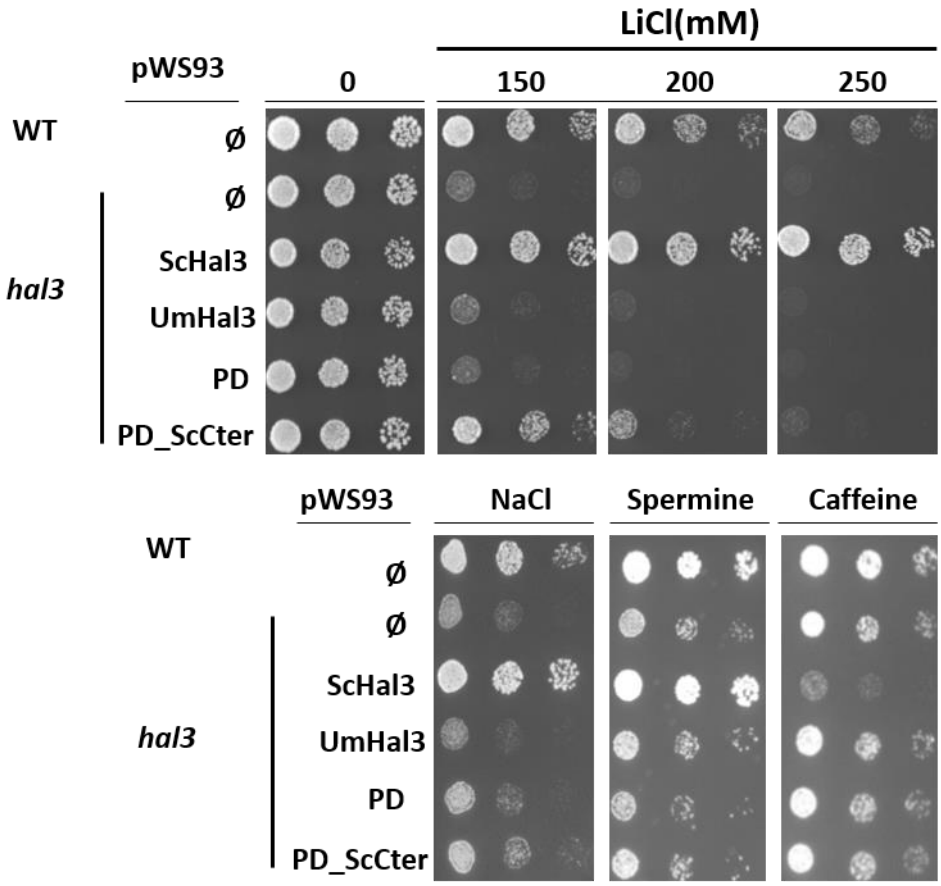

Figure 3.3.1 Effects of the expression of UmHal3 in *S. cerevisiae* on the tolerance to diverse stress conditions.

Wild type BY4741 (WT) and its *hal3* derivative were transformed with plasmid pWS93 (episomal, *URA3* marker) and the same plasmid expressing ScHal3, full-length UmHal3, its PPCDC domain (PD) and this domain followed by the acidic C-terminal tail form ScHal3 (PD_ScCter). Cells were spotted on synthetic medium plates lacking uracil supplemented with the indicated compounds. Growth was recorded after 48 hours.

The virtual lack of effects derived from the introduction in *S. cerevisiae* of the UmHal3 protein and its variants could be attributed to defective expression. To test this, we monitored the expression levels of these proteins taking advantage of the N-terminal 3xHA tag. However, as observed in Figure 3.3.2, all UmHal3 variants, including the very large full-length UmHal3 were expressed at considerable levels. Therefore, the absence of phenotypic effects must be attributed to the inherent properties of these proteins. Because the phenotypes tested are a consequence of the role of ScHal3 as inhibitor of Ppz1, our results suggest that UmHal3 is not able to inhibit Ppz1 in *S. cerevisiae*.

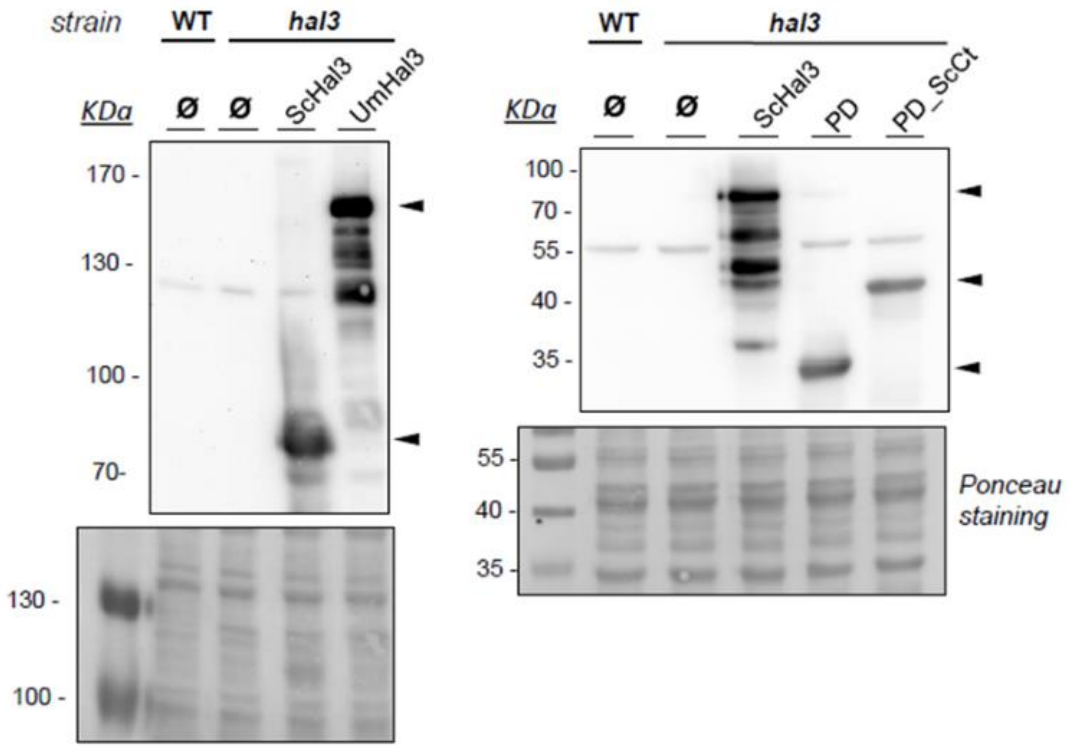

Figure 3.3.2 Evaluation of expression levels of UmHal3 proteins in *S. cerevisiae*

Protein extracts from cultures of the strains described were prepared, subjected to SDS-PAGE, and proteins were transferred to membranes. The different 3xHA-tagged proteins were detected with anti-HA antibodies (indicated by arrowheads). Ponceau staining of the membranes is shown.

3.4 Characterization of recombinant UmPpz1 and UmHal3 proteins

To this end, UmPpz1 was expressed in *E. coli* as a fusion protein with glutathione S-transferase (GST), purified by glutathione agarose affinity chromatography and the GST moiety removed by treatment with PreScission protease. The recombinant enzyme showed phosphatase activity against the synthetic substrate pNPP, with a specific activity similar to that observed for ScPpz1 or its C-terminal catalytic domain (ScPpz1-Cter). Our attempts to express and purify significant amounts of full-length UmHal3 in *E. coli* were unsuccessful, possibly due to the large size of the protein. In contrast, we were able to purify both the UmPD and UmPD_ScCter polypeptides.

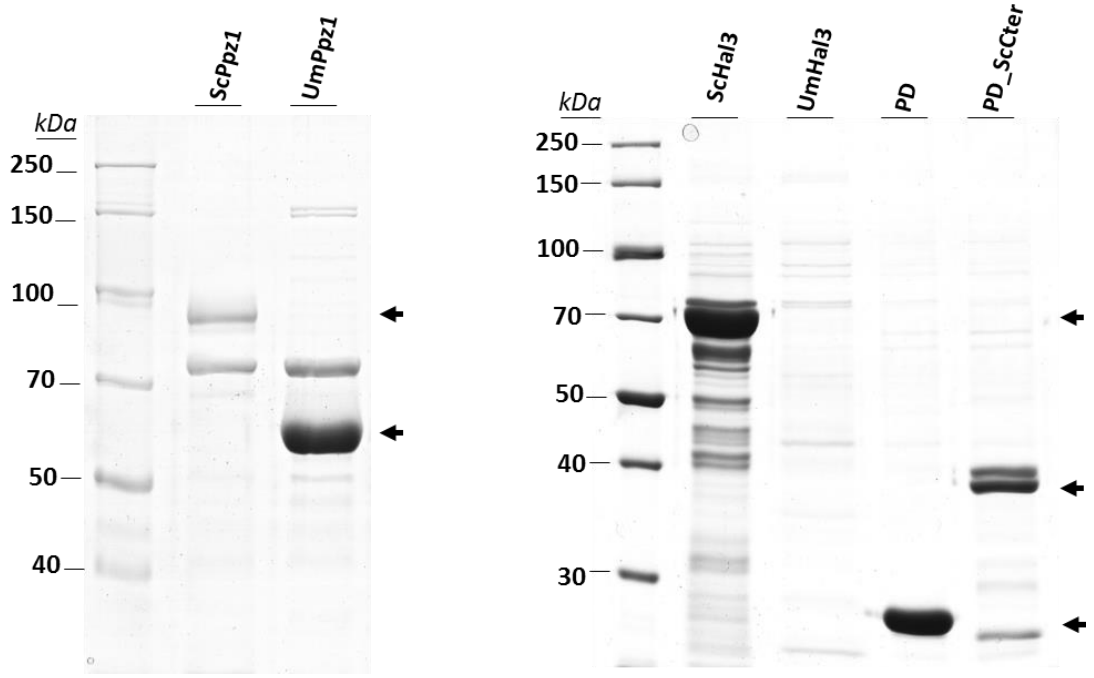

Figure 3.4 Expression in *E. coli* and purification of phosphatase proteins and Hal3-like proteins from *S. cerevisiae* and *U. maydis*.

Ten µl of purified phosphatase proteins as well as 5 µl of purified Hal3-like proteins from both *S. cerevisiae* and *U. maydis* were loaded in the SDS-PAGE (10%) after removing the GST tag by treatment with PreScission protease. The purified proteins were indicated by arrows.

3.4.1 Testing of the ScPpz1 and UmPpz1 inhibitory capacity of UmHal3 versions

We first set an assay to test the inhibitory properties of the Ustilago Hal3 proteins. As presented in Figure 3.4.1, neither UmHal3_PD nor UmPD_ScCter were able to inhibit recombinant ScPpz1, ScPpz1-Cter, or even UmPpz1. In contrast, ScHal3 was fully effective as an *in vitro* inhibitor of UmPpz1. This implies that UmPpz1 retains the structural features required to be inhibited by functional Hal3 proteins and suggest that the UmHal3_PD and UmPD_ScCter variants of UmHal3 are devoid of Ppz1 inhibitory properties.

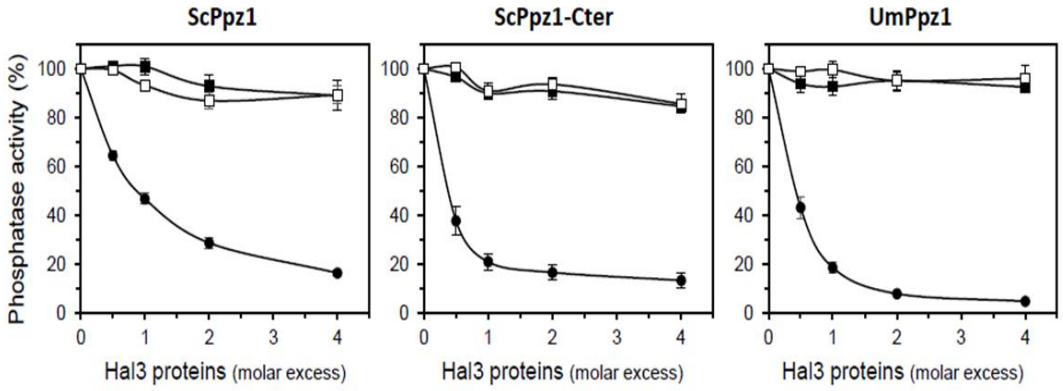

Figure 3.4.1 Inhibitory capacity of different UmHal3 versions on ScPpz1 and UmPpz1.

Five to ten pmols of ScPpz1, ScPpz1-Cter, or UmPpz1 were pre-incubated for 5 min at 30 °C with different amounts of ScHal3 (-●-), UmHal3_PD (-■-) or UmPD_ScCter (-□-), and the assay was initiated by addition of the substrate. Data are means ± SEM from 4 to 7 different assays and correspond to the ratio of phosphatase activity in the presence and the absence of inhibitor, expressed as percentage. Two different preparations of the phosphatases and the inhibitors were tested.

3.4.2 Evaluation of the interaction of UmHal3 variants with ScPpz1 and UmPpz1

The inability of UmHal3 proteins to inhibit ScPpz1 or UmPpz1 could be due to the incapacity for these proteins to effectively interact with the phosphatases. To test this, we set a pull-down assay using as baits the recombinant GST-tagged phosphatases bound to the glutathione resin that were incubated with *S. cerevisiae* extracts containing equivalent amounts of HA-tagged ScHal3, UmHal3, UmHal3_PD or UmPD_ScCter. As shown in Figure 3.4.2A, ScHal3 effectively interacts with UmPpz1, whereas full-length UmHal3 and UmHal3_PD are barely visible in the assay (see Figure 3.4.2B) and UmPD_ScCter cannot be detected. On the other hand (Figure 3.4.2C), full-length UmHal3 weakly interacts with both ScPPz1 and ScPpz1-Cter. Weak signals can be also observed for UmHal3_PD and UmPD_ScCter when ScPpz1 is used as bait, but they are not detected when the interaction with ScPpz1-Cter is tested (even if these lanes are overloaded, as in Figure 3.4.2A). Collectively, our results indicate that ScHal3 can effectively bind to and inhibit UmPpz1, and that UmHal3 can (even weakly) interact with ScPpz1 and ScPpz1-Cter, but it is completely unable to inhibit their phosphatase activity.

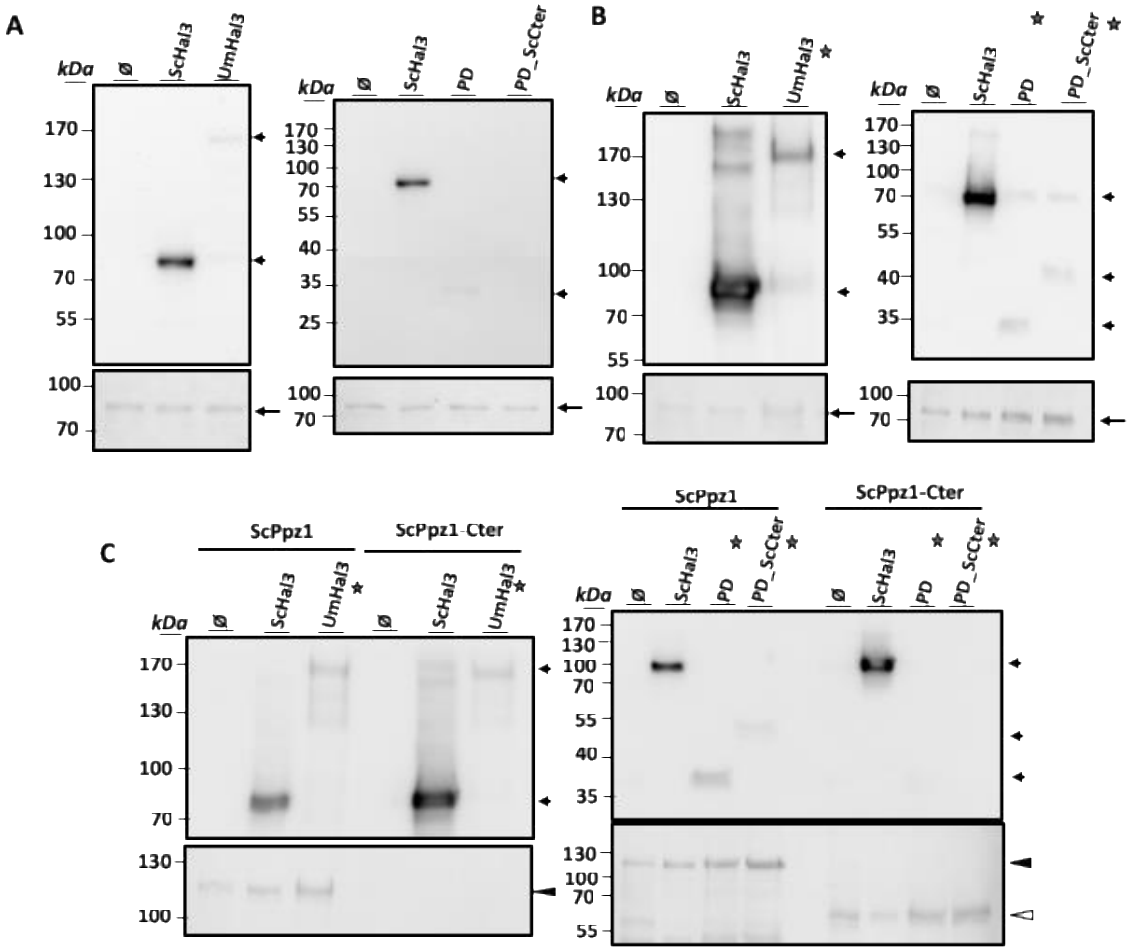

Figure 3.4.2 Evaluation of the interaction between UmHal3 variants with ScPpz1 and CnPpz1.

Glutathione beads containing 4 μg of the GST-tagged UmPpz1 (panel A), 8 μg of the GST-tagged UmPpz1 (panel B), or 8 μg of ScPpz1 and ScPpz1-Cter (panel C) were immobilized on glutathione beads and mixed with extracts from IM021 (*ppz1 hal3*) cells expressing 3HA-tagged ScHal3, UmHal3, UmHal3_PD (PD) or UmHal3_PD_ScCter from the pWS93 plasmid. Beads were washed, resuspended in 100 μl of 2x sample buffer and processed for SDS-PAGE (6% gels for UmHal3 and 10% for PD and PD_ScCter). Typically, 25 μl of the samples was used, except in lanes marked with an asterisk, where 50 μl was employed. Proteins were immunoblotted using anti-HA antibodies as described in Methods. Ponceau staining of the membranes is shown to evaluate for correct loading and transfer (ScPpz1-Cter was not seen in the left blot in panel B because due to its relatively low molecular mass run with the front of the 6% gel). The arrow indicates GST-UmPpz1, the black triangle indicates GST-ScPpz1 and the white triangle indicates GST-ScPpz1-Cter.

3.5 UmHal3 is a functional PPCDC enzyme

3.5.1 UV-visible scanning of purified recombinant UmHal3_PD

UV-visible scanning of purified recombinant UmHal3_PD preparations showed peaks at 382 and 452 nm, characteristic of the presence of an oxidized flavin, which is a cofactor involved in the PPCDC catalytic process. In addition, UmHal3 contains all the structural determinants necessary for PPCDC activity (such as catalytic His, Asn and Cys residues, see Figure 3.1). To confirm the possible PPCDC function of UmHal3 we set out two functional tests.

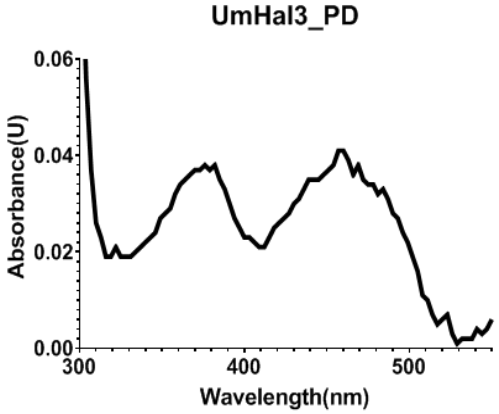

Figure 3.5.1 UV-spectrum of recombinant UmHal3_PD

GST-UmHal3_PD was expressed in *E. coli* and, after removal of the GST moiety, the visible-UV absorption profile was recorded. Note the appearance in the protein of two peaks characteristic of flavin-containing proteins.

3.5.2 Functional evaluation of UmHal3 proteins as PPCDC in *E. coli*

As described for the *Cryptococcus* study, we transformed the temperature-sensitive *E. coli* strain BW369 with pGEX-derived vectors containing UmHal3, UmHal3_PD and UmPD_ScCter. In parallel, this strain was transformed with AtHal3 (positive control) or ScHal3 (negative control). As shown in Figure 3.5.2, all three versions of UmHal3 were able to restore growth of the BW369 strain at 37 ˚C, suggesting that all three are able to provide PPCDC activity (even if UmHal3 is presumably expressed at very low levels, see Figure 3.4).

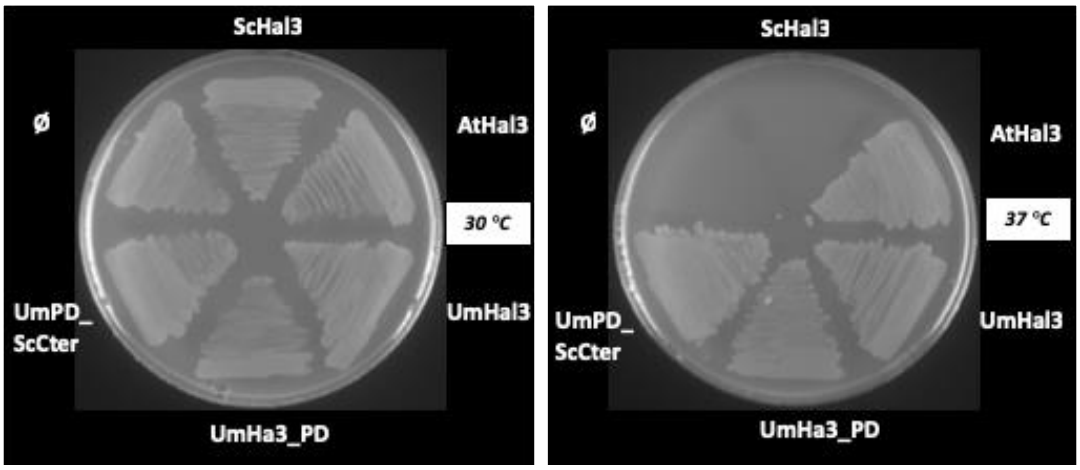

Figure 3.5.2 Evaluation of UmHal3 as functional PPCDC in *E. coli*

The empty pGEX6P-1 plasmid (∅) and the same vector bearing the *Arabidopsis* AtHal3 (as positive control), ScHal3 (as negative control), full-length UmHal3, and the indicated UmHal3 variants were introduced into the *E. coli* strain BW369, which carries the *dfp-707*^{ts} mutation that abolish PPCDC activity when cells are grown at 37 °C. Transformants were grown at 30 °C, diluted till OD_{600} = 0.05, transferred to the permissive (30 °C) or 37°C (non-permissive) temperatures for 6 h, and then plated at the indicated temperatures. Growth at 37 °C indicate complementation of the *ts* PPCDC mutation.

3.5.3 PPCDC functional evaluation of UmHal3 proteins in *S. cerevisiae*

In a second test, UmHal3 derivatives were introduced in diploid *S. cerevisiae* strains heterozygous for the *cab3* or the *hal3 vhs3* mutations, and the ability of the *Ustilago* proteins to rescue the deletion mutants was monitored by random spore analysis and/or tetrad analysis. As observed in Figure 3.5.3, expression of all three *Ustilago* variants allowed growth of the mutant haploid strains, as deduced from the germination of all four spores in the tetrads. Therefore, full-length UmHal3 can substitute either Cab3 and Hal3 (and Vhs3) in *S. cerevisiae* and provide PPCDC activity. As expected, this property can be assigned to the most C-terminal section of the protein.

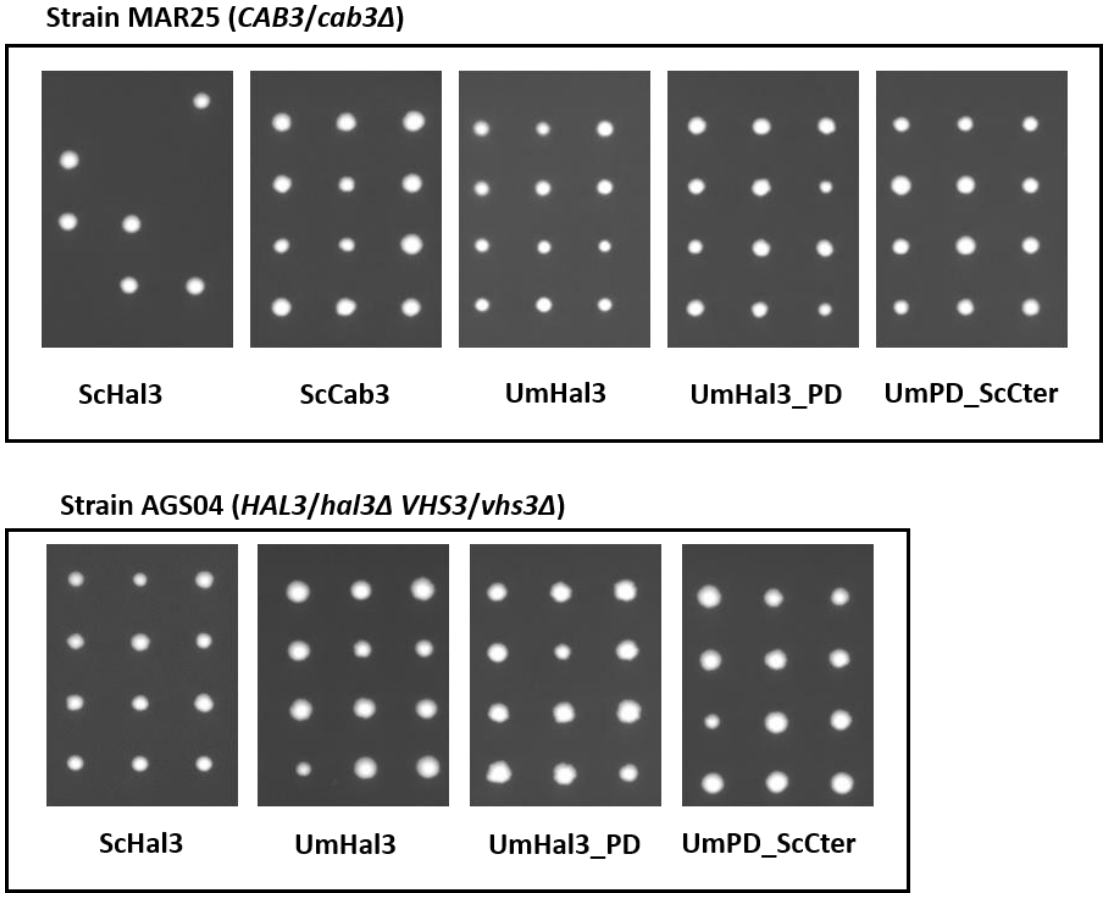

Figure 3.5.3 Evaluation of UmHal3 as functional PPCDC in *S. cerevisiae*

The heterozygous diploid strains MAR25 (*CAB3*/*cab3*Δ) and AGS04 (*HAL3*/*hal3*Δ *VHS3/vhs3*Δ) were transformed with the indicated plasmids, sporulation was induced, and spores from diverse asci (9 to 26 per transformation) were isolated with a micromanipulator and incubated for 3 days to form colonies. Note that *U. maydis* full-length UmHal3, as well as of its variants containing the PD domain, rescue the lethal phenotype of the *cab3* and *hal3 vhs3* mutations in haploidy, as denoted by germination and growth of all four spores in the tetrad.

Discussion

The fungus-specific serine/threonine phosphatase Ppz1 has been postulated as a potential novel target for antifungal therapy (Adam *et al.* 2012; Chen *et al.* 2016; Molero *et al.* 2017). A previous genome-wide study has established in *S. cerevisiae* that Ppz1 is one of the most toxic protein when overexpressed under the control of the *GAL1-10* promoter (Makanae *et al*. 2012). However, the knowledge of the molecular basis of Ppz1 toxicity is virtually null. Two negative regulators of Ppz1, Hal3 and Vhs3, have been characterized in the past (Muñoz *et al*. 2004). Furthermore, Ruiz and coworkers demonstrated that these two regulators also perform a functional role in CoA biosynthesis (Ruiz *et al.* 2009), thus explaining the requirement for the presence of at least one of these proteins in the yeast cell. Overall, these facts point out to two possible explanations for Ppz1 toxicity: one is that the excess phosphatase activity from overexpressing *PPZ1* might be deleterious (i.e., by blocking the cell cycle); the other is that the excess of Ppz1 might titrate down its negative regulators, Vhs3 and/or Hal3, resulting in shortage of components for functional PPCDC trimer formation.

To seek the potential explanation, and to avoid overexpression of Ppz1 from a plasmid vector, we constructed strain ZCZ01, which allows chromosomal expression of Ppz1 from a galactose-inducible promoter. Strain ZCZ01 displayed a clear-cut growth defect under induction using various galactose concentrations. Further immunoblot analysis confirmed the strong overexpression of Ppz1 in these conditions in a matter of less than one hour when cells were gown in a non-repressing carbon source (raffinose). Therefore, the behavior of this conditional Ppz1-overexpressing ZCZ01 strain mimic the one resulting from overexpression of Ppz1 from plasmid vectors. The observation that the introduction of high-copy vectors bearing Hal3 or Vhs3 was able to overcome the toxicity of Ppz1 overexpression was not sufficient to eliminate any of the two alternative possibilities. However, we found that expression of Hal3 was able to allow virtually normal growth to strain ZCZ01, while that of Vhs3 was also positive, but less effective compared to Hal3. Because it has been shown that Vhs3 exhibits *in vivo* lesser capacity to inhibit Ppz1 than Hal3 (Muñoz *et al.* 2004)., this observation may suggest that, indeed, the beneficial effect of Hal3 overexpression would be the counteraction of the excess of Ppz1 activity. This notion was finally confirmed by the observation that the human HsHal3 cDNA, which has been shown to be a functional PPCDC in *S. cerevisiae* able to fully support growth in a triple *hal3 vhs3 cab3 S. cerevisiae* mutant (Ruiz *et al.* 2009), was totally ineffective in rescuing the deleterious phenotype. This failure strongly supports the hypothesis that the toxic effects of Ppz1 overexpression derive from excessive Ppz1 activity and not from interference with

the PPCDC function. Further support came from experiments employing diverse Hal3 variants with differences in their ability to bind to and inhibit Ppz1, since it was observed that the Hal3 versions retaining most of the capacity to inhibit the phosphatase activity could rescue the lethal phenotype while the versions lacking such ability did not. Final evidence was provided by the observation that overexpression of the inactive phosphatase version $Ppz1^{R451L}$ was not toxic. In summary, these results suggest that there is a close association between excessive Ppz1 phosphatase activity and cellular toxicity.

The relevant point was now to investigate the reason(s) behind the toxicity of the excessive Ppz1 activity. It was known that Ppz1 inhibits the entry of potassium via the Trk transporters, thus making the defective transport of potassium an evident reason for Ppz1 toxicity. However, we have observed that a surplus of potassium enough to support growth in a *trk1 trk2* mutant, could not ameliorate the detrimental effect of the excess of Ppz1. Therefore, the relevant Ppz1 targets were still unclear.

Transcriptomic time-course profiling of the galactose-induced Ppz1 strain ZCZ01 provided some insights into cellular functions possibly altered by the excess of Ppz1. The analysis of the data after overexpressing Ppz1 for 2 and 4 hours, showed many up-regulated genes known to respond to oxidative stress. For example, *TSA2*, *SRX1* and *AHP1* are described as cytoplasmic 2-Cys peroxiredoxins which have multiple roles in stress protection, acting as antioxidants, molecular chaperones, and in the regulation of signal transduction (Wood *et al.* 2003; Biteau *et al.* 2003; Morgan and Veal 2007); *GTT1*, encoding a functional glutathione transferase, is involved in converting glutathione to its oxidized disulfide form (Choi *et al.* 1998); *GPX1*, encoding a phospholipid hydroperoxide glutathione peroxidase, is able to protect membrane lipids against peroxidation (Inoue *et al.* 1999; Avery and Avery 2001); *CTT1* encodes the cytosolic catalase, which plays important roles in the maintenance of redox balance (Izawa *et al.* 1996). Overall, these genes have been identified to be up regulated in response to reactive oxygen species (ROS) (Morano *et al.* 2012). In fact, parallel work in the laboratory has proven that, indeed, ROS markedly increase between 2 and 4 h after Ppz1 induction (Marcel Albacar, personal communication). Therefore, increased levels of Ppz1 do triggers generation of ROS, which leads to transcriptional activation of genes involved in oxidative stress response.

It is worth noting that oxidative stress conditions impact on protein synthesis at multiple levels (Shenton *et al.* 2006; Simpson and Ashe 2012). For instance, cells lacking eEF1Bα, the catalytic subunit of the elongation factor eEF1B, have shown increased

resistance to oxidative stress (Olarewaju *et al.* 2004); oxidative stress conditions have been shown to promote misreading including translational read-through of stop codons and frameshifting (Gerashchenko *et al.* 2012; Jamar *et al.* 2017). Moreover, Ppz1 was demonstrated to interact with eEF1Bα and affect the translation fidelity (de Nadal *et al.* 2001). In addition, Ppz1 was reported to influence the read-through efficiency and manifestation of non-Mendelian anti-suppressor determinant [ISP(+)] (Aksenova *et al.* 2007; Rogoza *et al.* 2009; Ivanov *et al.* 2010; Nizhnikov *et al.* 2014). Remarkably, current evidence gathered in our laboratory suggest that the excess of Ppz1 negatively affect translation, possibly at the initiation step. Therefore, it is conceivable that this effect could be secondary to the generation of intracellular ROS by the excess of Ppz1.

The *ADE* genes were found to be down-regulated after overexpression of Ppz1 for 4 hours. These genes encode the *de novo* pathway converting PRPP (5-phosphoribosyl-α-1-pyrophosphate) into the first purine nucleotide, IMP (inosine monophosphate), which is regulated by two *trans*-acting factors, Bas1 and Pho2 (Bas2) (Daignan-Fornier and Fink 1992; Denis *et al.* 1998; Tibbetts and Appling 2000). Purine nucleotides occupy a central position in cellular metabolism (Rolfes 2006), as they are the source for DNA and RNA molecules, as well as for ATP and redox cofactors (NAD^+, FAD). Interestingly, impaired expression of most AMP biosynthetic genes was also reported in response to oxidative stress, and this effect could be explained by a defective interaction between Bas1 and Bas2 (Pinson *et al.* 2000). We specifically observed that *ADE17*, but not *ADE16*, was clearly repressed upon overexpression of *PPZ1* (Figure 1.5.2). Both *ADE16* and *ADE17* genes encode 5-aminoimidazole-4-carboxamide ribonucleotide (AICAR) transformylase isozymes that catalyze the penultimate step of the *de novo* purine biosynthesis pathway. Although these two proteins are 80% identical to each other in amino acid sequence, the *ADE17* gene product accounts for approximately 90% of the total AICAR transformylase activity *in vivo* (Tibbetts and Appling 1997). In contrast to *ADE17, ADE16* is not regulated by Bas1 and is not repressed by oxidative stress (Pinson *et al.* 2000). This parallelism in the *ADE* transcriptional response suggest that the effect of Ppz1 overexpression on *ADE* genes expression could be the consequence of the oxidative stress generated upon overexpression of the phosphatase.

The study of Ppz1 protein phosphatases from pathogenic fungi is relatively recent, but evidence for the involvement of this enzyme in virulence has already been obtained in *Candida albicans* and *Aspergillus fumigatus* (Adam *et al*. 2012; Leiter *et al*. 2012; Manfiolli *et al*. 2017). In addition, the elucidation of the three-dimensional structure of CaPpz1

revealed several novel elements present in the catalytic domain of the phosphatase, which creates novel binding surfaces, suggesting that these unique structural elements are suitable for the development of CaPpz1-specific inhibitors (Chen *et al.* 2016). Taken together, these evidences suggest that Ppz1 has the potential to become a novel target for antifungal therapy (Adam *et al.* 2012; Chen *et al.* 2016; Molero *et al.* 2017). Therefore, we decided to characterize the Ppz/Hal3 phosphatase system from the human pathogenic fungus *C. neoformans* and the plant pathogenic fungus *U. maydis*.

To characterize the Ppz/Hal3 phosphatase system from *C. neoformans*, we expressed CnPpz1 in *S. cerevisiae*, and purified the protein from *E. coli*. We observed that CnPpz1 is able to replace endogenous Ppz1 in *S. cerevisiae* to some extent, indicating the ability of the *Cryptococcus* phosphatase to impact on specific *S. cerevisiae* intracellular targets. However, in contrast to ScPpz1 and under the same strong overexpression conditions, CnPpz1 did not block growth. Since we have confirmed that ScPpz1 toxicity is related to its phosphatase activity (see section 1), this disparity might be due to a lower phosphatase activity, either because the *Cryptococcus* enzyme is intrinsically less active (in agreement with the 3- to 5-fold lower specific activity measured for recombinant CnPpz1), or could be caused by more unstable mRNA or protein, yielding lower amounts of enzyme that might be insufficient for cell growth blockage. However, this possibility is less likely, since toxicity is not seen even in the absence of Hal3 (see below). Alternatively, the lack of toxicity could be derived from the inability of CnPpz1 to interact with the relevant *S. cerevisiae* targets.

We also showed that CnPpz1 contains the structural requirements for interaction with both homologous and heterologous Hal3 proteins. Since both *C. neoformans* Hal3-like proteins bind to the *Cryptococcus* phosphatase as well as to the C-terminal half of ScPpz1, it can be deduced that the structural elements required for interaction with Ppz1-like enzymes are retained in these putative regulatory proteins. It should be noted that, although the level of identity of both *Cryptococcus* proteins with ScHal3 is roughly similar (~29%), only CnHal3b shows detectable interaction with full length ScPpz1. CnHal3a binds to the catalytic domain of ScPpz1, but the interaction with the full-length form of the phosphatase is hardly detectable. This suggests that the long N-terminal extension present in ScPpz1 may act as a discriminator between both *Cryptococcus* Hal3-like proteins. It has been previously hypothesized that the long N-terminal region of ScPpz1 may serve to protect the phosphatase against excessive interaction with Hal3 and subsequent inhibition (de Nadal *et al*. 1998; Clotet *et al*. 1999). Indeed, ScHal3 interacts very strongly with full

length CnPpz1 (even more than with full length ScPpz1). In comparison with ScPpz1, CnPpz1 features a rather short N-terminal region. Therefore, this region may be unable to provide protection against ScHal3, a notion supported by the fact that removal of the CnPpz1 N-terminal region does not strengthen the interaction. Remarkably, despite the ability to interact up to some extent with ScPpz1 or CnPpz1, the *Cryptococcus* Hal3-like proteins are completely ineffective as phosphatase inhibitors *in vitro*. The failure of CnHal3a and CnHal3b to inhibit Ppz phosphatases is not due to the different sequence within the loop in ScHal3 known to be relevant for inhibition but not necessary for interaction(Muñoz *et al.* 2004), since replacement of this region in CnHal3b with the *S. cerevisiae* sequence did not improve inhibition *in vitro* (Figure 2.4.2). In comparison with AtHal3, ScHal3 has an extra insert (residues 312-350) that is also present in both CnHal3a and CnHal3b but about half in length. However, it is unlikely that such a difference could explain the lack of regulatory competence, since deletion of that region in ScHal3 did not abolish its inhibitory ability (Abrie *et al.* 2012).

Phenotypic analysis of the overexpression of CnHal3a and CnHal3b in Hal3-deficient cells indicated that only the latter significantly increased the tolerance to Li^+ cations (Figure 2.3). In contrast, the *C. neoformans* proteins were unable to decrease tolerance to caffeine in wild type cells or induce cell lysis in the *slt2* mutant, even if the proteins were expressed at substantial levels. In fact, expression of CnHal3b conferred a slight increase in tolerance to caffeine in the *slt2* background. We show that CnHal3b binds to ScPpz1 but cannot inhibit the phosphatase (Figure 2.4.1). Therefore, the increase in tolerance can be interpreted as a displacement of native ScHal3, the effective regulator, from its normal interaction with ScPpz1, thus yielding a phenotype reminiscent to that of a *hal3* mutant (hypertolerant to caffeine). A similar effect was observed upon overexpression of ScCab3, which binds to ScPpz1 but cannot inhibit its activity (Ruiz *et al.* 2009). The observation that replacement of the C-terminal tail of CnHal3b (which is not rich in acidic residues) with the equivalent region of ScHal3 further increased tolerance to LiCl without effecting tolerance to caffeine supports previous reports (Ferrando *et al*. 1995; Abrie *et al*. 2012) on the importance of an acidic region at the C-terminus of the Hal3 proteins to be effective modulators of the Ppz1 function on cation homeostasis *in vivo*.

We show that both CnHal3a and CnHal3b can independently function as PPCDCs in *S. cerevisiae* and *E. coli*, suggesting that they are able to form productive homotrimeric enzymes. Although the ability to form homotrimers was confirmed *in vitro* for CnHal3b, we cannot rule out the possibility that in *C. neoformans* CnHal3a and CnHal3b may combine to

form different heterotrimers and that these combinations could be the preferred forms *in vivo*. Alternatively, each protein could be specifically expressed under particular conditions. In any case, this work provides the first evidence of a fungus equipped with two functional PPCDCs, raising the question as to why these apparently redundant proteins have been conserved through evolution.

To assess the characteristics of the Ppz/Hal3 phosphatase system from *U. maydis*, in this study UmPpz1 was expressed/overexpressed in *S. cerevisiae* and purified from *E. coli*. We observed that UmPpz1 could partially replace endogenous Ppz1 in *S. cerevisiae*, suggesting that the *Ustilago* phosphatase has the capacity to impact on specific intracellular targets of *Saccharomyces* phosphatase. Our collaborator, Dr. Pérez-Martín (IBFG, Salamanca), observed that the *Ustilago ppz1* mutant was sensitive to CFW, indicating that UmPpz1 is potentially involved in the CWI pathway. Previous researches suggested that the link between Ppz phosphatases and the Slt2/Mpk1 pathway in *S. cerevisiae* is based on the regulatory role of the phosphatase on potassium uptake (Yenush *et al.* 2002; Merchan *et al.* 2004). However, ionic homeostasis mechanisms have been shown to be different in *U. maydis* and *S. cerevisiae* (Benito *et al.* 2009). Thus, the internal Na^+/K^+ ratio in *U. maydis* can be > 2 without detrimental effects. In addition, *U. maydis* has two ENA ATPases, UmEna1 and UmEna2. UmEna1 is a typical ENA ATPase, althouhg it shows low-Na^+/K^+ discrimination, whereas UmEna2 shows a different endosomal/ plasma membrane distribution and itsfunction is still unclear (Benito *et al.* 2009). Also, it has been demonstrated that *U. maydis* escapes from G_2 phase by activating the CWI pathway promotes (Carbó and Pérez-Martín 2010), which contrasts with the G_2 cell cycle arrest that occurs in *S. cerevisiae* in response to CWI pathway activation (Harrison *et al.* 2001). Therefore, even if the phosphatases in both organisms are functionally related to the CWI, the underlying mechanisms are likely different.

In contrast to CnPpz1 (Figure 2.2), expression of UmPpz1 was unable to reduce the tolerance of *ppz1* mutant cells to Li^+ cations. It could be hypothetised that the lack of the arginine-rich conserved motif in the N-terminal half of UmPpz1, which was found to be important for cation tolerance in *D. hansenii* (Minhas *et al.* 2012), was the reason for such failure. However, this motif is also absent in the N-terminal region of CnPpz1. Besides, a CaPpz1 mutated version lacking this conserved motif retains the ability to restore normal Li^+ tolerance *in vivo* (Szabó *et al.* 2019). Therefore, the dissimilarity in cation tolerance fucntions does not necessarily stem from the presence or absence of such motif, but most likely from the disparate abilities of Ppz1 orthologs to interact with the relevant *S. cerevisiae*

targets. On the other hand, when UmPpz1 was strongly overexpressed from the *GAL1-10* promoter, growth of *S. cerevisiae* was not blocked even if the expression levels of UmPpz1 and ScPpz1 were confirmed to be similar by immunoblot analysis and UmPpz1 and ScPpz1 exhibited similar *in vitro* phosphatase activity. Overall, these results suggest that the phosphatase activity level of UmPpz1 and ScPpz1 are alike *in vivo*. It must be noted that work in our laboratory (Carlos Calafí, personal communication) has shown that when the myristoylation site is mutated, the toxicity of Ppz1 in *S. cerevisiae* significantly decreases. Remarkably, in contrast to other characterized Ppz1 orthologs in diverse fungal species, such as *D. hansenii*, *C. albicans*, *A. fumigatus* and *C. neoformans,* the myristoylation site does not exist in UmPpz1 (see supplementary information 1). However, it is difficult to reconcile the presence or absence of this structural feature with Ppz1 toxicity, since it has been found that overexpression of DhPpz1 in *D. hansenii* does not affect growth (Minhas *et al*. 2012), and overexpression of CnPpz1 in *S. cerevisiae* has no harmful effects (this work).

The structures required for interaction with both homologous and heterologous Hal3 proteins also exist in UmPpz1. We observed that the *Ustilago* phosphatase could bind to *U. maydis* Hal3 proteins and *S. cerevisiae* Hal3, while the interactions between UmPpz1 and UmHal3_PD/UmPD_ScCter are hardly detectable. In addition, the interactions between ScPpz1 and all three Hal3 versions from *U. maydis* are quantitatively similar to that observed for the UmPpz1, but only the interaction between the full-length UmHal3 and ScPpz1-Cter is detected. Together, these results suggest that the long N-terminal extension of UmHal3 does not influence the interaction with the phosphatases from both *U. maydis* and *S. cerevisiae*. However, in contrast to what is seen for the *S. cerevisiae* and *C. neoformans* proteins (de Nadal *et al.* 1998; Clotet *et al.* 1999; Zhang *et al.* 2019), none of the *Ustilago* Hal3 versions showed increased interaction with ScPpz1-Cter than with ScPpz1. This suggests that the N-terminal region of ScPpz1 does not influence the weak interaction between UmHal3 proteins and *S. cerevisiae* phosphatase. Remarkably, despite the ability to interact up to some extent with ScPpz1 or UmPpz1, the *Ustilago* Hal3-like proteins are completely ineffective as phosphatase inhibitors *in vitro*. This fact, also observed for the *C. neoformans* Hal3a and Hal3b proteins, provide additional support to the idea that the structural determinants in Hal3 responsible for binding and inhibition of Ppz1 are different (Muñoz *et al*. 2004; Molero *et al*. 2017; Zhang *et al*. 2019).

We also observed that the overexpression of UmHal3 and UmHal3_PD in *S. cerevisiae* cells lacking ScHal3 could not increase the tolerance to Li^+ and Na^+ cations (Figure 3.3.1). Besides, both the entire and PD region of *U. maydis* Hal3 were unable to decrease

tolerance to caffeine in the *hal3* mutant, although the immunoblot analysis revealed that the proteins were expressed at substantial levels. However, addition of the C-terminal tail of ScHal3 to the UmHal3 PD region, resulted in an increase in tolerance to Li^+ and Na^+ without effecting tolerance to caffeine, similarly to what observed for CnHal3b (Figure 2.5.1). Both phenotypes support previous reports (Ferrando *et al*. 1995; Abrie *et al*. 2012) highlighting the importance of the acidic-rich tail of ScHal3 in cation homeostasis.

We explored the capacities of *Ustilago* Hal3 proteins to be an independently functional PPCDCs in *S. cerevisiae* and *E. coli*, including the entire protein, the PD domain UmHal3_PD and the PD domain with the ScHal3 C-terminal tail. The observations supported the idea that all UmHal3 versions could act as effective PPCDC enzymes, indicating that they are able to form productive homotrimeric enzymes. The apparent absence in UmHal3 of Ppz1 regulatory functions suggest that, as we found for CnHal3b and CnHal3a in *C. neoformans*, the biological role of this protein may be restricted to the participation in the biosynthesis of CoA and, in this case, it would be the unique PPCDC encoded in the *U. maydis* genome. This would fit with evidence gathered by Dr. Pérez-Martín (IBFG, Salamanca), who recently demonstrated that UmHal3 is an essential gene in *U. maydis*.

It is worth noting, however, that the long N-terminal extension of UmHal3 contains a putative VPS9 domain. Vsp9 is a guanine nucleotide exchange factor involved in vesicle-mediated vacuolar protein transport (Hama *et al.* 1999). A similar combination of VPS9 domain and PD domain in one Hal3-like protein also exists in the maize pathogenic fungus *Sporisorium scitamineum* and the sugarcane pathogenic fungus *Sporisorium reilianum*, which are closely related to *U. maydis* while have different infection symptoms (Schirawski *et al.* 2010; Dutheil *et al.* 2016). Therefore, the UmHal3-like protein may have the potential to perform as a moonlighting protein, as it is the case in *S. cerevisiae* and *C. albicans* although, if so, the non-PPCDC function would be different. It must be noted, however, that UmHal3 is not likely the *bona fide* Vps9 in *Ustilago*, since a closer protein (UM05369.1) is encoded in the genome of this fungus.

We demonstrated that both UmPpz1 and CnPpz1 are not controlled by Hal3-like proteins, which raises the question as how the activity of these phosphatases is regulated in *C. neoformans* and *U. maydis*. One possibility would be through phosphorylation. Although little data is available on the phosphoproteome of *C. neoformans*, two phosphorylated residues very near the C-terminal end (S497 and S506) of CnPpz1 have been identified (Selvan *et al.* 2014). This is interesting because in *S. cerevisiae* two

phosphorylated Ser have been found at positions similar to those described for CnPpz1 [(Holt *et al.* 2009; Swaney *et al.* 2013) and our own unpublished data]. Therefore, based on the conservation of specific phosphorylated sites, it could be hypothesized that phosphorylation and not the interaction with Hal3-like proteins could be a regulatory mechanism for the Ppz1 phosphatase in *Cryptococcus*. Unfortunately, as far as we know, no phosphoprotomic data has been deposited for *U. maydis*. However, it is worth noting that the C-terminal tail of CnPpz1 and UmPpz1 are rather conserved (Supplementary Information 2), and the mentioned Ser residues are also found in the *Ustilago* phosphatase (Ser487 and Ser 496). In fact, analysis of potential phosphorylatable sites using the NetPhosYeast 1.0 (Ingrell *et al.* 2007). Server reveals that Ser487 and Ser 496 have high chance (score 0.918 and 0.772, respectively) to be phosphorylated. Therefore, the possible regulation of Ppz1 phosphatases by phosphorylation is worth investigating, because the question of how this activity is regulated in the plant pathogenic fungus *U. maydis* and the human pathogenic fungus *C. neoformans* is still open and remain a challenge.

In contrast with what has been described for human pathogenic fungi *C. albicans* (Adam *et al.* 2012) and *A. fumigatus* (Manfiolli *et al.* 2017), lack of Ppz1 in *C. neoformans* does not affect virulence (Zhang *et al.* 2019). Experiments to evaluate the virulence of a *U. maydis* strain lacking UmPpz1 are under way in the laboratory of our collaborator Dr. Pérez-Martín at the IBFG in Salamanca and should be ready by the end of spring 2019. UmPpz1 is not among the transcripts whose expression is altered in the genome-wide analysis of the response of the *U. maydis* upon infection of the host surface (Lanver *et al.* 2014). However, very often regulatory proteins involved in the control of key cellular processes are controlled post-translationally and not at the level of expression. In addition, many of the *U. maydis* effectors contributing to virulence are completely novel, lacking known structural or functional domains (Lanver *et al.* 2017), leaving open the possibility that UmPpz1 may be relevant in virulence because of its involvement of the regulation of the phosphorylation status of components of new pathways.

On the other hand, CnHal3b protein (but not CnHal3a) is demonstrated to be important for full virulence of *C. neoformans*, most likely due to its requirement for growth at 37 °C (Zhang *et al.* 2019). Further study revealed the 3D-structure of CnHal3b which is very similar to that of AtHal3a (the PPCDC from the plant *A. thaliana*) while predicts an extra α-helix in the CnHal3b structure not present in AtHal3 (nor in human PPCDC), due to the 17-residue sequence insertion from Val^{86} to Gly^{102} (Zhang *et al.* 2019). Similarly, UmHal3 has an even larger extra insert (residues 1256-1289) in comparison with AtHal3 and human

PPCDC (Figure 4). The presence of the inserted structural feature might serve as basis for the development of selective drugs for human beings and antifungal treatments for maize (as mentioned above, UmHal3 is an essential protein), targeting Coenzyme A biosynthesis by interfering with PPCDC catalytic site or trimerization interface. Drugs targeting this step in the pathway have not yet been reported (Moolman *et al.* 2014).

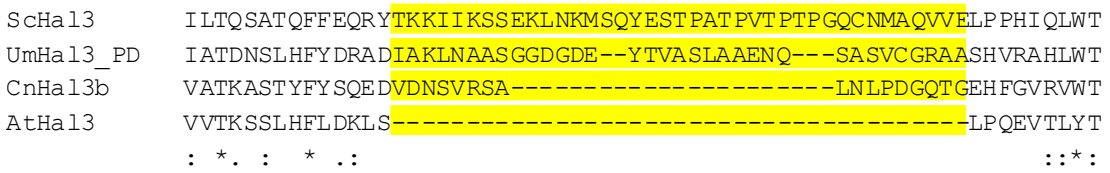

Figure 4 Comparison of ScHal3, UmHal3_PD, CnHal3b and AtHal3 protein sequences.

The amino acid sequences were aligned by the Clustal Omega multiple sequence alignment tool (https://www.ebi.ac.uk/Tools/msa/clustalo/). Yellow background indicates the extra inserts from ScHal3, UmHal3_PD and CnHal3b compared with AtHal3. Only the relevant insertion region is shown.

Conclusions

1.- We demonstrate that the toxic effect of the overexpression of Ppz1 is due to the increase in catalytic activity and not to a possible titration of the Hal3 and Vhs3 regulatory subunits, which are essential moonlighting proteins involved in the CoA biosynthetic pathway.

2.- We have constructed a yeast strain (ZCZ01) in which the Ppz1 ORF is expressed from the powerful regulatable promoter *GAL1-10*. This strain perfectly reproduces the toxic effects observed upon from *GAL1-10*-driven overexpression from Ppz1 episomal plasmids.

3.- Strain ZCZ01 has been used to investigate by RNA-Seq the transcriptional changes induced by overexpression of Ppz1 from 0.5 to 4 hours. Altogether, 890 genes were induced and 420 were repressed at least at one time-point.

4.- Analysis of the transcriptional response to Ppz1 overexpression revealed a strong response to oxidative stress, which might be the basis for the observed decrease in expression of the *ADE* biosynthetic pathway.

5.- We have identified in genome of *Cryptococcus neoformans* a likely gene encoding a Ppz1 phosphatase (CNAG_03673) named here CnPpz1, and two possible Hal3-like proteins, CnHal3a (CNAG_00909) and CnHal3b (CNAG_07348). These genes have been cloned and expressed in *S. cerevisiae* and *E. coli*.

6.- CnPpz1 is a functional phosphatase and partially replaced endogenous ScPpz1. Overexpression of CnPpz1 in *S. cerevisiae* was not toxic.

7.- Both CnHal3a and CnHal3b interact with ScPpz1 and CnPpz1 *in vitro* but did not inhibit their phosphatase activity. Consistently, when expressed in *S. cerevisiae,* they poorly reproduced the Ppz1-regulatory properties of ScHal3.

8.- In contrast, both CnHal3a and CnHal3b were functional monogenic PPCDCs and replaced the absence of Vhs3/Hal3 or Cab3 in *S. cerevisiae*, or bacterial PPCDC function in *E. coli*. This is the first description of a fungus with two functional PPCDC isoforms.

9.- Analysis of the *Ustilago maydis* genome revealed the presence of one gene encoding a putative Ppz phosphatase (UM04827.1, named here UmPpz1) and a single gene encoding a possible Hal3-like protein (UM05916.1, named here UmHal3). UmHal3 presents an anomalous structure: it is a very large protein (1430 residues) in which the PPCDC domain (PD region) is located at the very C-terminus.

10.- UmPpz1 is a functional phosphatase, but episomal expression of UmPpz1 in a *ppz1 S. cerevisiae* mutant did not normalize tolerance to Li^+ but restored normal tolerance to caffeine. Strong overexpression of UmPpz1 in *S. cerevisiae* did not negatively affected growth.

11.- Expression of UmHal3 or its PD region (UmHal3_PD) in a *hal3* strain did not improve tolerance to LiCl or NaCl nor affected tolerance to caffeine, suggesting that these proteins cannot regulate ScPpz1 *in vivo*. However, addition of the acidic tail present in ScHal3 (UmPD_ScCt) increased somewhat tolerance to LiCl, but not to caffeine.

12.- Neither UmPD nor UmPD_ScCt were able to inhibit recombinant ScPpz1, ScPpz1-Cter, or even UmPpz1. In contrast, ScHal3 was fully effective as an *in vitro* inhibitor of UmPpz1.

13.- Both full length UmHal3 and UmPD provide PPCDC function in *S. cerevisiae* and *E. coli* PPCDC-deficient strains. Therefore, UmHal3 does not reproduce the moonlighting properties of ScHal3.

References

Abrie J. A., A. González, E. Strauss, and J. Ariño, 2012 Functional mapping of the disparate activities of the yeast moonlighting protein Hal3. Biochem. J. 442: 357–368. https://doi.org/10.1042/bj20111466

Adam C., E. Erdei, C. Casado, L. Kovacs, A. Gonzalez, *et al.*, 2012 Protein phosphatase CaPpz1 is involved in cation homeostasis, cell wall integrity and virulence of Candida albicans. Microbiology 158: 1258–1267. https://doi.org/10.1099/mic.0.057075-0

Adams A., D. E. Gottschling, C. A. Kaiser, and T. Stearns, 1997 *Methods in Yeast Genetics*. Cold Spring Harbor Laboratory Press, NY , Cold Spring Harbor, NY.

Aggarwal M., and A. K. Mondal, 2006 Role of N-terminal hydrophobic region in modulating the subcellular localization and enzyme activity of the bisphosphate nucleotidase from Debaryomyces hansenii. Eukaryot. Cell 5: 262–71. https://doi.org/10.1128/EC.5.2.262-271.2006

Aggarwal M., and A. K. Mondal, 2009 Debaryomyces hansenii: An Osmotolerant and Halotolerant Yeast, pp. 65–84 in *Yeast Biotechnology: Diversity and Applications*, Springer Netherlands, Dordrecht.

Agrios G. N., 2005 *Plant pathology*. Elsevier Academic Press.

Aksenova A., I. Muñoz, K. Volkov, J. Ariño, and L. Mironova, 2007 The HAL3-PPZ1 dependent regulation of nonsense suppression efficiency in yeast and its influence on manifestation of the yeast prion-like determinant [ISP+]. Genes to Cells 12: 435–445. https://doi.org/10.1111/j.1365-2443.2007.01064.x

Albert A., M. Martínez-Ripoll, A. Espinosa-Ruiz, L. Yenush, F. A. Culiáñez-Macià, *et al.*, 2000 The X-ray structure of the FMN-binding protein AtHal3 provides the structural basis for the activity of a regulatory subunit involved in signal transduction. Structure 8: 961–969. https://doi.org/10.1016/S0969-2126(00)00187-8

Alepuz P. M., K. W. Cunningham, and F. Estruch, 1997 Glucose repression affects ion homeostasis in yeast through the regulation of the stress-activated ENA1 gene. Mol. Microbiol. 26: 91–98. https://doi.org/10.1046/j.1365-2958.1997.5531917.x

Andrews B., and V. Measday, 1998 The cyclin family of budding yeast: abundant use of a good idea. Trends Genet. 14: 66–72.

Andrews P. D., and M. J. Stark, 2000 Type 1 protein phosphatase is required for maintenance of cell wall integrity, morphogenesis and cell cycle progression in Saccharomyces cerevisiae. J. Cell Sci. 113: 507 LP-520.

Ariño J., 2002 Novel protein phosphatases in yeast. Eur. J. Biochem. 269: 1072–1077. https://doi.org/10.1046/j.0014-2956.2002.02753.x

Ariño J., J. Ramos, and H. Sychrova, 2010 Alkali metal cation transport and homeostasis in yeasts. Microbiol Mol Biol Rev 74: 95–120. https://doi.org/10.1128/MMBR.00042-09

Avery A. M., and S. V. Avery, 2001 Saccharomyces cerevisiae Expresses Three Phospholipid Hydroperoxide Glutathione Peroxidases. J. Biol. Chem. 276: 33730–33735. https://doi.org/10.1074/jbc.M105672200

Balcells L., N. Gomez, A. Casamayor, J. Clotet, and J. Ariño, 1997 Regulation of Salt Tolerance in Fission Yeast by a Protein-Phosphatase-Z-Like Ser/Thr Protein Phosphatase. Eur. J. Biochem. 250: 476–483. https://doi.org/10.1111/j.1432-1033.1997.0476a.x

Balcells L., R. Martín, M. C. Ruiz, N. Gómez, J. Ramos, *et al.*, 1998 The Pzh1 protein phosphatase and the Spm1 protein kinase are involved in the regulation of the plasma membrane H^+-ATPase in fission yeast. FEBS Lett. 435: 241–244. https://doi.org/10.1016/S0014-5793(98)01082-5

Balcells L., F. Calero, N. Gomez, J. Ramos, and J. Ariño, 1999 The Schizosaccharomyces pombe Pzh1 protein phosphatase regulates Na+ ion influx in a Trk1-independent fashion. Eur. J. Biochem. 260: 31–37. https://doi.org/10.1046/j.1432-1327.1999.00129.x

Banuett F., and I. Herskowitz, 1996 Discrete developmental stages during teliospore formation in the corn smut fungus, Ustilago maydis. Development 122: 2965–76.

Barford D., A. K. Das, and M.-P. Egloff, 1998 The Structure and Mechanism of Protein Phosphatases: Insights into Catalysis and Regulation. Annu. Rev. Biophys. Biomol. Struct. 27: 133–164. https://doi.org/10.1146/annurev.biophys.27.1.133

Barreto L., D. Canadell, D. Valverde-Saubí, A. Casamayor, and J. Ariño, 2012 The short-term response of yeast to potassium starvation. Environ. Microbiol. 14: 3026–3042. https://doi.org/10.1111/j.1462-2920.2012.02887.x

Basi G., E. Schmid, and K. Maundrell, 1993 TATA box mutations in the Schizosaccharomyces pombe nmt1 promoter affect transcription efficiency but not the transcription start point or thiamine repressibility. Gene 123: 131–136. https://doi.org/10.1016/0378-1119(93)90552-E

Bastians H., and H. Ponstingl, 1996 The novel human protein serine/threonine phosphatase 6 is a functional homologue of budding yeast Sit4p and fission yeast ppe1, which are involved in cell cycle regulation. J. Cell Sci. 109 (Pt 1: 2865–74.

Bastians H., H. Krebber, J. Hoheisel, S. Ohl, P. Lichter, *et al.*, 1997 Assignment of the human serine/ threonine protein phosphatase 4 gene (PPP4C) to chromosome 16p11-p12 by fluorescence in situ hybridization. Genomics 42: 181–182. https://doi.org/10.1006/geno.1997.4693

Battley E. H., 1992 *Yeasts: Characteristics and Identification.* Cambridge University Press.

Bauer R., F. Oberwinkler, and K. Vánky, 1997 Ultrastructural markers and systematics in smut fungi and allied taxa. Can. J. Bot. 75: 1273–1314. https://doi.org/10.1139/b97-842

Begley T. P., C. Kinsland, and E. Strauss, 2001 The biosynthesis of coenzyme A in bacteria. Vitam. Horm. 61: 157–71.

Ben-Ami R., R. E. Lewis, K. Leventakos, J.-P. Latgé, and D. P. Kontoyiannis, 2010 Cutaneous model of invasive aspergillosis. Antimicrob. Agents Chemother. 54: 1848–54. https://doi.org/10.1128/AAC.01504-09

Benito B., B. Garciadeblás, J. Pérez-Martín, and A. Rodríguez-Navarro, 2009 Growth at High pH and Sodium and Potassium Tolerance in Media above the Cytoplasmic pH Depend on ENA ATPases in Ustilago maydis . Eukaryot. Cell 8: 821–829. https://doi.org/10.1128/ec.00252-08

Bertl A., J. Ramos, J. Ludwig, H. Lichtenberg-Fraté, J. Reid, *et al.*, 2003 *Characterization of potassium transport in wild-type and isogenic yeast strains carrying all combinations of trk1, trk2 and tok1 null mutations*.

Biteau B., J. Labarre, and M. B. Toledano, 2003 ATP-dependent reduction of cysteine–sulphinic acid by S. cerevisiae sulphiredoxin. Nature 425: 980–984. https://doi.org/10.1038/nature02075

Bloecher A., and K. Tatchell, 1999 Defects in Saccharomyces cerevisiae protein phosphatase type I activate the spindle/kinetochore checkpoint. Genes Dev. 13: 517–22.

Bollen M., W. Peti, M. J. Ragusa, and M. Beullens, 2010 The extended PP1 toolkit: designed to create specificity. Trends Biochem. Sci. 35: 450–8. https://doi.org/10.1016/j.tibs.2010.03.002

Borkovich K. A., L. A. Alex, O. Yarden, M. Freitag, G. E. Turner, *et al.*, 2004 Lessons from the genome sequence of Neurospora crassa: tracing the path from genomic blueprint to multicellular organism. Microbiol. Mol. Biol. Rev. 68: 1–108.

Bosveld F., A. Rana, P. E. van der Wouden, W. Lemstra, M. Ritsema, *et al.*, 2008 De novo CoA biosynthesis is required to maintain DNA integrity during development of the Drosophila nervous system. Hum. Mol. Genet. 17: 2058–2069. https://doi.org/10.1093/hmg/ddn105

Brefort T., G. Doehlemann, A. Mendoza-Mendoza, S. Reissmann, A. Djamei, *et al.*, 2009 Ustilago maydis as a Pathogen. https://doi.org/10.1146/annurev-phyto-080508-081923

Calero F., and J. Ramos, 2003 K+fluxes in Schizosaccharomyces pombe. FEMS Yeast Res. 4: 1–6. https://doi.org/10.1016/S1567-1356(03)00111-9

Carbó N., and J. Pérez-Martín, 2010 Activation of the Cell Wall Integrity Pathway Promotes

Escape from G2 in the Fungus Ustilago maydis. PLoS Genet 6: 1001009. https://doi.org/10.1371/journal.pgen.1001009

Chang J. S., K. Henry, B. L. Wolf, M. Geli, and S. K. Lemmon, 2002 Protein phosphatase-1 binding to scd5p is important for regulation of actin organization and endocytosis in yeast. J. Biol. Chem. 277: 48002–8. https://doi.org/10.1074/jbc.M208471200

Chen M. X., A. E. McPartlin, L. Brown, Y. H. Chen, H. M. Barker, *et al.*, 1994 A novel human protein serine/threonine phosphatase, which possesses four tetratricopeptide repeat motifs and localizes to the nucleus. EMBO J. 13: 4278–90.

Chen E., M. S. Choy, K. Petrényi, Z. Kónya, F. Erdődi, *et al.*, 2016 Molecular Insights into the Fungus-Specific Serine/Threonine Protein Phosphatase Z1 in Candida albicans. MBio 7: e00872-16. https://doi.org/10.1128/MBIO.00872-16

Cho H., T. K. Kim, H. Mancebo, W. S. Lane, O. Flores, *et al.*, 1999 A protein phosphatase functions to recycle RNA polymerase II. Genes Dev. 13: 1540–52.

Choi J. H., W. Lou, and A. Vancura, 1998 A novel membrane-bound glutathione S-transferase functions in the stationary phase of the yeast Saccharomyces cerevisiae. J. Biol. Chem. 273: 29915–22.

Clotet J., F. Posas, A. Casamayor, I. Schaaff-Gerstenschlger, and J. Ariño, 1991 The gene DIS2S1 is essential in Saccharomyces cerevisiae and is involved in glycogen phosphorylase activation. Curr. Genet. 19: 339–342. https://doi.org/10.1007/BF00309593

Clotet J., F. Posas, E. de Nadal, and J. Ariño, 1996 The NH2-terminal extension of protein phosphatase PPZ1 has an essential functional role. J Biol Chem 271: 26349–26355.

Clotet J., E. Garí, M. Aldea, and J. Ariño, 1999 The yeast ser/thr phosphatases sit4 and ppz1 play opposite roles in regulation of the cell cycle. Mol. Cell. Biol. 19: 2408–15. https://doi.org/10.1128/MCB.19.3.2408

Cohen P., 1989 The structure and regulation of protein phosphatases. Annu Rev Biochem 58: 453–508.

Cohen P. T. W., 1997 Novel protein serine/threonine phosphatases: Variety is the spice of life. Trends Biochem. Sci. 22: 245–251. https://doi.org/10.1016/S0968-0004(97)01060-8

Cohen P. T. W., 2002 Protein phosphatase 1--targeted in many directions. J. Cell Sci. 115: 241–56.

Cohen P. T. W., A. Philp, and C. Vázquez-Martin, 2005 Protein phosphatase 4 - from obscurity to vital functions. FEBS Lett. 579: 3278–3286. https://doi.org/10.1016/j.febslet.2005.04.070

Como C. J. Di, R. Bose, and K. T. Arndt, 1995 Overexpression of SIS2, which contains an

extremely acidic region, increases the expression of SWI4, CLN1 and CLN2 in sit4 mutants. Genetics 139: 95–107.

Cooper G. M., 2000 The Eukaryotic Cell Cycle, in *The Cell: A Molecular Approach. 2nd edition.*, Sinauer Associates.

Csuros M., I. B. Rogozin, and E. V Koonin, 2011 A detailed history of intron-rich eukaryotic ancestors inferred from a global survey of 100 complete genomes. PLoS Comput. Biol. 7: e1002150. https://doi.org/10.1371/journal.pcbi.1002150

Cullen P. J., and G. F. Sprague, 2002 The Glc7p-interacting protein Bud14p attenuates polarized growth, pheromone response, and filamentous growth in Saccharomyces cerevisiae. Eukaryot. Cell 1: 884–94. https://doi.org/10.1128/EC.1.6.884-894.2002

Cyert M. S., and C. C. Philpott, 2013 Regulation of cation balance in Saccharomyces cerevisiae. Genetics 193: 677–713. https://doi.org/10.1534/genetics.112.147207

D'Souza C. A., J. W. Kronstad, G. Taylor, R. Warren, M. Yuen, *et al.*, 2011 Genome variation in Cryptococcus gattii, an emerging pathogen of immunocompetent hosts. MBio 2: e00342-10. https://doi.org/10.1128/mBio.00342-10

Dagenais T. R. T., and N. P. Keller, 2009 Pathogenesis of Aspergillus fumigatus in Invasive Aspergillosis. Clin. Microbiol. Rev. 22: 447–465. https://doi.org/10.1128/CMR.00055-08

Daignan-Fornier B., and G. R. Fink, 1992 Coregulation of purine and histidine biosynthesis by the transcriptional activators BAS1 and BAS2. Proc. Natl. Acad. Sci. U. S. A. 89: 6746–50. https://doi.org/10.1073/PNAS.89.15.6746

Daugherty M., B. Polanuyer, M. Farrell, M. Scholle, A. Lykidis, *et al.*, 2002 Complete Reconstitution of the Human Coenzyme A Biosynthetic Pathway via Comparative Genomics. J. Biol. Chem. 277: 21431–21439. https://doi.org/10.1074/jbc.M201708200

Dean R., J. A. L. Van Kan, Z. A. Pretorius, K. E. Hammond-Kosack, A. Di Pietro, *et al.*, 2012 The Top 10 fungal pathogens in molecular plant pathology. Mol. Plant Pathol. 13: 414–430.

Denis V., H. Boucherie, C. Monribot, and B. Daignan-Fornier, 1998 Role of the Myb-like protein Bas1p in Saccharomyces cerevisiae: a proteome analysis. Mol. Microbiol. 30: 557–566. https://doi.org/10.1046/j.1365-2958.1998.01087.x

Dever T. E., and R. Green, 2012 The elongation, termination, and recycling phases of translation in eukaryotes. Cold Spring Harb. Perspect. Biol. 4: 1–16. https://doi.org/10.1101/cshperspect.a013706

Dever T. E., T. G. Kinzy, and G. D. Pavitt, 2016 Mechanism and Regulation of Protein Synthesis in Saccharomyces cerevisiae. Genetics 203: 65–107. https://doi.org/10.1534/genetics.115.186221

Dibrov P., J. J. Smith, P. G. Young, and L. Fliegel, 1997 Identification and localization of the sod2 gene product in fission yeast. FEBS Lett. 405: 119–124. https://doi.org/10.1016/S0014-5793(97)00169-5

Djamei A., and R. Kahmann, 2012 Ustilago maydis: Dissecting the Molecular Interface between Pathogen and Plant, (J. Heitman, Ed.). PLoS Pathog. 8: e1002955. https://doi.org/10.1371/journal.ppat.1002955

Doehlemann G., R. Wahl, M. Vranes, R. P. de Vries, J. Kämper, *et al.*, 2008 Establishment of compatibility in the Ustilago maydis/maize pathosystem. J. Plant Physiol. 165: 29–40. https://doi.org/10.1016/J.JPLPH.2007.05.016

Doehlemann G., B. Ökmen, W. Zhu, and A. Sharon, 2017 Plant Pathogenic Fungi, pp. 703–726 in *The Fungal Kingdom*, American Society of Microbiology.

Dutheil J. Y., G. Mannhaupt, G. Schweizer, C. M. K. Sieber, M. Münsterkötter, *et al.*, 2016 A tale of genome compartmentalization: The evolution of virulence clusters in smut fungi. Genome Biol. Evol. 8: 681–704. https://doi.org/10.1093/gbe/evw026

Egloff M. P., P. T. Cohen, P. Reinemer, and D. Barford, 1995 Crystal structure of the catalytic subunit of human protein phosphatase 1 and its complex with tungstate. J. Mol. Biol. 254: 942–59. https://doi.org/10.1006/jmbi.1995.0667

Espinosa-Ruiz A., J. M. Bellés, R. Serrano, and F. A. Culiáñez-Maclà, 1999 Arabidopsis thaliana AtHAL3: a flavoprotein related to salt and osmotic tolerance and plant growth. Plant J. 20: 529–39.

FAOSTAT, 2013 *Statistical yearbook. World food and agriculture*. Food and Agriculture Organization of the United Nations (FAO), Roma.

Feng Z. H., S. E. Wilson, Z. Y. Peng, K. K. Schlender, E. M. Reimann, *et al.*, 1991 The yeast GLC7 gene required for glycogen accumulation encodes a type 1 protein phosphatase. J. Biol. Chem. 266: 23796–801.

Fernandez-Sarabia M. J., A. Sutton, T. Zhong, and K. T. Arndt, 1992 SIT4 protein phosphatase is required for the normal accumulation of SWI4, CLN1, CLN2, and HCS26 RNAs during late G1. Genes Dev. 6: 2417–28.

Ferrando A., S. J. Kron, G. Rios, G. R. Fink, and R. Serrano, 1995 Regulation of cation transport in Saccharomyces cerevisiae by the salt tolerance gene HAL3. Mol. Cell. Biol. 15: 5470–5481. https://doi.org/10.1128/mcb.15.10.5470

Fisher M. C., D. A. Henk, C. J. Briggs, J. S. Brownstein, L. C. Madoff, *et al.*, 2012 Emerging fungal threats to animal, plant and ecosystem health. Nature 484: 186–194. https://doi.org/10.1038/nature10947

Fones H. N., M. C. Fisher, and S. J. Gurr, 2017 Emerging Fungal Threats to Plants and Animals Challenge Agriculture and Ecosystem Resilience, pp. 787–809 in *The Fungal Kingdom*,

American Society of Microbiology.

Foulkes J. G., S. J. Strada, P. J. Henderson, and P. Cohen, 1983 A Kinetic Analysis of the Effects of Inhibitor-1 and Inhibitor-2 on the Activity of Protein Phosphatase-1. Eur. J. Biochem. 132: 309–313. https://doi.org/10.1111/j.1432-1033.1983.tb07363.x

Gaber R. F., C. A. Styles, and G. R. Fink, 1988 TRK1 encodes a plasma membrane protein required for high-affinity potassium transport in Saccharomyces cerevisiae. Mol. Cell. Biol. 8: 2848–59. https://doi.org/10.1128/MCB.8.7.2848

Gancedo C., and C.-L. Flores, 2008 Moonlighting proteins in yeasts. Microbiol. Mol. Biol. Rev. 72: 197–210, table of contents. https://doi.org/10.1128/MMBR.00036-07

Gancedo C., C.-L. Flores, and J. M. Gancedo, 2016 The Expanding Landscape of Moonlighting Proteins in Yeasts. Microbiol. Mol. Biol. Rev. 80: 765–777. https://doi.org/10.1128/MMBR.00012-16

García-Gimeno M. A., I. Muñoz, J. Ariño, and P. Sanz, 2003 Molecular characterization of Ypi1, a novel Saccharomyces cerevisiae type 1 protein phosphatase inhibitor. J. Biol. Chem. 278: 47744–52. https://doi.org/10.1074/jbc.M306157200

García-Muse T., G. Steinberg, and J. Pérez-Martín, 2003 Pheromone-induced G2 arrest in the phytopathogenic fungus Ustilago maydis. Eukaryot. Cell 2: 494–500.

García-Rodas R., R. J. B. Cordero, N. Trevijano-Contador, G. Janbon, F. Moyrand, *et al.*, 2014 Capsule growth in Cryptococcus neoformans is coordinated with cell cycle progression. MBio 5: e00945-14. https://doi.org/10.1128/mBio.00945-14

Garciadeblas B., F. Rubio, F. J. Quintero, M. A. Bañuelos, R. Haro, *et al.*, 1993 Differential expression of two genes encoding isoforms of the ATPase involved in sodium efflux in Saccharomyces cerevisiae. Mol. Gen. Genet. 236: 363–8.

Gerashchenko M. V, A. V Lobanov, and V. N. Gladyshev, 2012 Genome-wide ribosome profiling reveals complex translational regulation in response to oxidative stress. Proc. Natl. Acad. Sci. U. S. A. 109: 17394–9. https://doi.org/10.1073/pnas.1120799109

Ghosh A., S. Shuman, and C. D. Lima, 2008 Molecular Cell The Structure of Fcp1, an Essential RNA Polymerase II CTD Phosphatase. Mol. Cell 32: 478–490. https://doi.org/10.1016/j.molcel.2008.09.021

Gibbons J. A., D. C. Weiser, and S. Shenolikar, 2005 Importance of a surface hydrophobic pocket on protein phosphatase-1 catalytic subunit in recognizing cellular regulators. J. Biol. Chem. 280: 15903–11. https://doi.org/10.1074/jbc.M500871200

Gietz R. D., and A. Sugino, 1988 New yeast-Escherichia coli shuttle vectors constructed with in vitro mutagenized yeast genes lacking six-base pair restriction sites. Gene 74: 527–534.

Giga-Hama Y., H. Tohda, K. Takegawa, and H. Kumagai, 2007 Schizosaccharomyces pombe

minimum genome factory. Biotechnol. Appl. Biochem. 46: 147. https://doi.org/10.1042/BA20060106

Giraldo M. C., and B. Valent, 2013 Filamentous plant pathogen effectors in action. Nat. Rev. Microbiol. 11: 800–814. https://doi.org/10.1038/nrmicro3119

Goebels C., A. Thonn, S. Gonzalez-Hilarion, O. Rolland, F. Moyrand, *et al.*, 2013 Introns regulate gene expression in Cryptococcus neoformans in a Pab2p dependent pathway. PLoS Genet. 9: e1003686. https://doi.org/10.1371/journal.pgen.1003686

Goldberg J., H. Huang, Y. Kwon, P. Greengard, A. C. Nairn, *et al.*, 1995 Three-dimensional structure of the catalytic subunit of protein serine/threonine phosphatase-1. Nature 376: 745–753. https://doi.org/10.1038/376745a0

Gómez M. J., K. Luyten, and J. Ramos, 1996 The capacity to transport potassium influences sodium tolerance in Saccharomyces cerevisiae. FEMS Microbiol. Lett. 135: 157–160. https://doi.org/10.1016/0378-1097(95)00441-6

Greenberger P. A., R. K. Bush, J. G. Demain, A. Luong, R. G. Slavin, *et al.*, 2014 Allergic bronchopulmonary aspergillosis. J. allergy Clin. Immunol. Pract. 2: 703–8. https://doi.org/10.1016/j.jaip.2014.08.007

Hadfield C., B. E Jordan, R. C Mount, G. H. J. Pretorius, and E. Burak, 1990 G418-resistance as a dominant marker and reporter for gene expression in Saccharomyces cerevisiae. Curr. Genet. 18: 303–313. https://doi.org/10.1007/BF00318211

Hajjeh R. A., L. A. Conn, D. S. Stephens, W. Baughman, R. Hamill, *et al.*, 1999 *Cryptococcosis: Population-Based Multistate Active Surveillance and Risk Factors in Human Immunodeficiency Virus–Infected Persons*.

Hama H., G. G. Tall, and B. F. Horazdovsky, 1999 Vps9p is a guanine nucleotide exchange factor involved in vesicle-mediated vacuolar protein transport. J. Biol. Chem. 274: 15284–91.

Haro R., B. Garciadeblas, and A. Rodriguez-Navarro, 1991 A novel P-type ATPase from yeast involved in sodium transport. FEBS Lett. 291: 189–191. https://doi.org/10.1016/0014-5793(91)81280-L

Harrison J. C., E. S. G. Bardes, Y. Ohya, and D. J. Lew, 2001 A role for the Pkc1p/Mpk1p kinase cascade in the morphogenesis checkpoint. Nat. Cell Biol. 3: 417–420. https://doi.org/10.1038/35070104

Heitman J., A. Casadevall, J. K. Lodge, and J. R. Perfect, 1999 The Cryptococcus neoformans genome sequencing project. Mycopathologia 148: 1–7.

Hernández-Acosta P., D. G. Schmid, G. Jung, F. A. Culiáñez-Macià, and T. Kupke, 2002 Molecular characterization of the Arabidopsis thaliana flavoprotein AtHAL3a reveals the general reaction mechanism of 4’-phosphopantothenoylcysteine decarboxylases.

J. Biol. Chem. 277: 20490–8. https://doi.org/10.1074/jbc.M201557200

Heroes E., B. Lesage, J. Görnemann, M. Beullens, L. Van Meervelt, *et al.*, 2013 The PP1 binding code: a molecular-lego strategy that governs specificity. FEBS J. 280: 584–595. https://doi.org/10.1111/j.1742-4658.2012.08547.x

Herzog S., M. R. Schumann, and A. Fleißner, 2015 Cell fusion in Neurospora crassa. Curr. Opin. Microbiol. 28: 53–59. https://doi.org/10.1016/J.MIB.2015.08.002

Hisamoto N., K. Sugimoto, and K. Matsumoto, 1994 The Glc7 type 1 protein phosphatase of Saccharomyces cerevisiae is required for cell cycle progression in G2/M. Mol. Cell. Biol. 14: 3158–65.

Holt L. J., B. B. Tuch, J. Villén, A. D. Johnson, S. P. Gygi, *et al.*, 2009 Global analysis of Cdk1 substrate phosphorylation sites provides insights into evolution. Science 325: 1682–6. https://doi.org/10.1126/science.1172867

Honkanen R. E., J. Zwiller, R. E. Moore, S. L. Daily, B. S. Khatra, *et al.*, 1990 Characterization of microcystin-LR, a potent inhibitor of type 1 and type 2A protein phosphatases. J. Biol. Chem. 265: 19401–4.

Huberts D. H. E. W., and I. J. van der Klei, 2010 Moonlighting proteins: An intriguing mode of multitasking. Biochim. Biophys. Acta - Mol. Cell Res. 1803: 520–525. https://doi.org/10.1016/J.BBAMCR.2010.01.022

Hughes V., A. Mulles, M. J. R. Stark, and P. T. W. Cohen, 1993 Both isoforms of protein phosphatase Z are essential for the maintenance of cell size and integrity in Saccharomyces cerevisiae in response to osmotic stress. Eur. J. Biochem. 216: 269–279. https://doi.org/10.1111/j.1432-1033.1993.tb18142.x

Idnurm A., Y. S. Bahn, K. Nielsen, X. Lin, J. A. Fraser, *et al.*, 2005 Deciphering the model pathogenic fungus Cryptococcus neoformans. Nat. Rev. Microbiol. 3: 753–764. https://doi.org/10.1038/nrmicro1245

Ingrell C. R., M. L. Miller, O. N. Jensen, and N. Blom, 2007 NetPhosYeast: Prediction of protein phosphorylation sites in yeast. Bioinformatics 23: 895–897. https://doi.org/10.1093/bioinformatics/btm020

Inoue Y., T. Matsuda, K. Sugiyama, S. Izawa, and A. Kimura, 1999 Genetic analysis of glutathione peroxidase in oxidative stress response of Saccharomyces cerevisiae. J. Biol. Chem. 274: 27002–9.

Ivanov M. S., E. A. Radchenko, and L. N. Mironova, 2010 Protein complex Ppz1p/Hal3p and the efficiency of nonsense suppression in yeasts Saccharomyces cerevisiae. Mol. Biol. 44: 907–914. https://doi.org/10.1134/s0026893310060075

Izawa S., Y. Inoue, and A. Kimura, 1996 Importance of catalase in the adaptive response to hydrogen peroxide: analysis of acatalasaemic Saccharomyces cerevisiae. Biochem. J.

320 (Pt 1): 61–7.

Jamar N. H., P. Kritsiligkou, and C. M. Grant, 2017 The non-stop decay mRNA surveillance pathway is required for oxidative stress tolerance. Nucleic Acids Res. 45: 6881–6893. https://doi.org/10.1093/nar/gkx306

Janbon G., K. L. Ormerod, D. Paulet, E. J. Byrnes 3rd, V. Yadav, *et al.*, 2014 Analysis of the genome and transcriptome of Cryptococcus neoformans var. grubii reveals complex RNA expression and microevolution leading to virulence attenuation. PLoS Genet 10: e1004261. https://doi.org/10.1371/journal.pgen.1004261

Janssens V., S. Longin, and J. Goris, 2008 PP2A holoenzyme assembly: in cauda venenum (the sting is in the tail). Trends Biochem. Sci. 33: 113–121. https://doi.org/10.1016/j.tibs.2007.12.004

Jeffery C. J., 1999 Moonlighting proteins. Trends Biochem. Sci. 24: 8–11. https://doi.org/10.1016/S0968-0004(98)01335-8

Jeffery C. J., 2003 Moonlighting proteins: old proteins learning new tricks. Trends Genet. 19: 415–7. https://doi.org/10.1016/S0168-9525(03)00167-7

Jeffery C. J., 2009 Moonlighting proteins--an update. Mol. Biosyst. 5: 345–50. https://doi.org/10.1039/b900658n

Jia Z. P., N. McCullough, R. Martel, S. Hemmingsen, and P. G. Young, 1992 Gene amplification at a locus encoding a putative Na+/H+ antiporter confers sodium and lithium tolerance in fission yeast. EMBO J. 11: 1631–40.

Jiang Y., 2006 Regulation of the cell cycle by protein phosphatase 2A in Saccharomyces cerevisiae. Microbiol. Mol. Biol. Rev. 70: 440–449. https://doi.org/10.1128/mmbr.00049-05

Jimenez A., and J. Davies, 1980 Expression of a transposable antibiotic resistance element in Saccharomyces. Nature 287: 869.

Johnson A., and J. M. Skotheim, 2013 Start and the restriction point. Curr. Opin. Cell Biol. 25: 717–723. https://doi.org/10.1016/j.ceb.2013.07.010

Jung K.-W., A. K. Strain, K. Nielsen, K.-H. Jung, and Y.-S. Bahn, 2012 Two cation transporters Ena1 and Nha1 cooperatively modulate ion homeostasis, antifungal drug resistance, and virulence of Cryptococcus neoformans via the HOG pathway. Fungal Genet Biol 49: 332–345. https://doi.org/10.1016/j.fgb.2012.02.001

Kahm M., and M. Kschischo, 2016 Mathematical Modelling of Cation Transport and Regulation in Yeast, pp. 291–305 in Springer, Cham.

Kämper J., R. Kahmann, M. Bölker, L.-J. Ma, T. Brefort, *et al.*, 2006 Insights from the genome of the biotrophic fungal plant pathogen Ustilago maydis. Nature 444: 97–101. https://doi.org/10.1038/nature05248

Kim H.-S., G. Fernandes, and C.-W. Lee, 2016 Protein Phosphatases Involved in Regulating Mitosis: Facts and Hypotheses. Mol. Cells 39: 654–62. https://doi.org/10.14348/molcells.2016.0214

Kinclova-Zimmermannova O., D. Gaskova, and H. Sychrova, 2006 The Na^+,K^+/H^+-antiporter Nha1 influences the plasma membrane potential of *Saccharomyces cerevisiae*. FEMS Yeast Res. 6: 792–800. https://doi.org/10.1111/j.1567-1364.2006.00062.x

Klis F. M., A. Boorsma, and P. W. J. De Groot, 2006 Cell wall construction inSaccharomyces cerevisiae. Yeast 23: 185–202. https://doi.org/10.1002/yea.1349

Knoke M., and G. Schwesinger, 1994 One hundred years ago: the history of cryptococcosis in Greifswald. Medical mycology in the nineteenth century. Mycoses 37: 229–33.

Ko C. H., A. M. Buckley, and R. F. Gaber, 1990 TRK2 is required for low affinity K+transport in Saccharomyces cerevisiae. Genetics 125: 305–312.

Ko C. H., and R. F. Gaber, 1991 TRKI and TRK2 Encode Structurally Related K+ Transporters in Saccharomyces cerevisiae. Mol. Cell. Biol. 4266–4273.

Kobor M. S., F. Kouyoumdjian, J. Archambault, F. C. . Holstege, J. Greenblatt, *et al.*, 1999 An Unusual Eukaryotic Protein Phosphatase Required for Transcription by RNA Polymerase II and CTD Dephosphorylation in S. cerevisiae. Mol. Cell 4: 55–62. https://doi.org/10.1016/s1097-2765(00)80187-2

Koch C., A. Schleiffer, G. Ammerer, and K. Nasmyth, 1996 Switching transcription on and off during the yeast cell cycle: Cln/Cdc28 kinases activate bound transcription factor SBF (Swi4/Swi6) at Start, whereas Clb/Cdc28 kinases displace it from the promoter in G2. Genes Dev. 10: 129–141. https://doi.org/10.1101/gad.10.2.129

Kovács L., I. Farkas, L. Majoros, M. Miskei, I. Pócsi, *et al.*, 2010 The polymorphism of protein phosphatase Z1 gene in Candida albicans. J. Basic Microbiol. 50: S74–S82. https://doi.org/10.1002/jobm.200900434

Kupke T., P. Hernandez-Acosta, S. Steinbacher, and F. A. Culianez-Macia, 2001 Arabidopsis thaliana flavoprotein AtHAL3a catalyzes the decarboxylation of 4'-Phosphopantothenoylcysteine to 4'-phosphopantetheine, a key step in coenzyme A biosynthesis. J. Biol. Chem. 276: 19190–6. https://doi.org/10.1074/jbc.M100776200

Kupke T., 2001 Molecular characterization of the 4'-phosphopantothenoylcysteine decarboxylase domain of bacterial Dfp flavoproteins. J. Biol. Chem. 276: 27597–604. https://doi.org/10.1074/jbc.M103342200

Kupke T., P. Hernández-Acosta, and F. A. Culiáñez-Macià, 2003 4'-phosphopantetheine and coenzyme A biosynthesis in plants. J. Biol. Chem. 278: 38229–37. https://doi.org/10.1074/jbc.M306321200

Kutuzov M. A., D. E. Evans, and A. V Andreeva, 1998 Expression and characterization of PP7, a novel plant protein Ser/Thr phosphatase distantly related to RdgC/PPEF and PP5. FEBS Lett. 440: 147–52.

Kwon-Chung K. J., J. A. Fraser, T. L. Doering, Z. Wang, G. Janbon, *et al.*, 2014 Cryptococcus neoformans and Cryptococcus gattii, the etiologic agents of cryptococcosis. Cold Spring Harb. Perspect. Med. 4: a019760. https://doi.org/10.1101/cshperspect.a019760

Lammers T., and S. Lavi, 2007 Role of type 2C protein phosphatases in growth regulation and in cellular stress signaling. Crit. Rev. Biochem. Mol. Biol. 42: 437–461. https://doi.org/10.1080/10409230701693342

Lanver D., P. Berndt, M. Tollot, V. Naik, M. Vranes, *et al.*, 2014 Plant surface cues prime Ustilago maydis for biotrophic development. PLoS Pathog 10: e1004272. https://doi.org/10.1371/journal.ppat.1004272

Lanver D., M. Tollot, G. Schweizer, L. Lo Presti, S. Reissmann, *et al.*, 2017 Ustilago maydis effectors and their impact on virulence. Nat Rev Microbiol 15: 409–421. https://doi.org/10.1038/nrmicro.2017.33

Leal S. M., C. Vareechon, S. Cowden, B. A. Cobb, J.-P. Latgé, *et al.*, 2012 Fungal antioxidant pathways promote survival against neutrophils during infection. J. Clin. Invest. 122: 2482–98. https://doi.org/10.1172/JCI63239

Lee K. S., K. Irie, Y. Gotoh, Y. Watanabe, H. Araki, *et al.*, 1993a A yeast mitogen-activated protein kinase homolog (Mpk1p) mediates signalling by protein kinase C. Mol. Cell. Biol. 13: 3067–75.

Lee K. S., L. K. Hines, and D. E. Levin, 1993b A pair of functionally redundant yeast genes (PPZ1 and PPZ2) encoding type 1-related protein phosphatases function within the PKC1-mediated pathway. Mol. Cell. Biol. 13: 5843–53. https://doi.org/10.1128/MCB.13.9.5843.Updated

Leiter É., A. González, É. Erdei, C. Casado, L. Kovács, *et al.*, 2012 Protein phosphatase Z modulates oxidative stress response in fungi. Fungal Genet. Biol. 49: 708–716. https://doi.org/10.1016/j.fgb.2012.06.010

Levin D. E., 2005 Cell Wall Integrity Signaling in Saccharomyces cerevisiae. Microbiol. Mol. Biol. Rev. 69: 262–291. https://doi.org/10.1128/MMBR.69.2.262-291.2005

Levin D. E., 2011 Regulation of cell wall biogenesis in Saccharomyces cerevisiae: The cell wall integrity signaling pathway. Genetics 189: 1145–1175. https://doi.org/10.1534/genetics.111.128264

Liu H., T. R. Cottrell, L. M. Pierini, W. E. Goldman, and T. L. Doering, 2002 RNA interference in the pathogenic fungus Cryptococcus neoformans. Genetics 160: 463–70.

Loftus B. J., E. Fung, P. Roncaglia, D. Rowley, P. Amedeo, *et al.*, 2005 The genome of the basidiomycetous yeast and human pathogen Cryptococcus neoformans. Science (80-.). 307: 1321–1324. https://doi.org/10.1126/science.1103773

Longtine M. S., A. M. K. Iii, D. J. Demarini, and N. G. Shah, 1998 Additional Modules for Versatile and EconomicalPCR-based Gene Deletion and Modification in Saccharomyces cerevisiae. Yeast 961: 1–9. https://doi.org/10.1002/(SICI)1097-0061(199807)14

MacKintosh C., K. A. Beattie, S. Klumpp, P. Cohen, and G. A. Codd, 1990 Cyanobacterial microcystin-LR is a potent and specific inhibitor of protein phosphatases 1 and 2A from both mammals and higher plants. FEBS Lett. 264: 187–92.

Madrid R., M. J. Gómez, J. Ramos, and A. Rodríguez-Navarro, 1998 Ectopic potassium uptake in trk1 trk2 mutants of Saccharomyces cerevisiae correlates with a highly hyperpolarized membrane potential. J. Biol. Chem. 273: 14838–44. https://doi.org/10.1074/JBC.273.24.14838

Makanae K., R. Kintaka, T. Makino, H. Kitano, and H. Moriya, 2012 Identification of dosage-sensitive genes in Saccharomyces cerevisiae using the genetic tug-of-war method. Genome Res. 23: 300–311. https://doi.org/10.1101/gr.146662.112

Manfiolli A. O., P. A. de Castro, T. F. dos Reis, S. Dolan, S. Doyle, *et al.*, 2017 Aspergillus fumigatus protein phosphatase PpzA is involved in iron assimilation, secondary metabolite production, and virulence. Cell. Microbiol. 19: e12770. https://doi.org/10.1111/cmi.12770

Martinez R., M. T. Latreille, and M. Mirande, 1991 A PMR2 tandem repeat with a modified C-terminus is located downstream from the KRS1 gene encoding lysyl-tRNA synthetase in Saccharomyces cerevisiae. Mol. Gen. Genet. 227: 149–54.

McGowan C. H., and P. Cohen, 1988 Protein Phosphatase-2C from Rabbit Skeletal Muscle and Liver: An Mg2+-Dependent Enzyme. Methods Enzymol. 159: 416–426. https://doi.org/10.1016/0076-6879(88)59041-9

Mendenhall M. D., and A. E. Hodge, 1998 *Regulation of Cdc28 Cyclin-Dependent Protein Kinase Activity during the Cell Cycle of the Yeast Saccharomyces cerevisiae*.

Merchan S., D. Bernal, R. Serrano, and L. Yenush, 2004 Response of the Saccharomyces cerevisiae Mpk1 mitogen-activated protein kinase pathway to increases in internal turgor pressure caused by loss of Ppz protein phosphatases. Eukaryot. Cell 3: 100–7. https://doi.org/10.1128/EC.3.1.100-107.2004

Merchan S., L. Pedelini, G. Hueso, A. Calzada, R. Serrano, *et al.*, 2011 Genetic alterations leading to increases in internal potassium concentrations are detrimental for DNA integrity in Saccharomyces cerevisiae. Genes to Cells 16: 152–165. https://doi.org/10.1111/j.1365-2443.2010.01472.x

Miller M. E., and F. R. Cross, 2001 Cyclin specificity: how many wheels do you need on a

unicycle? J. Cell Sci. 114: 1811–20.

Minhas A., A. Sharma, H. Kaur, Y. Rawal, K. Ganesan, *et al.*, 2012 Conserved Ser/Arg-rich motif in PPZ orthologs from fungi is important for its role in cation tolerance. J Biol Chem 287: 7301–7312. https://doi.org/10.1074/jbc.M111.299438

Molero C., K. Petrényi, A. González, M. Carmona, S. Gelis, *et al.*, 2013 The *Schizosaccharomyces pombe* fusion gene *hal3* encodes three distinct activities. Mol. Microbiol. 90: n/a-n/a. https://doi.org/10.1111/mmi.12370

Molero C., C. Casado, and J. Ariño, 2017 The inhibitory mechanism of Hal3 on the yeast Ppz1 phosphatase: A mutagenesis analysis. Sci. Rep. 7: 8819. https://doi.org/10.1038/s41598-017-09360-5

Moolman W. J. A., M. de Villiers, and E. Strauss, 2014 Recent advances in targeting coenzyme A biosynthesis and utilization for antimicrobial drug development. Biochem. Soc. Trans. 42: 1080–6. https://doi.org/10.1042/BST20140131

Moorhead G. B. G., L. Trinkle-Mulcahy, and A. Ulke-Lemée, 2007 Emerging roles of nuclear protein phosphatases. Nat. Rev. Mol. Cell Biol. 8: 234–244. https://doi.org/10.1038/nrm2126

Moorhead G. B. G., V. De Wever, G. Templeton, and D. Kerk, 2009 Evolution of protein phosphatases in plants and animals. Biochem. J. 417: 401–9. https://doi.org/10.1042/BJ20081986

Morano K. A., C. M. Grant, W. S. Moye-Rowley, T. K. Van Dyk, M. B. Ficke, *et al.*, 2012 The response to heat shock and oxidative stress in Saccharomyces cerevisiae. Genetics 190: 1157–95. https://doi.org/10.1534/genetics.111.128033

Morgan B. A., and E. A. Veal, 2007 Functions of typical 2-Cys peroxiredoxins in yeast, pp. 253–265 in *Peroxiredoxin Systems*, Springer.

Mulet J. M., M. P. Leube, S. J. Kron, G. Rios, G. R. Fink, *et al.*, 1999 A novel mechanism of ion homeostasis and salt tolerance in yeast: the Hal4 and Hal5 protein kinases modulate the Trk1-Trk2 potassium transporter. Mol. Cell. Biol. 19: 3328–37. https://doi.org/10.1128/MCB.19.5.3328

Muñoz I., E. Simón, N. Casals, J. Clotet, and J. Ariño, 2003 Identification of multicopy suppressors of cell cycle arrest at the G_1-S transition in *Saccharomyces cerevisiae*. Yeast 20: 157–169. https://doi.org/10.1002/yea.938

Muñoz I., A. Ruiz, M. Marquina, A. Barceló, A. Albert, *et al.*, 2004 Functional Characterization of the Yeast Ppz1 Phosphatase Inhibitory Subunit Hal3. J. Biol. Chem. 279: 42619–42627. https://doi.org/10.1074/jbc.m405656200

Nadal E. de, J. Clotet, F. Posas, R. Serrano, N. Gomez, *et al.*, 1998 The yeast halotolerance determinant Hal3p is an inhibitory subunit of the Ppz1p Ser/Thr protein phosphatase.

Proc Natl Acad Sci U S A 95: 7357–7362.

Nadal E. de, R. P. Fadden, A. Ruiz, T. Haystead, and J. Ariño, 2001 A role for the Ppz Ser/Thr protein phosphatases in the regulation of translation elongation factor 1Balpha. J. Biol. Chem. 276: 14829–34. https://doi.org/10.1074/jbc.M010824200

Nagy G., G. W. Hennig, K. Petrenyi, L. Kovacs, I. Pocsi, *et al.*, 2014 Time-lapse video microscopy and image analysis of adherence and growth patterns of Candida albicans strains. Appl. Microbiol. Biotechnol. 98: 5185–5194. https://doi.org/10.1007/s00253-014-5696-5

Navarrete C., S. Petrezsélyová, L. Barreto, J. L. Martínez, J. Zahrádka, *et al.*, 2010 Lack of main K+ uptake systems in Saccharomyces cerevisiae cells affects yeast performance in both potassium-sufficient and potassium-limiting conditions. FEMS Yeast Res. 10: no-no. https://doi.org/10.1111/j.1567-1364.2010.00630.x

Nizhnikov A. A., K. S. Antonets, S. G. Inge-Vechtomov, and I. L. Derkatch, 2014 Modulation of efficiency of translation termination in Saccharomyces cerevisiae: Turning nonsense into sense. Prion 8: 247–260. https://doi.org/10.4161/pri.29851

Noble S. M., S. French, L. A. Kohn, V. Chen, and A. D. Johnson, 2010 Systematic screens of a Candida albicans homozygous deletion library decouple morphogenetic switching and pathogenicity. Nat. Genet. 42: 590–8. https://doi.org/10.1038/ng.605

O'Meara T. R., and J. A. Alspaugh, 2012 The Cryptococcus neoformans capsule: a sword and a shield. Clin. Microbiol. Rev. 25: 387–408. https://doi.org/10.1128/CMR.00001-12

Ohkura H., N. Kinoshita, S. Miyatani, T. Toda, and M. Yanagida, 1989 The fission yeast dis2+ gene required for chromosome disjoining encodes one of two putative type 1 protein phosphatases. Cell 57: 997–1007. https://doi.org/10.1016/0092-8674(89)90338-3

Olarewaju O., P. A. Ortiz, W. Q. Chowdhury, I. Chatterjee, and T. G. Kinzy, 2004 The translation elongation factor eEF1B plays a role in the Oxidative stress response pathway. RNA Biol. 89–94.

Olsen J. V, B. Blagoev, F. Gnad, B. Macek, C. Kumar, *et al.*, 2006 Global, in vivo, and site-specific phosphorylation dynamics in signaling networks. Cell 127: 635–48. https://doi.org/10.1016/j.cell.2006.09.026

Pappas P. G., J. H. Rex, J. Lee, R. J. Hamill, R. A. Larsen, *et al.*, 2003 A Prospective Observational Study of Candidemia: Epidemiology, Therapy, and Influences on Mortality in Hospitalized Adult and Pediatric Patients. Clin. Infect. Dis. 37: 634–643. https://doi.org/10.1086/376906

Park B. J., K. A. Wannemuehler, B. J. Marston, N. Govender, P. G. Pappas, *et al.*, 2009 Estimation of the current global burden of cryptococcal meningitis among persons living with HIV/AIDS. Aids 23: 525–530. https://doi.org/10.1097/QAD.0b013e328322ffac

Peng Z. Y., R. J. Trumbly, and E. M. Reimann, 1990 *Purification and characterization of glycogen synthase from a glycogen-deficient strain of Saccharomyces cerevisiae*.

Pennisi E., 2010 Armed and dangerous. Science 327: 804–5. https://doi.org/10.1126/science.327.5967.804

Pérez-Valle J., H. Jenkins, S. Merchan, V. Montiel, J. Ramos, *et al.*, 2007 Key role for intracellular K+ and protein kinases Sat4/Hal4 and Hal5 in the plasma membrane stabilization of yeast nutrient transporters. Mol. Cell. Biol. 27: 5725–36. https://doi.org/10.1128/MCB.01375-06

Perfect J. R., and A. Casadevall, 2002 Cryptococcosis. Infect. Dis. Clin. North Am. 16: 837–874. https://doi.org/10.1016/S0891-5520(02)00036-3

Peti W., A. C. Nairn, and R. Page, 2013 Structural basis for protein phosphatase 1 regulation and specificity. FEBS J. 280: 596–611. https://doi.org/10.1111/j.1742-4658.2012.08509.x

Petrényi K., C. Molero, Z. Kónya, F. Erdődi, J. Ariño, *et al.*, 2016 Analysis of Two Putative Candida albicans Phosphopantothenoylcysteine Decarboxylase / Protein Phosphatase Z Regulatory Subunits Reveals an Unexpected Distribution of Functional Roles. https://doi.org/10.1371/journal.pone.0160965

Pfaller M. A., and D. J. Diekema, 2010 Epidemiology of Invasive Mycoses in North America. Crit. Rev. Microbiol. 36: 1–53. https://doi.org/10.3109/10408410903241444

Pinson B., O. S. Gabrielsen, and B. Dalgnan-Fornier, 2000 Redox regulation of AMP synthesis in yeast: A role of the Bas1p and Bas2p transcription factors. Mol. Microbiol. 36: 1460–1469. https://doi.org/10.1046/j.1365-2958.2000.01966.x

Posas F., A. Casamayors, N. Morral, and J. Ariño, 1992 Molecular Cloning and Analysis of a Yeast Protein Phosphatase with an Unusual Amino-terminal Region. J. Biol. Chem. 267: 11734–11740.

Posas F., A. Casamayor, and J. Ariño, 1993 The PPZ protein phosphatases are involved in the maintenance of osmotic stability of yeast cells. FEBS Lett. 318: 282–286. https://doi.org/10.1016/0014-5793(93)80529-4

Posas F., M. Camps, and J. Ariño, 1995a The PPZ protein phosphatases are important determinants of salt tolerance in yeast cells. J. Biol. Chem. 270: 13036–13041. https://doi.org/10.1074/jbc.270.22.13036

Posas F., M. Bollen, W. Stalmans, and J. Ariño, 1995b Biochemical characterization of recombinant yeast PPZ1, a protein phosphatase involved in salt tolerance. FEBS Lett. 368: 39–44. https://doi.org/10.1016/0014-5793(95)00593-X

Prior C., S. Potier, J.-L. Souciet, and H. Sychrova, 1996 Characterization of the *NHA1* gene encoding a Na^+/H^+-antiporter of the yeast *Saccharomyces cerevisiae*. FEBS Lett. 387:

89–93. https://doi.org/10.1016/0014-5793(96)00470-X

Prista C., M. C. Loureiro-Dias, V. Montiel, R. García, and J. Ramos, 2005 Mechanisms underlying the halotolerant way of Debaryomyces hansenii. FEMS Yeast Res. 5: 693–701. https://doi.org/10.1016/j.femsyr.2004.12.009

Ptacek J., G. Devgan, G. Michaud, H. Zhu, X. Zhu, *et al.*, 2005 Global analysis of protein phosphorylation in yeast. Nature 438: 679–684. https://doi.org/10.1038/nature04187

Rebelo S., M. Santos, F. Martins, E. F. da Cruz e Silva, and O. A. B. da Cruz e Silva, 2015 Protein phosphatase 1 is a key player in nuclear events. Cell. Signal. 27: 2589–2598. https://doi.org/10.1016/J.CELLSIG.2015.08.007

Robert V. A., and A. Casadevall, 2009 Vertebrate Endothermy Restricts Most Fungi as Potential Pathogens. J. Infect. Dis. 200: 1623–1626. https://doi.org/10.1086/644642

Rocco M. La, 1992 Cryptococcus neoformans. Clin. Microbiol. Newsl. 14: 177–181. https://doi.org/10.1016/0196-4399(92)90044-A

Rodriguez-Navarro A., and J. Ramos, 1984 Dual System for Potassium Transport in Saccharomyces cerevisiae. J. Bacteriol. 159: 940–945.

Rodríguez-Navarro A., F. J. Quintero, and B. Garciadeblás, 1994 Na+-ATPases and Na+/H+ antiporters in fungi. Biochim. Biophys. Acta - Bioenerg. 1187: 203–205. https://doi.org/10.1016/0005-2728(94)90111-2

Rodríguez-Navarro A., 2000 Potassium transport in fungi and plants. Biochim. Biophys. Acta 1469: 1–30.

Rodríguez-Navarro A., and B. Benito, 2010 Sodium or potassium efflux ATPase. Biochim. Biophys. Acta - Biomembr. 1798: 1841–1853. https://doi.org/10.1016/j.bbamem.2010.07.009

Rodríguez-Navarro A., B. Garciadeblás, and B. Benito, 2002 Potassium- or sodium-efflux ATPase, a key enzyme in the evolution of fungi. Microbiology 148: 933–941. https://doi.org/10.1099/00221287-148-4-933

Rogoza T. M., M. S. Ivanov, O. V. Viktorovskaya, K. V. Volkov, S. A. Rodionova, *et al.*, 2009 Search for genes influencing the maintenance of the [ISP +] prion-like antisuppressor determinant in yeast with the use of an insertion gene library. Mol. Biol. 43: 360–366. https://doi.org/10.1134/s0026893309030029

Rolfes R. J., 2006 Regulation of purine nucleotide biosynthesis: in yeast and beyond. Biochem. Soc. Trans. 34: 786–790. https://doi.org/10.1042/bst0340786

Rovenich H., J. C. Boshoven, and B. P. Thomma, 2014 Filamentous pathogen effector functions: of pathogens, hosts and microbiomes. Curr. Opin. Plant Biol. 20: 96–103. https://doi.org/10.1016/J.PBI.2014.05.001

Roy S. W., and W. Gilbert, 2006 The evolution of spliceosomal introns: Patterns, puzzles and progress. Nat. Rev. Genet. 7: 211–221. https://doi.org/10.1038/nrg1807

Ruiz A., L. Yenush, and J. Ariño, 2003 Regulation of ENA1 Na-ATPase Gene Expression by the Ppz1 Protein Phosphatase Is Mediated by the Calcineurin Pathway. Eukaryot. Cell 2: 937–948. https://doi.org/10.1128/EC.2.5.937-948.2003

Ruiz A., I. Muñoz, R. Serrano, A. González, E. Simón, *et al.*, 2004a Functional Characterization of the Saccharomyces cerevisiae VHS3 Gene. J. Biol. Chem. 279: 34421–34430. https://doi.org/10.1074/jbc.M400572200

Ruiz A., M. del Carmen Ruiz, M. A. Sánchez-Garrido, J. Ariño, and J. Ramos, 2004b The Ppz protein phosphatases regulate Trk-independent potassium influx in yeast. FEBS Lett. 578: 58–62. https://doi.org/10.1016/j.febslet.2004.10.069

Ruiz A., A. Gonzalez, I. Munoz, R. Serrano, J. A. Abrie, *et al.*, 2009 Moonlighting proteins Hal3 and Vhs3 form a heteromeric PPCDC with Ykl088w in yeast CoA biosynthesis. Nat Chem Biol 5: 920–928. https://doi.org/10.1038/nchembio.243

Sadowski I., B.-J. Breitkreutz, C. Stark, T.-C. Su, M. Dahabieh, *et al.*, 2013 The PhosphoGRID Saccharomyces cerevisiae protein phosphorylation site database: version 2.0 update/database/bat026. ID bat026 2013. https://doi.org/10.1093/database/bat026

Sakumoto N., I. Matsuoka, Y. Mukai, N. Ogawa, Y. Kaneko, *et al.*, 2002 A series of double disruptants for protein phosphatase genes inSaccharomyces cerevisiae and their phenotypic analysis. Yeast 19: 587–599. https://doi.org/10.1002/yea.860

Sambrook J., E. F. Fritsch, and T. Maniatis, 2012 *Molecular cloning: a laboratory manual.* Cold spring harbor laboratory press.

Sangrador A., I. Andrés, A. Eguiraun, M. L. Lorenzo, and J. M. Ortiz, 1998 Growth arrest of Schizosaccharomyces pombe following overexpression of mouse type 1 protein phosphatases. Mol. Gen. Genet. 259: 449–56.

Santolaria C., D. Velázquez, E. Strauss, and J. Ariño, 2018 Mutations at the hydrophobic core affect Hal3 trimer stability, reducing its Ppz1 inhibitory capacity but not its PPCDC moonlighting function. Sci. Rep. 8: 14701. https://doi.org/10.1038/s41598-018-32979-x

Sassoon I., F. F. Severin, P. D. Andrews, M. R. Taba, K. B. Kaplan, *et al.*, 1999 Regulation of Saccharomyces cerevisiae kinetochores by the type 1 phosphatase Glc7p. Genes Dev. 13: 545–55.

Scherer M., K. Heimel, V. Starke, and J. Kämper, 2006 The Clp1 protein is required for clamp formation and pathogenic development of Ustilago maydis. Plant Cell 18: 2388–401. https://doi.org/10.1105/tpc.106.043521

Schirawski J., G. Mannhaupt, K. Münch, T. Brefort, K. Schipper, *et al.*, 2010 Pathogenicity

determinants in smut fungi revealed by genome comparison. Science 330: 1546–8. https://doi.org/10.1126/science.1195330

Selvan L. D. N., S. Renuse, J. E. Kaviyil, J. Sharma, S. M. Pinto, *et al.*, 2014 Phosphoproteome of Cryptococcus neoformans. J. Proteomics 97: 287–295. https://doi.org/10.1016/J.JPROT.2013.06.029

Serrano R., M. C. Kielland-Brandt, and G. R. Fink, 1986 Yeast plasma membrane ATPase is essential for growth and has homology with (Na+ + K+), K+- and Ca2+-ATPases. Nature 319: 689–93. https://doi.org/10.1038/319689a0

Serrano R., 1996 Salt Tolerance in Plants and Microorganisms: Toxicity Targets and Defense Responses. Int. Rev. Cytol. 165: 1–52. https://doi.org/10.1016/S0074-7696(08)62219-6

Shenton D., J. B. Smirnova, J. N. Selley, K. Carroll, S. J. Hubbard, *et al.*, 2006 Global Translational Responses to Oxidative Stress Impact upon Multiple Levels of Protein Synthesis. J. Biol. Chem. 281: 29011–29021. https://doi.org/10.1074/jbc.m601545200

Sherman F., and J. Hicks, 1991 [2] Micromanipulation and dissection of asci, pp. 21–37 in *Methods in enzymology*, Elsevier.

Shi Y., 2009 Serine/threonine phosphatases: mechanism through structure. Cell 139: 468–84. https://doi.org/10.1016/j.cell.2009.10.006

Silva-Rojas H. V., A. Espinosa-Calderón, L. Córdova-Téllez, P. R. Galicia-García, H. A. Zavaleta-Mancera, *et al.*, 2017 Selection of aggressive pathogenic and solopathogenic strains of Ustilago maydis to improve Huitlacoche production. Acta Bot. Brasilica 30: 683–692. https://doi.org/10.1590/0102-33062016abb0097

Simón E., J. Clotet, F. Calero, J. Ramos, and J. Ariño, 2001 A screening for high copy suppressors of the sit4 hal3 synthetically lethal phenotype reveals a role for the yeast Nha1 antiporter in cell cycle regulation. J. Biol. Chem. 276: 29740–7. https://doi.org/10.1074/jbc.M101992200

Simpson C. E., and M. P. Ashe, 2012 Adaptation to stress in yeast: to translate or not?: Figure 1. Biochem. Soc. Trans. 40: 794–799. https://doi.org/10.1042/bst20120078

Simwami S. P., K. Khayhan, D. A. Henk, D. M. Aanensen, and T. Boekhout, 2011 Low Diversity Cryptococcus neoformans Variety grubii Multilocus Sequence Types from Thailand Are Consistent with an Ancestral African Origin. PLoS Pathog 7: 1001343. https://doi.org/10.1371/journal.ppat.1001343

Snetselaar K. M., and C. W. Mims, 1994 Light and electron microscopy of Ustilago maydis hyphae in maize. Mycol. Res. 98: 347–355. https://doi.org/10.1016/S0953-7562(09)80463-2

Song W., and M. Carlson, 1998 Srb/mediator proteins interact functionally and physically

with transcriptional repressor Sfl1. EMBO J 17: 5757–5765. https://doi.org/10.1093/emboj/17.19.5757

Spitzer E. D., and B. Weiss, 1985 dfp Gene of Escherichia coli K-12, a locus affecting DNA synthesis, codes for a flavoprotein. J. Bacteriol. 164: 994–1003.

Spitzer E. D., H. E. Jimenez-Billini, and B. Weiss, 1988 -Alanine Auxotrophy Associated with dfp, a Locus Affecting DNA Synthesis in Escherichia coli. J. Bacteriol. 170: 872476.

Srikanta D., F. H. Santiago-Tirado, and T. L. Doering, 2014 Cryptococcus neoformans: Historical curiosity to modern pathogen. Yeast 31: 47–60. https://doi.org/10.1002/yea.2997

Stark M. J. R., 1996 Yeast protein serine/threonine phosphatases: Multiple roles and diverse regulation. Yeast 12: 1647–1675. https://doi.org/10.1002/(SICI)1097-0061(199612)12:16<1647::AID-YEA71>3.0.CO;2-Q

Steinbacher S., P. Hernández-Acosta, B. Bieseler, M. Blaesse, R. Huber, *et al.*, 2003 Crystal Structure of the Plant PPC Decarboxylase AtHAL3a Complexed with an Ene-thiol Reaction Intermediate. J. Mol. Biol. 327: 193–202. https://doi.org/10.1016/S0022-2836(03)00092-5

Stotz H. U., G. K. Mitrousia, P. J. G. M. de Wit, and B. D. L. Fitt, 2014 Effector-triggered defence against apoplastic fungal pathogens. Trends Plant Sci. 19: 491–500. https://doi.org/10.1016/j.tplants.2014.04.009

Strauss E., C. Kinsland, Y. Ge, F. W. McLafferty, and T. P. Begley, 2001 Phosphopantothenoylcysteine synthetase from Escherichia coli. Identification and characterization of the last unidentified coenzyme A biosynthetic enzyme in bacteria. J. Biol. Chem. 276: 13513–6. https://doi.org/10.1074/jbc.C100033200

Sukroongreung S., K. Kitiniyom, C. Nilakul, and S. Tantimavanich, 1998 Pathogenicity of basidiospores of Filobasidiella neoformans var. neoformans. Med. Mycol. 36: 419–24.

Sutton A., D. Immanuel, and K. T. Arndt, 1991 The SIT4 Protein Phosphatase Functions in Late G1 for Progression into S Phase Saccharomyces cerevisiae strains containing temperature-sensitive mutations in the SIT4 protein phosphatase arrest in late G1 at the nonpermissive temperature. Order-of-functio. Mol. Cell. Biol. 11: 2133–2148.

Swaney D. L., P. Beltrao, L. Starita, A. Guo, J. Rush, *et al.*, 2013 Global analysis of phosphorylation and ubiquitylation cross-talk in protein degradation. Nat. Methods 10: 676–82. https://doi.org/10.1038/nmeth.2519

Swingle M. R., R. E. Honkanen, and E. M. Ciszak, 2004 Structural basis for the catalytic activity of human serine/threonine protein phosphatase-5. J. Biol. Chem. 279: 33992–33999. https://doi.org/10.1074/jbc.M402855200

Sychrová H., 2004 Yeast as a model organism to study transport and homeostasis of alkali

metal cations. Physiol. Res. 53 Suppl 1: S91-8.

Szabó K., Z. Kónya, F. Erdődi, I. Farkas, and V. Dombrádi, 2019 Dissection of the regulatory role for the N-terminal domain in Candida albicans protein phosphatase Z1. PLoS One 14. https://doi.org/10.1371/journal.pone.0211426

Szöőr B., Z. Fehér, T. Zeke, P. Gergely, E. Yatzkan, *et al.*, 1998 pzl-1 encodes a novel protein phosphatase-Z-like Ser/Thr protein phosphatase in Neurospora crassa. Biochim. Biophys. Acta - Protein Struct. Mol. Enzymol. 1388: 260–266. https://doi.org/10.1016/S0167-4838(98)00201-5

Tachikawa H., A. Bloecher, K. Tatchell, and A. M. Neiman, 2001 A Gip1p-Glc7p phosphatase complex regulates septin organization and spore wall formation. J. Cell Biol. 155: 797–808. https://doi.org/10.1083/jcb.200107008

Takahashi H., J. M. McCaffery, R. A. Irizarry, and J. D. Boeke, 2006 Nucleocytosolic Acetyl-Coenzyme A Synthetase Is Required for Histone Acetylation and Global Transcription. Mol. Cell 23: 207–217. https://doi.org/10.1016/j.molcel.2006.05.040

Tamura S., M. G. Li, K. Komaki, M. Sasaki, and T. Kobayashi, 2004 Roles of mammalian protein phosphatase 2C family members in the regulation of cellular functions, pp. 91–105 in Springer, Berlin, Heidelberg.

Tibbetts A. S., and D. R. Appling, 1997 Saccharomyces cerevisiae expresses two genes encoding isozymes of 5- aminoimidazole-4-carboxamide ribonucleotide transformylase. Arch. Biochem. Biophys. 340: 195–200. https://doi.org/10.1006/abbi.1997.9919

Tibbetts A. S., and D. R. Appling, 2000 Characterization of two 5-aminoimidazole-4-carboxamide ribonucleotide transformylase/inosine monophosphate cyclohydrolase isozymes from Saccharomyces cerevisiae. J. Biol. Chem. 275: 20920–7. https://doi.org/10.1074/jbc.M909851199

Tollot M., D. Assmann, C. Becker, J. Altmuller, J. Y. Dutheil, *et al.*, 2016 The WOPR Protein Ros1 Is a Master Regulator of Sporogenesis and Late Effector Gene Expression in the Maize Pathogen Ustilago maydis. PLoS Pathog 12: e1005697. https://doi.org/10.1371/journal.ppat.1005697

Tompa P., C. Szász, and L. Buday, 2005 Structural disorder throws new light on moonlighting. Trends Biochem. Sci. 30: 484–9. https://doi.org/10.1016/j.tibs.2005.07.008

Tu J., W. Song, and M. Carlson, 1996 *Protein Phosphatase Type 1 Interacts with Proteins Required for Meiosis and Other Cellular Processes in Saccharomyces cerevisiae*.

Tyson J. J., A. Csikasz-Nagy, and B. Novak, 2002 The dynamics of cell cycle regulation. BioEssays 24: 1095–1109. https://doi.org/10.1002/bies.10191

Virgilio S., and M. C. Bertolini, 2018 Functional diversity in the pH signaling pathway: an overview of the pathway regulation in Neurospora crassa. Curr. Genet. 64: 529–534. https://doi.org/10.1007/s00294-017-0772-x

Virshup D. M., and S. Shenolikar, 2009 From Promiscuity to Precision: Protein Phosphatases Get a Makeover. Mol. Cell 33: 537–545. https://doi.org/10.1016/j.molcel.2009.02.015

Vissi E., J. Clotet, E. de Nadal, A. Barceló, E. Bako, *et al.*, 2001 Functional analysis of theNeurospora crassa PZL-1 protein phosphatase by expression in budding and fission yeast. Yeast 18: 115–124. https://doi.org/10.1002/1097-0061(20010130)18:2<115::AID-YEA653>3.0.CO;2-G

Wera S., and B. A. Hemmings, 1995 Serine/threonine protein phosphatases. Biochem. J. 311: 17.

Wickerham L. J., 1953 *The yeasts, a taxonomic study*. Elsevier.

Wieland J., A. M. Nitsche, J. Strayle, H. Steiner1, and H. K. Rudolph2, 1995 *The PMR2 gene cluster encodes functionally distinct isoforms of a putative Na+ pump in the yeast plasma membrane*.

Wittenberg C., 2005 Cell cycle: Cyclin guides the way. Nature 434: 34–35. https://doi.org/10.1038/434034a

Wood Z. A., E. Schröder, J. R. Harris, and L. B. Poole, 2003 Structure, mechanism and regulation of peroxiredoxins. Trends Biochem. Sci. 28: 32–40. https://doi.org/10.1016/S0968-0004(02)00003-8

Ye Y., A. Osterman, R. Overbeek, and A. Godzik, 2005 Automatic detection of subsystem/pathway variants in genome analysis. Bioinformatics 21: i478–i486. https://doi.org/10.1093/bioinformatics/bti1052

Yenush L., J. M. Mulet, J. Ariño, and R. Serrano, 2002 The Ppz protein phosphatases are key regulators of K+ and pH homeostasis: Implications for salt tolerance, cell wall integrity and cell cycle progression. EMBO J. 21: 920–929. https://doi.org/10.1093/emboj/21.5.920

Yenush L., S. Merchan, J. Holmes, and R. Serrano, 2005 pH-Responsive, posttranslational regulation of the Trk1 potassium transporter by the type 1-related Ppz1 phosphatase. Mol. Cell. Biol. 25: 8683–92. https://doi.org/10.1128/MCB.25.19.8683-8692.2005

Yenush L., 2016 Potassium and Sodium Transport in Yeast, pp. 187–228 in Springer, Cham.

Yonamine I., K. Yoshida, K. Kido, A. Nakagawa, H. Nakayama, *et al.*, 2004 Overexpression of NtHAL3 genes confers increased levels of proline biosynthesis and the enhancement of salt tolerance in cultured tobacco cells. J. Exp. Bot. 55: 387–395. https://doi.org/10.1093/jxb/erh043

Zhang S., S. Guha, and F. C. Volkert, 1995 The Saccharomyces SHP1 Gene, Which Encodes a

Regulator of Phosphoprotein Phosphatase 1 with Differential Effects on Glycogen Metabolism, Meiotic Differentiation, and Mitotic Cell Cycle Progression. Mol. Cell. Biol. 15: 2037–2050.

Zhang C., R. García-Rodas, C. Molero, H. C. de Oliveira, L. Tabernero, *et al.*, 2019 Characterization of the atypical Ppz/Hal3 phosphatase system from the pathogenic fungus Cryptococcus neoformans. Mol. Microbiol. 111: 898–917. https://doi.org/10.1111/mmi.14181

Zhao Y., and H. B. Lieberman, 1995 *Schizosaccharomyces pombe: A model for molecular studies of eukaryotic genes*. Mary Ann Liebert, Inc., Publishers Pp.

Zhao S., and E. Y. C. Lee, 1997 A Protein Phosphatase-1-binding Motif Identified by the Panning of a Random Peptide Display Library*

Zhi X., H. Zhang, C. He, Y. Wei, L. Bian, *et al.*, 2015 Serine/Threonine Protein Phosphatase-5 Accelerates Cell Growth and Migration in Human Glioma. Cell. Mol. Neurobiol. 35: 669–677. https://doi.org/10.1007/s10571-015-0162-1

Supplementary Information

Supplementary Information 1

Protein sequences from *C. neoformans* and *U. maydis* used in this study.

CnPpz1

MGQGQSSSKKLGRTSSKQLPPQDLADSLARTSIADRDAAAGHPPPPDALSPAKLAAKRRGSTRDAP
PASYASSTSDAPPAPAPPSPSPSSIPTTQNILAAPREGLKSSFLGSSPPPPSAMSVSPASTTGGRV
RSSSPPPSSSPTRQTGGHLSRDSASSLSPGFTLTQTVSRTESAAGGFQILDVDNMIQRLLEAGYSG
KVTKSPPLKNAEITSVCAAAREVFLSQPTLIELSPPVKIVGDVHGQYADLLRMFEMCGFPPAANYL
FLGDYVDRGKQSLETILLLLCYKIKYPENFFLLRGNHECANVTRVYGFYDECKRRTNIKIWKTFID
VFNTLPIASIVASKIFCVHGGLSPSLKSMDDIRRIQRPTDVPDYGLLNDLVWSDPSDTALDWEDNE
RGVSFCYGKSVINAFLATHDMDLICRAHMVVEDGYEFYNDRTLVTVFSAPNYCGEFDNFGAVMSVS
EDLLCSFELLKPLDGAALKKEMTKSKRKSLQAHQSPPNNPMAQSF

CnHal3a

MQPAQTHAAPVRKKPSRPFVSSHHRPADDVDDGIFRVVLITSGSVASIKAPDIVGALVKSPNIDVQ
VVATKASTYFYSQEDVDNSVRSALNLPDGQTGEHFGVRVWTDEDEWSDWKQVGEPILHIELRRWAD
LVVIAPCSADLLAKIAGGICDSLATSLLRALGPSTPVIVCPAMNTYMYQHRLTTRHLAVVQEDLGY
LVSGPQGAGRLACGDDGPGKMTDWRDIVSLIEGFATMHQDRRAVVHPGHPLQESSDPPLPPPTETP
PTPGRPSKSSSAVGSSSVSTQDRAPAKAPSDDVLTGIADWRSMTNELGGDGTAWRRKWWLG

CnHal3b

MQPAQTHAAPVRKKPSRPFVSSHHRPADDVDDGIFRVVLITSGSVASIKAPDIVGALVKSPNIDVQ
VVATKASTYFYSQEDVDNSVRSALNLPDGQTGEHFGVRVWTDEDEWSDWKQVGEPILHIELRRWAD
LVVIAPCSADLLAKIAGGICDSLATSLLRALGPSTPVIVCPAMNTYMYQHRLTTRHLAVVQEDLGY
LVSGPQGAGRLACGDDGPGKMTDWRDIVSLIEGFATMHQDRRAVVHPGHPLQESSDPPLPPPTETP
PTPGRPSKSSSAVGSSSVSTQDRAPAKAPSDDVLTGIADWRSMTNELGGDGTAWRRKWWLG

Purple background: putative myristoylation site

Blue background: potential phosphorylatable site

Yellow background: extra insert compared with AtHal3

UmPpz1

MFKSFGKIMGGSSRKGKSKLQDGDDSVDASNGLPGSDSSNLLRAKSKDSLAVTENGSGNFANNGSS
APAKIEKRGGVSRHESPLPSPSPSARNVLEGQEESSEVGSSAVARSAPASDVGGPRPANDAASQST
SVPTANTILSNPLAQSGSTGFPSSVGKNAQAAAGGDQVRTFDIDDMISRLLEAGYSGKIPKPALKN
AEITAVCQAAREIFLSQPTLIELSPPVKIVGDTHGQYHDLLRLFEMCGFPPSANYLFLGDYVDRGK
QSLETILLLLCYKIKYPENFFLLRGNHECANVTRVYGFYDECKRRVNIKIWKTFIDVFNTLPIAAV
VASKIFCVHGGLSPSLSNMDDIRRIERPTDVPDYGLLNDLLWSDPSDTALDWEDNERGVSYCFGKA
VIQQFLAQYDFDLICRAHMVVEDGYEFWNERTLVTIFSAPNYCGEFDNFGAVMSVSEDLLCAFELL
KPLDGAALKKEMAKNKRRSLLQHQSPPARGSQQSY

UmHal3

MQRTPSDSLDPSIAASKALDASQSGSDCSSRTTSPRFPIARLEPTDRAEWQSQTVGRSSHRRDSQH
PFGDHTAQRIVPTSSSTPSTPTSALPTSRTYHSLNYAPRQRNSMLRPNAASVFQPHSPQSAQQQQA
VTTAFTGLALPSGRVSPALPSYSSPLSATSYLRTSPSYPTISLPDAVPPRDSSRVRDSVSLQADTA
PTSLARMQLQQMQDEARRLGLNEKSAGWLILEALQAATEGEWAAVAELLANGDATLLLPRDPPSVF
TSSSQLSASFAYDHTIFNAASASSTKPSPSAVPSSATCPDALSILTLSGLRGSLSRAPSDQSEPDT
LVQAVESQQFQLILQSFVVKTSQSAISNLKDASSRQETLEMLAPLPIITSLDKSNCRYPSFSLLAS
NAQFPLPPPLNVRKASSQSQAGGKNRARSNSKLNAAGSRASASFASIFGGSGRERRRQAEAAGTTG
SEMLDAQRLSVNATHLDVQPFQGANVAQDGLEIESGAQIPSSLGVELRGDLQHTTNDEATSIKEST
CATTQRRSVSVWVVDHLVRRSTVMKMIRKALDTRIKERLLAKSIPESISDVVASFAATYLPPAPSL
NDVSASRSGGAERGQASHSNRSRAASPVNVVNPPYLADPDELSENFQDFFNSIREQLYNFDSSQAE
YLRADSDTAAAIARNPAPNASLEEQHAQHDRIERQLEAVETVLCEEVYDRIFCPVTSRDRYHDDAL
ASRIAALNVLGLSLRHLGLVVPSERLQEDEIEATESNALLDGIERIVQQCGDELQRLESAMCRSPQ
AKLDVLVRAHKIAVEGVAQLPSIKMRDDDTAVEGQEKEQTARPSSGKKGDGSTSADLILPILIYSI
VSSNPSHLASNLLYIQRFRAESLVQGETSYCLVNVQAAVAFLENVDVKDLGLDSNQIGAHLPVHSR
DEGHAPRSSTGSSHSLVPSSKIAETSSATLAMPARIRGRLTQEIGDLAGASNKVITGVMGSSISAF
SRMMGANASVAEAGVDESLGRKRAKSSASLNAAHSEGAVAPTQADAQRPLRSRTSSSVTPTDDSYL
GEQSKEKEKDTVGTPSTDKPSIGDRLAMLSRLGTSALSSSPSSSLGSGLPSDSGLGVSASGQSLIA
SPRAVSRELPGPPPPTKTKTTRPVQNRTTSYLASQLSRTTATPPRTSSGSLSAVLADEVVAAAKPL
PASLRSPYAPLSRPPTCDRPLHIVLASTGSVASVKIPLIVQELLTYANVRVQVIATDNSLHFYDRA
DIAKLNAASGGDGDEYTVASLAAENQSASVCGRAASHVRAHLWTNADEWTSFSRIGDPILHIELRR
WADMVLIAPCSANTLAKIYGGMCDDLLTSFVRALARDTPKWMFPAMNTLMWENEVTEVHVDALRRR
GWVVHGPVEKMLACGDMGTGAMVEWTELVQTLVQWAHLVRDESR

Blue background: potential phosphorylatable site

Yellow background: extra insert compared with AtHal3

Green background: putative VPS9 domain

Supplementary Information 2

Comparison of CnPpz1 and UmPpz1 protein sequences

```
CnPpz1             1 ----MGQGQSSSKKLGRT----------SSKQLPPQDLADSL---ARTSI     33
                       .|:....|.:.|::          :|..||..|.::.|   ::.|:
UmPpz1             1 MFKSFGKIMGGSSRKGKSKLQDGDDSVDASNGLPGSDSSNLLRAKSKDSL     50

CnPpz1            34 ADRDAAAGHPPPPDALSPAKLAAKRRGSTRDAPPASYASSTSDAPPAPAP     83
                     |..:..:|:.....:.:|||: .||.|.:|...|.
UmPpz1            51 AVTENGSGNFANNGSSAPAKI-EKRGGVSRHESPL---------------     84

CnPpz1            84 PSPSPSSIPTTQNILAAPREGLKSSFLGSSPPPPSAMSVSPASTTGG-RV    132
                     ||||||:    :|:|....|   ||.:|||....||    |||..|| |.
UmPpz1            85 PSPSPSA----RNVLEGQEE---SSEVGSSAVARSA----PASDVGGPRP    123

CnPpz1           133 RSSSPPPSSS-PTRQTGGHLSRDSASSLSPGFTLTQTVSRTESAAGGFQI    181
                     .:.:...|:| ||..|  .||...|.|.|.||. :......::||||.|:
UmPpz1           124 ANDAASQSTSVPTANT--ILSNPLAQSGSTGFP-SSVGKNAQAAAGGDQV    170

CnPpz1           182 --LDVDNMIQRLLEAGYSGKVTKSPPLKNAEITSVCAAAREVFLSQPTLI    229
                       .|:|:||.||||||||||:.| |.|||||||:||.||||:||||||||
UmPpz1           171 RTFDIDDMISRLLEAGYSGKIPK-PALKNAEITAVCQAAREIFLSQPTLI    219

CnPpz1           230 ELSPPVKIVGDVHGQYADLLRMFEMCGFPPAANYLFLGDYVDRGKQSLET    279
                     ||||||||||.||||.||||:||||||||:||||||||||||||||||||
UmPpz1           220 ELSPPVKIVGDTHGQYHDLLRLFEMCGFPPSANYLFLGDYVDRGKQSLET    269

CnPpz1           280 ILLLLCYKIKYPENFFLLRGNHECANVTRVYGFYDECKRRTNIKIWKTFI    329
                     ||||||||||||||||||||||||||||||||||||||.|||||||||
UmPpz1           270 ILLLLCYKIKYPENFFLLRGNHECANVTRVYGFYDECKRRVNIKIWKTFI    319

CnPpz1           330 DVFNTLPIASIVASKIFCVHGGLSPSLKSMDDIRRIQRPTDVPDYGLLND    379
                     |||||||||::||||||||||||||||.:|||||||:||||||||||||||
UmPpz1           320 DVFNTLPIAAVVASKIFCVHGGLSPSLSNMDDIRRIERPTDVPDYGLLND    369

CnPpz1           380 LVWSDPSDTALDWEDNERGVSFCYGKSVINAFLATHDMDLICRAHMVVED    429
                     |:||||||||||||||||||:|:||:||..|||.:|.||||||||||||
UmPpz1           370 LLWSDPSDTALDWEDNERGVSYCFGKAVIQQFLAQYDFDLICRAHMVVED    419

CnPpz1           430 GYEFYNDRTLVTVFSAPNYCGEFDNFGAVMSVSEDLLCSFELLKPLDGAA    479
                     ||||:|:||||||||||||||||||||||||||||:||||||||||||||
UmPpz1           420 GYEFWNERTLVTIFSAPNYCGEFDNFGAVMSVSEDLLCAFELLKPLDGAA    469

CnPpz1           480 LKKEMTKSKRKSLQAHQSPPNNPMAQSF*    508
                     |||||.|:||:||..|||||.....||:
UmPpz1           470 LKKEMAKNKRRSLLQHQSPPARGSQQSY-    497
```

Blue background: potential phosphorylatable site

Supplementary Table 1. Yeast strains used in this study

Strain	Genotype	Source/Reference
BY4741	*MAT* a *his3D1 leu2D0 met15D0 ura3D0*	Euroscarf
ppz1	BY4741 *ppz1::kanMx4*	Euroscarf
hal3	BY4741 *hal3::kanMx4*	Euroscarf
slt2	BY4741 *slt2::kanMx4*	Euroscarf
trk1 trk2	BY4741 *trk2::nat1 trk1::LEU2*	(Barreto *et al.* 2012)
trk1	BY4741 *trk1::LEU2*	(Barreto *et al.* 2012)
nha1	BY4741 *nha1::LEU2*	This study
ZCZ01	BY4741 *promotor ppz1*::*pGAL*::*kanMX6*	This study
ZCZ06	ZCZ01 *NHA1*::*LEU*	This study
IM21	1788 (*MAT* a/α, *ura3-52 leu2-3,112 trp1-1 his4 can-1*r) *ppz1::kanMx4 hal3::LEU2*	(Ruiz *et al.* 2004a)
AGS04	1788 (*MAT* a/α, *ura3-52 leu2-3,112 trp1-1 his4 can-1*r) *vhs3::kanMx4 hal3::LEU2*	(Ruiz *et al.* 2004a)
MAR25	1788 (*MAT* a/α, *ura3-52 leu2-3,112 trp1-1 his4 can-1*r) *ykl088w::kanMx4*	(Ruiz *et al*. 2009)

Supplementary Table 2. Plasmids used in the study

Plasmids	Description	Source/Reference
pYES2	High copy number plasmid is designed to express inserted ORF controlled by the galactose-induced promoter *GAL1-10* in *S. cerevisia*e	Invitrogen
pYES-Ppz1	pYES2-based plasmid, expressing *ScPPZ1* in *S. cerevisiae*	(Clotet *et al.* 1996)
pYES2-Ppz1^{R451L}	pYES2-based plasmid, expressing the *ScPPZ1* inactive version *PPZ1^{R451L}* in *S. cerevisiae*	This study
pYES-ScPpz1-HA	pYES2-based plasmid, expressing *ScPPZ1* with HA tag added to C-terminal region in *S. cerevisiae*	This study
pYES-CnPpz1	pYES2-based plasmid, expressing *CnPPZ1* in *S. cerevisiae*	This study
pYES-UmPpz1-HA	pYES2-based plasmid, expressing *UmPPZ1* with HA tag in C-terminal region in *S. cerevisiae*	This study
YCplac111	Low copy number plasmid of *S. cerevisiae*	(Gietz and Sugino 1988)
YCp-Ppz1	YCplac111-based plasmid, expressing *ScPPZ1* controlled by *ScPPZ1* promoter in *S. cerevisiae*	(Clotet *et al.* 1996)
YCp-Ppz1^{R451L}	YCplac111-based plasmid, expressing the *PPZ1* inactive version *PPZ1^{R451L}* controlled by *PPZ1* promoter in *S. cerevisiae*	(Clotet *et al.* 1996)
YCp-CnPpz1	YCplac111-based plasmid, expressing *CnPPZ1* controlled by *ScPPZ1* promoter in *S. cerevisiae*	This study
YCp-UmPpz1	YCplac111-based plasmid, expressing *UmPPZ1* controlled by *ScPPZ1* promoter in *S. cerevisiae*	This study
YCp-UmPpz1-HA	YCplac111-based plasmid, expressing *UmPPZ1* with HA tag in the C-terminal region controlled by *ScPPZ1* promoter in *S. cerevisiae*	This study
YCp-CaPpz1	YCplac111-based plasmid, expressing *CaPPZ1* controlled by *ScPPZ1* promoter in *S. cerevisiae*	(Adam *et al.* 2012)
YEplac181	High copy number plasmids with a *LEU2* marker of *S. cerevisiae*	(Gietz and Sugino 1988)
YEplac195	High copy number plasmids with a *URA3* marker of *S. cerevisiae*	(Gietz and Sugino 1988)

YEp-ScPpz1	YEplac181-based plasmid, expressing *ScPPZ1* controlled by *ScPPZ1* promoter in *S. cerevisiae*	(Clotet *et al.* 1996)
YEp-HAL3^{Y313D}, HAL3^{V390G}, HAL3^{W452G}, HAL3^{V462A}, HAL3^{E460G}	YEplac195 based plasmid, expressing specific mutated *HAL3* versions in *S. cerevisiae*	(Ruiz *et al.* 2004a)
pRS699-HsHal3	pRS699 (high copy number plasmids with a *URA3* marker) based plasmid, expressing *HsHAL3* in *S. cerevisiae*	(Ruiz *et al.* 2009)
YEp-CnPpz1	YEplac181-based plasmid, expressing *CnPPZ1* controlled by *ScPPZ1* promoter in *S. cerevisiae*	This study
YEp-UmPpz1	YEplac181-based plasmid, expressing *UmPPZ1* controlled by *ScPPZ1* promoter in *S. cerevisiae*	This study
pWS93	High copy number plasmid to express N-terminally 3xHA-tagged proteins from the strong promoter *ADH1* in *S. cerevisia*e	(Song and Carlson 1998)
pWS-ScPpz1	pWS93-based plasmid expressing *ScPPZ1* in *S. cerevisiae*	This study
pWS-UmPpz1	pWS93-based plasmid expressing *UmPPZ1* in *S. cerevisiae*	This study
pWS-ScHal3	pWS93-based plasmid expressing *ScHAL3* in *S. cerevisiae*	This study
pWS-CnHal3a	pWS93-based plasmid expressing *CnHAL3a* in *S. cerevisiae*	This study
pWS-CnHal3b	pWS93-based plasmid expressing *CnHAL3b* in *S. cerevisiae*	This study
pWS-CnHal3b_ScL	pWS93-based plasmid expressing *CnHAL3b* with the catalytic loop ^{204}QGAGRLAC^{211} replaced by ^{458}SEKVMDIN^{466} from *ScHAL3* in *S. cerevisiae*	This study
pWS-CnHal3b_ScCter	pWS93-based plasmid expressing *CnHAL3b* with the C-tail replaced by the C-tail region from *ScHAL3* in *S. cerevisiae*	This study
pWS-CnHal3b_ScL _Cter	pWS93-based plasmid expressing *CnHAL3b* with both catalytic loop and C-tail region replaced by the ones from *ScHAL3* in *S. cerevisiae*	This study
pWS-UmHal3	pWS93-based plasmid expressing *UmHAL3* in *S. cerevisiae*	This study
pWS-UmHal3_PD	pWS93-based plasmid expressing the PD region of *UmHAL3* in *S. cerevisiae*	This study
pWS-UmPD_ScCter	pWS93-based plasmid expressing the PD region of *UmHAL3* with the C-tail region from *ScHAL3* in *S. cerevisiae*	This study
pGEX-6p-1	Bacterial vector for expressing GST fusion proteins with a PreScission protease site.	GE Healthcare
pGEX-ScPpz1	pGEX-based plasmid, expressing *ScPPZ1* in *E. coli*	(Ruiz *et al.* 2004a)
pGEX-ScPpz1_cat	pGEX-based plasmid, expressing the catalytic region of *ScPPZ1* in *E. coli*	(Ruiz *et al.* 2004a)
pGEX-CnPpz1	pGEX-based plasmid, expressing *CnPPZ1* in *E. coli*	This study
pGEX-CnPpz1_cat	pGEX-based plasmid, expressing the catalytic region of *CnPPZ1* in *E. coli*	This study
pGEX-UmPpz1	pGEX-based plasmid, expressing *UmPPZ1* in *E. coli*	This study
pGEX-AtHal3	pGEX-based plasmid, expressing *AtHAL3* in *E. coli*	(Santolaria *et al.* 2018)
pGEX-ScHal3	pGEX-based plasmid, expressing *ScHAL3* in *E. coli*	(Ruiz *et al.* 2004a)
pGEX-CnHal3a	pGEX-based plasmid, expressing *CnHAL3a* in *E. coli*	This study
pGEX-CnHal3b	pGEX-based plasmid, expressing *CnHAL3b* in *E. coli*	This study
pGEX-CnHal3b_ScL	pGEX-based plasmid, expressing *CnHAL3b* with the catalytic loop ^{204}QGAGRLAC^{211} replaced by ^{458}SEKVMDIN^{466} from *ScHAL3* in *E. coli*	This study
pGEX-CnHal3b_ScCter	pGEX-based plasmid, expressing *CnHAL3b* with the C-tail replaced by the C-tail region from *ScHAL3* in *E. coli*	This study
pGEX-CnHal3b_ScL _Cter	pGEX-based plasmid, expressing *CnHAL3b* with both catalytic loop and C-tail region replaced by the ones from *ScHAL3* in *E. coli*	This study
pGEX-UmHal3	pGEX-based plasmid, expressing *UmHAL3* in *E. coli*	This study
pGEX-UmHal3_PD	pGEX-based plasmid, expressing the PD region of *UmHAL3* in *E. coli*	This study
pGEX-UmPD_ScCter	pGEX-based plasmid expressing the PD region of *UmHAL3* in *E. coli*	This study
pFA6a-KanMx6-pGAL1	Plasmid that contains the *KanMx6 GAL1-10* promoter cassette	(Longtine *et al.* 1998)
pCRII-NHA1::LEU	Plasmid containing the cassette *nha1::LEU2* used to knock out the gene *NHA1* in *S. cerevisiae*	Dr. Alonso Rodríguez-Navarro

Supplementary Table 3. Oligonucleotides used in this study

Name	Sequence	Function
PPZ1-F4	TCATCGTTATAGTCGCTTCTTTTCCCCTAGAGGCTTTGTCGAATTCGAGCTCGTTTAAAC	Oligo forward, to amplify the sequence containing *GAL1-10* promoter and part of *PPZ1* to replace the *PPZ1* promoter in *S. cerevisiae*
PPZ1-R2	TTTCGAAGATTTTGAACTTGAATTACCCATTTTGAGATCCGGGTTTT	Oligo reverse, to amplify the sequence containing *GAL1-10* promoter and part of *PPZ1* to replace the *PPZ1* promoter in *S. cerevisiae*
E1_kpnI	CGGGTACCATGTTCAGATAGCTGCC	Oligo forward, used to check ZCZ01
K3	GTTAAGTGCGCAGAAAGTAA	Oligo reverse, used to check ZCZ01
NHA1 anl disr 3'	TTGACGGCTGTGCTCAATGC	Oligo forward, used to check *NHA1::LEU2* cassette inserted.
leu2-3´	AAGTCAATACCTTCTTGAACC	Oligo reverse, used to check *NHA1::LEU2* cassette inserted.
RI-L	GC*GAATTC*GGCCAGGGCCAGTCCTCCTCGAAGAAACTGG	Oligo forward, to amplify the ORF of CnPpz1 to yield pGEX-CnPpz1
Cryp_PPZ1_XhoI_L_1	CGC*CTCGAG*AAAGCTTTGAGCCATAGGGTTATTGG	Oligo reverse, to amplify the ORF of CnPpz1 to yield pGEX-CnPpz1
Cryp_PPZ1prom_XbaI	CG*TCTAGA*TCAAAATGGGCCAGGGCCAGTCCTC	Oligo forward, to amplify the ORF of CnPpz1 to yield YCp/YEp-CnPpz1
Cryp_PPZ1prom_SphI	CGC*GCATGC*CTAAAAGCTTTGAGCCATAGG	Oligo reverse, to amplify the ORF of CnPpz1 to yield YCp/YEp-CnPpz1 and pYES-CnPpz1
CnPPZ1-R1-L-ATG	GC*GAATTC*TCAAAATGGGCCAGGGCCAGTCCTCCTC	Oligo forward, to amplify the ORF of CnPpz1 to yield pYES-CnPpz1
FUS FW	CTACAGCGGCAAGGTCACAAAGAGC	Oligo forward, to amplify the fragment used as the template to yield ORF of CnPpz1 by fusion PCR. Also, used to sequence the ORF.
FUS RV	CATGCACATCGCCGACAATCTTG	Oligo reverse, to amplify the fragment used as the template to yield ORF of CnPpz1 by fusion PCR. Also, used to sequence the ORF.
Cn_07348_EcoRI	GCT*GAATTC*AGCCCGCCCAGACCCATG	Oligo forward, to amplify the ORF of CnHal3b to yield pGEX-CnHal3b and pWS-CnHal3b.
Cn_07348_SalI	GCT*GTCGAC*TCAACCCAACCACCACTTTCTG	Oligo reverse, to amplify the ORF of CnHal3b to yield pGEX-CnHal3b and pWS-CnHal3b.
Cn_00909_EcoRI	CGC*GAATTC*CCATCCATCAGCCACGTCA	Oligo forward, to amplify the ORF of CnHal3a to yield pGEX-CnHal3a and pWS-CnHal3a.
Cn_00909_SalI	GCG*GTCGAC*TTAGACACCAAGCCACCATTTTC	Oligo reverse, to amplify the ORF of CnHal3a to yield pGEX-CnHal3a and pWS-CnHal3a.
CnPPZ1_5'_cat_EcoRI	CCG*GAATTC*CGGGGCTTCACACTCACCCA	Oligo forward, to amplify the ORF of the catalytic region of CnPpz1 to yield pGEX-CnPpz1_cat
Cn_00909_seq_FW	CCCACATGTACCAACAC	Oligo forward, used to sequence *CnHAL3a*.
Cn_00909_seq_RV	GCAAGGTGTTTGGGG	Oligo reverse, used to sequence *CnHAL3a*.

Cn_07348_seq_FW	CTTCTCTTCTCCGCG	Oligo forward, used to sequence *CnHAL3b*
Cn_07348_seq_RV	CATAGCGGGGCACA	Oligo reverse, used to sequence *CnHAL3b*.
5´insert Sc	TCTGAAAAAGTTATGGATATTAATGGTGATGACGGCCCTG GAAAA	Oligo forward, used to replace the catalytic loop ^{204}QGAGRLAC^{211} of CnHal3b by ^{458}SEKVMDIN^{466} from ScHal3 to yield pGEX/pWS-CnHal3b_ScL and pGEX/pWS-CnHal3b_ScL_Cter
3´insert Sc	ATTAATATCCATAACTTTTTCAGACGGTCCAGAGACAAGGT ACCC	Oligo reverse, used to replace the catalytic loop ^{204}QGAGRLAC^{211} of CnHal3b by ^{458}SEKVMDIN^{466} from ScHal3 to yield pGEX/pWS-CnHal3b_ScL and pGEX/pWS-CnHal3b_ScL_Cter
Cn07348_ScCtD_FW	GTGTCTCTGATCGAACCAAAAAATAACGAGGAA	Oligo forward, used to replace the C-tail of CnHal3b by the C-tail of ScHal3 to yield pGEX/pWS-CnHal3b_ScCter and pGEX/pWS-CnHal3b_ScL_Cter
Cn07348_ScCtD_RV	TTCCTCGTTATTTTTTGGTTCGATCAGAGACAC	Oligo reverse, used to replace the C-tail of CnHal3b by the C-tail of ScHal3 to yield pGEX/pWS-CnHal3b_ScCter and pGEX/pWS-CnHal3b_ScL_Cter
UmPpz1_BamHI	CGC*GGATCC*TTCAAATCTTTCGGCAAGAT	Oligo forward, to amplify the ORF of UmPpz1 to yield pGEX-UmPpz1
UmPpz1_EcoRI	CCG*GAATTC*TCAATACGACTGCTGCGA	Oligo reverse, to amplify the ORF of UmPpz1 to yield pGEX-UmPpz1
UmPpz1_ATG_BamHI	CGC*GGATCC*ATGTTCAAATCTTTCGGCAAGAT	Oligo forward, to amplify the ORF of UmPpz1 to yield pYES-UmPpz1
UmPpz1_XbaI	TGC*TCTAGA*ATGTTCAAATCTTTCGGCAA	Oligo forward, to amplify the ORF of UmPpz1 to yield YCp/YEp-UmPpz1
UmPpz1_HindIII	CCC*AAGCTT*TCAATACGACTGCTGCGA	Oligo reverse, to amplify the ORF of UmPpz1 to yield YCp/YEp-UmPpz1
UmPpz1_HA_HindIII	CCC*AAGCTT*TTAAGCGTAATCTGGAACATCGTATGGATAAT ACGACTGCTGCGA	Oligo reverse, to amplify the ORF of UmPpz1 with HA tag in the C-terminal region to yield YCp/YEp-UmPpz1-HA
UmPpz1_HA_EcoRI	CCG*GAATTC*TTAAGCGTAATCTGGAACATC	Oligo reverse, to amplify the ORF of UmPpz1 with HA tag in C-terminal region to yield pYES-UmPpz1-HA
ScPpz1-HA-NotI	CCG*CGGCCGC*TTAAGCGTAATCTGGAACATC	Oligo reverse, to amplify the ORF of ScPpz1 with HA tag in C-terminal region to yield pYES-ScPpz1-HA
ScPpz1_in_PacI	TTGGCTTAATTAATGATCTTTTGT	Oligo forward, to amplify the ORF of ScPpz1 with HA tag in C-terminal region to yield pYES-ScPpz1-HA
UmHal3_EcoRI	CG*GAATTC*CAACGCACACCAAGCGAC	Oligo forward, to amplify the ORF of UmHal3 to yield pGEX-UmHal3 and pWS-UmHal3.
UmHal3_NotI	ATAAGAAT*GCGGCCGC*TCATCGGCTCTCGTCTCTGA	Oligo reverse, to amplify the ORF of UmHal3 to yield pGEX-UmHal3
UmHal3_BamHI	CGC*GGATCC*TCATCGGCTCTCGTCTCTG	Oligo reverse, to amplify the ORF of UmHal3 to yield pWS-UmHal3.
UmHal3_seq 1	GCCTCCGCATCCTCTACAA	Oligo forward, used to sequence the inserted ORF of UmHal3 in both pGEX-UmHal3 and pWS-Hal3

UmHal3_seq 2	CTCGACACACGCATTAAAGA	Oligo forward, used to sequence the inserted ORF of UmHal3 in both pGEX-UmHal3 and pWS-Hal3
UmHal3_seq 3	TTGAAGGCCAAGAAAAAGAACAGACAGCT	Oligo forward, used to sequence the inserted ORF of UmHal3 in both pGEX-UmHal3 and pWS-Hal3
UmHal3_seq 4	AAGTGGTGGCTGCTGCCAA	Oligo forward, used to sequence the inserted ORF of UmHal3 in both pGEX-UmHal3 and pWS-Hal3
UmHal3_seq 5	TAAAGACAGAAGGAGGATCG	Oligo reverse, used to sequence the inserted ORF of UmHal3 in both pGEX-UmHal3 and pWS-Hal3
UmHal3_seq 6	TTCTTTTTCTTGGCCTTCAACGGCAGTGTCAT	Oligo reverse, used to sequence the inserted ORF of UmHal3 in both pGEX-UmHal3 and pWS-Hal3
UmHal3_ScCtD_FW	TCAGAGACGAGAGCCGACCAAAAAATAACGAGGAA	Oligo forward, used to add the C-tail of ScHal3 to UmHal3 to yield pGEX-UmPD_ScCter and pWS-UmPD_ScCter
UmHal3_ScCtD_RV	TTCCTCGTTATTTTTTGGTCGGCTCTCGTCTCTGA	Oligo reverse, used to add the C-tail of ScHal3 to UmHal3_PD to yield pGEX-UmPD_ScCter and pWS- UmPD_ScCter
Reverse HAL3-XhoI	AC*CTCGAG*TTATTGATGCTTATCTATTATACCTGGGG	Oligo reverse, used to add the C-tail of ScHal3 to UmHal3 by fusion PCR
UmHal3_PD_EcoRI	CG*GAATTC*CCGCTCCCGGCGTCGCTG	Oligo forward, to amplify the PD region of UmHal3 to yield pGEX/pWS-UmHal3_PD and pGEX/pWS-UmPD_ScCter

Underlined sequences denote artifically added restriction sites for cloning purposes